METHODS AND INSTRUMENTATION FOR MEASURING MOISTURE IN BUILDING STRUCTURES

Jukka Voutilainen

Dissertation for the degree of Doctor of Science in Technology to be presented with due permission of the Department of Electrical Engineering, for public examination and debate in Auditorium S2 at Helsinki University of Technology (Espoo, Finland) on the 18th of March, 2005, at 12 noon.

Abstract

Excess moisture in building structures may damage the structures and provide suitable conditions for microbe growth. As a consequence, moisture may cause different health effects to the occupants, and lead to costly refurbishments, if the damage is not perceived in time. Currently, there are several work-intensive, destructive methods for verifying suspected moisture problems and for monitoring the drying of concrete structures. However, it has not been previously feasible to monitor moisture routinely, on a regular basis.

This thesis introduces new methods for measuring moisture in building structures, and the instrumentation developed for implementing them. First of all, the study defines accurately the current need for new methods, and selects the specific problems to approach. The study then elucidates the physical principles of the novel measurement methods and presents the practical instrumentation. The functionality of the system is then verified in laboratory and field measurements. Finally, some guidelines are presented in how to apply the system to the building industry.

The developed measurement system consists of two components: low-cost passive LC circuit sensors and a separate reading device that couples inductively with each sensor. The sensors are assembled in contact with the structure of interest at the time of construction or renovation. The moisture conditions in the structure affect the resonant frequency and quality factor of the sensor. These parameters can be measured with the reading device from outside the structure, whenever needed. As a consequence, moisture conditions inside the structure can be measured without damaging the structure. As an improvement to existing moisture measurement methods, the developed system combines measurement accuracy at an exactly defined location with a fast and non-destructive measurement procedure. In addition to the methods, this thesis presents several, new moisture and temperature sensors, a hand-held device for reading the sensors wirelessly, and preliminary measurement results and experiences from using the system in the construction industry. The research lays a foundation for further research in the moisture measurement application, but also for applying the methods to other application areas, such as the packaging industry. The research has also led to the development of a new commercial product.

Keywords: moisture, humidity, measurement method, RFID, inductive coupling, embedded systems

Preface

This thesis is based on the work carried out in two moisture monitoring research projects (RAKO and RAKO2) that took place at the Applied Electronics Laboratory in Helsinki University of Technology, during the years 2000–2003. The projects were a part of the Healthy Building technology program organized by the National Technology Agency of Finland (Tekes). My research has also been supported financially by the Graduate School of Electronics Manufacturing, Jenny ja Antti Wihurin rahasto, and Tekniikan Edistämissäätiö, to all of which I am grateful.

First of all, I would like to thank Professor Raimo Sepponen for the opportunity to work with this interesting topic, and for his valuable guidance. I would also like to thank everyone at the Applied Electronics Laboratory for providing a pleasant working environment. I am especially grateful to my research team, Juho Partanen, Tuomo Reiniaho, Outi Savinen, and Eero Tommila for their scientific and creative contribution to the research. I would like to thank all the organizations and companies that participated in the two monitoring projects, and provided an active management team that shared their expertise with the projects. Especially the people at Humittest have been of enormous help with aspects related to the laboratory and field measurements.

I am grateful to my brother Tuomas for helping me out with the illustration of this thesis. For the circuit diagrams, I am grateful to Dr. Kimmo Silvonen and his excellent software tool. I would also like to thank the examiners of my thesis, Professor Kalevi Kalliomäki and Professor Pertti Silventoinen, for their suggestions and discussions on the manuscript.

I wish to thank all my friends in HäPS, and DIG-group for taking my thoughts away from the research, at least once in a while. I also want to thank my family for their support. Finally I would like to thank my fiancée Merja for her love and patience during my post-graduate studies.

Jukka Voutilainen

February 2005

Contents

Nomenclature

A Area

$\mathbf{A}$ Vector potential

B Bandwidth

$\mathbf{B}$ Magnetic flux density

c Contour

C Capacitance

C_{di} Capacitance of dielectric layer

C_L Capacitance of inductor

C_p Parallel capacitance

d Thickness

$\mathbf{D}$ Electric flux

$\mathbf{E}$ Electric field strength

f Frequency

$\mathbf{f}$ Vector field

f_{res} Resonant frequency

G Moisture production

$\mathbf{H}$ Magnetic field strength

i Current

I Current (phasor expression)

j Imaginary unit

J Current source

$\mathbf{J}$ Density of free currents

k Coefficient of coupling

L Inductance

L_C Inductance of capacitor

L_s Series inductance

m Mass

M Mutual inductance

n Air exchange rate

p_v Vapor pressure

p_s Saturated vapor pressure

P_l Power loss

Q Quality factor

$\mathbf{r}$ Location

R Resistance

R_C Resistance of capacitor

R_{eq} Equivalent resistance

R_{Lp} Parallel resistance of inductor

R_{Ls} Series resistance of inductor

R_p Parallel resistance

R_s Series resistance

S Surface

t time

T Temperature

u Voltage

U Voltage (phasor expression)

U_{det} Detected voltage

U_{RF} Radio frequency voltage

U_S Voltage signal

V Volume

w Moisture content

W Moisture quotient

W_e Electric energy

W_m Magnetic energy

Z_{in} Input impedance

Z_{mat} Impedance of material

Z_T Transfer impedance

β Current amplification factor

ϵ_0 Permittivity of vacuum

ϵ_r Relative permittivity

μ_0 Permeability of vacuum

μ_r Relative permeability

ν Absolute humidity

ν_s Saturation humidity

σ Conductivity

ϕ Phase angle

φ Relative humidity

ω Angular frequency

ω_{res} Angular resonance frequency

ADC	Analog-to-Digital Converter
BNC	Bayonet Navy Connector
C	C programming language
DAC	Digital-to-Analog Converter
DC	Direct Current
DSP	Digital Signal Processor
DIN	Deutsches Institut für Normung
ESR	Equivalent Series Resistance
FET	Field Effect Transistor
FFT	Fast Fourier Transform
FR-4	Flame Retardant class 4
HVAC	Heating, Ventilation, and Air-Conditioning
LC	Inductor and Capacitor
LCD	Liquid Crystal Display
LED	Light Emitting Diode
LO	Local Oscillator
MC	Moisture Content
MVOC	Microbial Volatile Organic Compounds
PC	Personal Computer
PVC	PolyVinyl Chloride
RF	Radio Frequency
RFID	Radio Frequency IDentification
RH	Relative Humidity
TVOC	Total Volatile Organic Compounds
USART	Universal Synchronous and Asynchronous Receiver Transmitter
VCO	Voltage Controlled Oscillator
VCCS	Voltage Controlled Current Source
VOC	Volatile Organic Compounds
µC	MicroController

1 Introduction

Excess moisture that drifts into structures at the time of construction or inhabitation may damage the structures and provide suitable conditions for the growth of hazardous microbes. Thus, occurred moisture damages often require costly refurbishment operations if they are not perceived in time. As a consequence, controlling moisture in buildings is an important task. However, the measurement methods currently available are predominantly suitable for verifying suspected moisture problems, not for routine monitoring of moisture.

This thesis introduces new methods for measuring moisture in building structures routinely and the instrumentation developed for implementing them. The methods and instrumentation are then applied in the actual building industry and the acquired results are reported. The research has been performed at the Applied Electronics Laboratory at Helsinki University of Technology during the years 2000–2004.

This chapter concentrates on describing the field of application and the role of the performed research within it. First, the concepts and the quantities used when assessing moisture are introduced. Then, the typical origins of structural moisture, the possible damage associated with it, and related health effects are discussed. Some figures of the economic significance of moisture damage are presented. The common methods currently used in measuring moisture are presented. Finally, the objectives of the performed research, the specific research problem, and the contribution of the research and the author are presented.

1.1 Definitions

Several different quantities are used to evaluate the amount of moisture in air or inside different materials. It is crucial to understand which quantities are relevant in each case and what quantities a specific moisture measurement device assesses. These matters are often ignored in practical measurements due to insufficient knowledge or plain negligence. In addition, the names used for the quantities differ slightly in the literature. This section defines the concepts used in this thesis.

1.1.1 Moisture in air

Water vapor is one of the many gases of the atmosphere. The amount of water vapor in a volume unit of air is referred to as the *absolute humidity* ν of the air, usually expressed as grams in a cubic meter of air. The maximum value of absolute humidity is the *saturated humidity* ν_s at the prevailing temperature, i.e. the

maximum amount of water vapor that the air can hold [1, pp. 236–238]. If additional moisture is introduced, it will condense into liquid water. The difference between the saturated humidity and the prevailing absolute humidity is known as *saturation deficit*, a measure of how much additional moisture the air can bind [2, p. 49]. Another measure for the amount of moisture in air is the *vapor pressure* p_v. Correspondingly, vapor pressure is limited to the *saturated vapor pressure* p_s [3, p. 43]. Both saturated humidity and saturated vapor pressure are temperature dependent being the larger the higher the temperature. The saturated humidity and saturated vapor pressure values in some temperatures often present in building structures are shown in Table 1.1 [3, p. 44].

Table 1.1: Saturated humidity and saturated vapor pressure values at some temperatures at a typical atmospheric pressure of 101 325 Pa. Symbols: T = temperature [℃] , ν_s = saturated humidity [g/m^3], p_s = saturated vapor pressure [Pa]. [3, p. 44]

T [℃]	ν_s [g/m^3]	p_s [Pa]
−20	0.87	102
−10	2.20	266
0	4.85	611
10	9.45	1234
20	17.28	2337
30	30.31	4237

In the majority of cases, the amount of moisture in air is expressed as *relative humidity* (RH), φ. By definition, relative humidity is the ratio of the absolute humidity to the saturated humidity at a given temperature [1, p. 239]. Correspondingly, RH can be expressed in terms of vapor pressure as the ratio of the vapor pressure and the saturated vapor pressure. RH is typically expressed as a percentage so that a relative humidity of 100 % corresponds to the saturated humidity at the prevailing temperature. In attempting to diagnose moisture related problems, both relative humidity and temperature should be measured [4, p. 3].

Another widely used approach to assessing the amount of moisture in air is the *dew point*. By definition, dew point is the temperature at which the air of a given absolute humidity saturates [1, p. 238]. When the prevailing temperature is known, absolute humidity, relative humidity and dew point can all be calculated from one another.

1.1.2 Moisture in construction materials

Water in construction materials is bound in several different ways. *Chemically bound water* is bound so tight that it typically is not taken into account when assessing moisture. *Physically bound water*, on the other hand, is the evaporable water typically known as moisture. Physically bound water is bound to the pores of the material both hygroscopically and capillarily. [1, pp. 241–242]

A porous material has the ability to absorb moisture from the atmosphere and to discharge it to the atmosphere. This property is known as *hygroscopicity* [3, p. 59]. When the relative humidity of the air inside the pores of a material, often referred to as the *relative humidity of the material*, is equal to the relative humidity of the atmosphere, a *hygroscopic equilibrium* is reached. Materials strive for this equilibrium by absorbing and discharging moisture. The equilibrium is possible when the material is in the *hygroscopic range*, i.e. the relative humidity of the material is 0–98 % [5, p. 6].

The majority of the water present in a substance is not in the air of the pores but physically bound to the surface of the pores. The amount of water in a material, relative to the volume of the substance (kg/m^3), is referred to as *moisture content* (MC) w. The maximum value of MC is limited to the density of water. Another widely used quantity is the *moisture quotient*, W, the weight of the water, as a percentage of the weight of the dry substance. [1, p. 243]

The interdependence between the moisture content of a material and the relative humidity of the atmosphere in hygroscopic equilibrium is described with *sorption isotherms*. Figure 1.1 shows the sorption isotherms of two materials, concrete of the strength class K25 and mineral wool [1, pp. 479, 481]. As can be seen from the figures, the moisture content at a given relative humidity varies significantly between different materials. The interdependence also depends on the prevailing temperature and features *hysteresis*, i.e. it depends on whether the material is drying (*desorption*) or wetting (*absorption*) [1, p. 250].
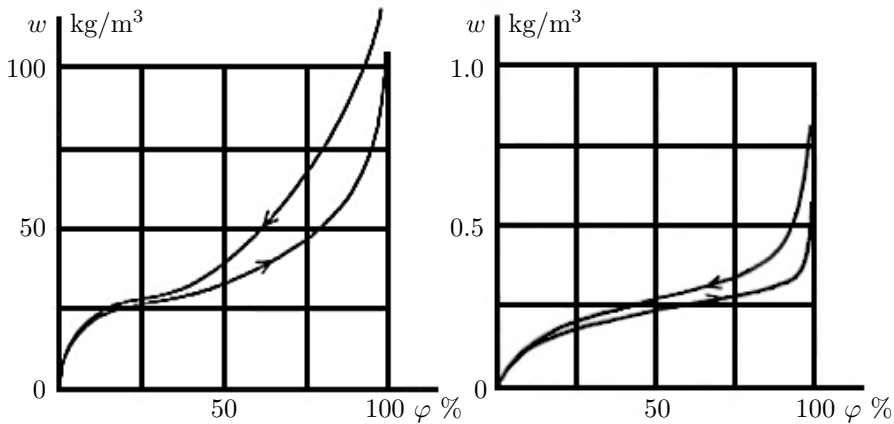
Figure 1.1: The hygroscopic sorption isotherms for concrete of the strength class K25 (on the left) and mineral wool of density 18 kg/m^3 (on the right) at the temperature of 20 ℃. Symbols: w = moisture content [kg/m^3], φ = relative humidity [%] [1, pp. 479, 481]

When a porous material is in contact with free water, water is absorbed into the pores of the material due to a negative pressure formed in the pores. The moisture content that the material reaches with time is referred to as a *capillary*

equilibrium and the material is said to be in the *capillary range*, i.e. the relative humidity range 98–100 % [2, p. 47] [6, p. 21]. A material may reach capillary equilibrium also due to moisture originating from the time of construction or when the material is in contact with another material in the capillary range, such as soil. For a capillary equilibrium, it is typical that the moisture content is significantly higher than in the hygroscopic range [5, p. 6].

1.2 Origins of moisture in building structures

All buildings include moisture both as water vapor in their indoor air and as physically bound water in building materials. This section assesses the moisture sources present in a building and the methods with which moisture migrates inside and into the structures.

1.2.1 Sources of moisture

The common sources of moisture in a building can be divided into internal and external sources. The most typical external moisture sources are the humidity of the outdoor air, rain, and soil. Internal moisture sources include people, animals, and plants living in the building, the use of water, pipe leaks and construction moisture. Some of these sources are shown in figure 1.2.

Outdoor humidity in the Nordic countries varies significantly between seasons, times of the day, and locations. Meteorological data from Finland and Sweden agree reasonably well. The average relative humidity in both countries is 80–90 % during the winter and 60–80 % during the summer [3, p. 47] [1, p. 275]. However, due to the large temperature differences between seasons, absolute humidity in the summer is significantly larger than in the winter, up to fivefold. Typical values are 8–12 g/m^3 in the summer and 1–4 g/m^3 in the winter [3, pp. 47–48]. Absolute humidity variations in a shorter period, such as one week or day, are even larger. Especially during the summer, sunshine has a large effect on outdoor humidity [2, p. 50]. However, these short term variations typically do not affect the behavior of the structures in terms of moisture.

Indoor humidity depends primarily on the humidity of the outdoor air, the moisture produced in the house, and the ventilation of the space. In a large time scale, indoor absolute humidity can be evaluated as

$$\nu_i = \nu_o + \frac{G}{n \cdot V},\tag{1.1}$$

where ν_i is the indoor absolute humidity [g/m^3], ν_o is the outdoor absolute humidity [g/m^3], G is the moisture produced in the house [g/h], n is the air exchange rate [1/h], and V is the volume of the indoor air [m^3] [2, p. 49]. The latter term is referred to as *moisture regain*. Typical values used for the term are 2 g/m^3 in office buildings, 3 g/m^3 in residential buildings, and 4 g/m^3 in moist and badly ventilated buildings [3, p. 48]. In other words, indoor absolute
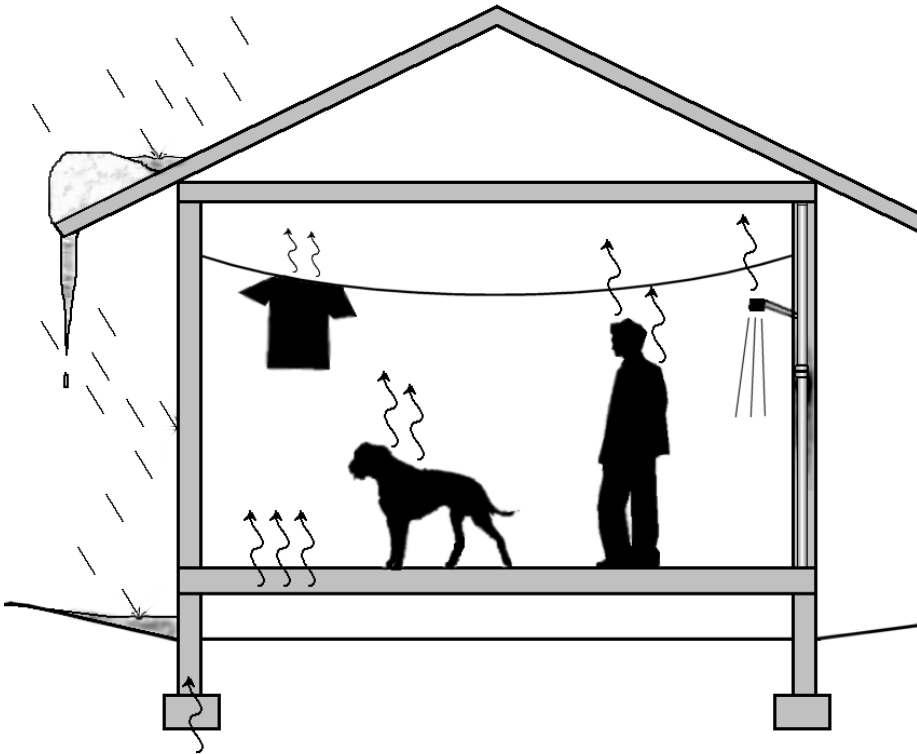
Figure 1.2: Different sources of moisture in building structures include external moisture sources such as rain, and soil, and internal moisture sources such as people, animals, the use of water, pipe leaks and construction moisture.

humidity in residential buildings is higher than outdoor absolute humidity by ca. 3 g/m^3, which leads to the approximate indoor relative humidities of 70–80 % during the summer and 30–40 % during the winter. However, it should be noted that equation 1.1 is a simplification for a long time period. Short term changes in indoor humidity are also significant. Indoor moisture is produced primarily by evaporation from people, animals, and plants, by the use of water, such as washing the dishes or the laundry, bathing, and using the shower, by cooking, and by artificial moisturizing of the air [1, p. 277].

The effect of rain on a building can be divided into two temporarily different periods: rain during the construction of the building and rain after construction. The former is discussed in more detail in the context of construction moisture. The moisture stress caused by the latter is directed towards the exterior surfaces of the envelope of the building. Water may penetrate the envelope through untight joints or cracks and drift a long distance inside the structure [3, p. 41]. This has to be taken into account when evaluating the location of the leak from inside the building. *Vertical rain* does not reach the vertical surfaces of the envelope of the building but when wind is involved, the rain also has a horizontal component. This kind of rain is referred to as *oblique rain* [1, p. 272]. The penetration of rainwater into buildings is significantly affected by the wind conditions present. In addition to the direct effects of rain, rainwater that reaches the ground may damage the lower parts of the envelope of the building. The moisture stress caused by rain is at its largest during the autumn, when the diurnal changes in temperature are at their smallest and drying is minor due to the frequency of rain [2, p. 51]. In the Nordic climate, snow and ice also need to be taken into account. Snow causes significant moisture stress on a small area when heaps of snow melt. Ice, on the other hand, may block the movement of water and help create puddles [2, p. 52].

In the soil, between the surface of the earth and the groundwater, water may appear as *gravitational water*, i.e. water sinking into the groundwater, as capillary moisture, and as water vapor inside the pores of the soil [1, p. 284]. Capillary moisture is a possible moisture stress to structures. The amount of water rising capillarily from the soil depends on the type of soil, its capillarity, the groundwater level and the functionality of the underdrain network [2, p. 52]. Especially the groundwater level may vary significantly with the time of year and with meteorological and climatological variations. The moisture content of soil is typically so large, that the relative humidity of the air inside the pores of soil is considered to be 100 % [3, p. 49].

Leaks in piping and waterproofing is the most common source of moisture damage [1, p. 286]. Pipe leaks may occur in water pipes, sewers or heating pipes that are located either on surfaces or inside structures. In addition, e.g. insufficient waterproofing, damages in the waterproofing, or insufficiently sealed penetrations and drains may cause leaks in bathrooms [6, p. 58–61]. A leak is always a large risk of moisture damage since the moisture stress on the structure is large. Pipes are typically located in the warm parts of the building and the

leaks often occur in locations where there is no waterproofing. In addition, a small, seeping leak may damage structures long before the damage is perceived [2, p. 52]. As a consequence, especially pipe leaks always require fast repairing and drying actions.

Moisture in construction materials may also originate from the time before or during construction. The amount of this kind of moisture that needs to leave a material for it to reach equilibrium with its environment is referred to as *construction moisture*. Construction moisture may originate e.g. from making the material, as with concrete, or from being exposed to rain, soil, or other wet construction materials during storage or construction. [1, p. 280–282]

1.2.2   Moisture migration

Moisture can migrate into and inside building structures in a vapor or liquid state. As vapor, moisture migrates with diffusion and air flow. As water, moisture migrates with capillary suction and gravity.

As already stated in subsection 1.1.2, water absorbs capillarily into a porous material if the material is in contact with liquid water. Capillary migration of moisture is caused by a negative pressure formed in the pores of the material. The smaller the pores are, the larger is the negative pressure and thus the higher the water rises in the material. As a consequence, water may migrate capillarily from one material to another if the pore size of the second material is smaller than that of the first material [5, p. 7]. The maximum height for the capillary rising of water is an equilibrium between capillary forces, gravity and the evaporation of water from the structure. Capillary migration of water is always present, when a structure is in contact with free water or in a capillary contact with soil or another construction material in the capillary range [2, p. 53].

Due to gravity, water migrates downwards on the vertical and inclined surfaces of a building. Inside materials with large capillary suction, *gravital migration of moisture* is negligent. However, moisture may still migrate in structural joints and possible cracks. In contrast, in materials with weak capillary suction, gravital migration is the dominant migration method. [2, p. 54]

Moisture diffuses through building structures from a larger vapor pressure to a smaller one. The amount of moisture migrating with *diffusion* through a structure is determined by the vapor pressure difference and the *vapor permeability* of the structure [1, p. 260]. Usually, the vapor pressure is larger inside a building than it is outside. As a consequence, diffusion usually moves moisture out from inside the building [2, p. 55].

Moisture migration with air flow is known as *moisture convection*. Air flows from a larger air pressure to a smaller one through porous materials or chinks [1, p. 265]. Since air includes water vapor, also moisture is transported. The

warmer the air, the more moisture it can transport. The most hazardous situation occurs when warm air flows through a cold structure, since some of the water vapor in the air may condense inside the structure if the air cools below dew point [5, p. 10].

1.3   Effects of moisture in structures

Excess moisture in buildings has several effects both on the durability of structures and on the indoor air of a building. These effects may occur once the moisture stress towards a structure is larger than the structure can endure, i.e. a moisture damage occurs [2, p. 45]. In this section, the concept of *critical moisture condition* is used as the relative humidity or moisture content where the risk of a moisture damage is significant [7, p. 72].

1.3.1   Damage to structures

Excess moisture is the single greatest factor that affects the durability of buildings [4, p. xi]. The effects that moisture has on construction materials are various and they can be classified in many different ways. In this context, the effects of moisture are classified by cause into physical, chemical and biological damages.

Physical damages

Materials sensitive to moisture may experience changes in their physical dimensions and mechanical properties when moisture is present. Such changes include freezing of a moist porous material, swelling due to moisture absorption and decreased strength. As a consequence, the materials may be damaged.

Moist porous materials may deteriorate when they freeze. The mechanism of frost induced deterioration is a hydraulic pressure originating from the sudden expansion of the water in the pores of the material when it freezes [7, p. 73]. For this to happen, the moisture content of the material has to be near saturation simultaneously as the temperature drops below 0 ℃ [1, p. 287].

Most porous materials tend to swell or shrink when moisture content and relative humidity vary. This may cause problems especially because different materials have different rates of thermal and moisture movement [8, p. 9]. Swelling due to moisture may lead to cracking, skewness and arching of structures. As extreme consequences, parquet may blister, wooden floors may move partition walls and ceiling panels may break. With many materials, most of the moisture induced swelling occurs at the upper hygroscopic range, say above 75 % RH [1, p. 289].

A form of physical damage concerning especially wood products as their moisture content increases is the loss of strength and increased elastic and plastic deformations [1, p. 289].

Chemical damages

Moisture has an important role in many chemical reactions that deteriorate construction materials. Water may dissolve and transport gases and ions between different materials. In addition, water itself participates in some chemical reactions. Typical chemical damages influenced by moisture include corrosion of metals, salt deposition, and deterioration of floor adhesives.

Corrosion of metals, or rusting, is an electrochemical process that requires water or a high RH and oxygen. Polished steel, typically used as an reinforcement in concrete, has a critical moisture condition of ca. 80 % RH both in free air and when embedded in concrete. Impurities may have an even larger influence on corrosion than moisture. For example, the presence of chlorides may lower the critical moisture condition below 80 % RH. [7, p. 75]

Water that penetrates a structure acts as a solvent and a transport media for different salts originating from the ground, the atmosphere, and from inside the building material. When drying out occurs, the salts come out of the solution and accumulate as crystals either on the surface of the structure as visible efflorescence or inside the pores of the material. The process of crystallization often involves swelling, which may lead to erosion, flaking or ultimate deterioration of the building material. In addition, some salts attract moisture, which results in more moisture accumulating in the structure. [8, p. 7]

Deterioration of a polymer based floor adhesive, that is used to attach e.g. a PVC carpet to a concrete surface, is influenced by moisture both chemically and physically. The deteriorative chemical reaction, referred to as alkali attack, requires water and calcium hydroxide originating from the underlying concrete. In addition, moisture causes the carpet to swell, thus causing a strain on the adhesive. If the adhesive is too deteriorated, damage will occur. A suggested critical moisture condition for floor adhesives is ca. 90 % RH. [7, p. 76–77]

Biological damages

Different microbes and insects cause biological damages to especially wooden structures. Typical microbes involved with moist wood include stain fungi, molds and rots. Both microbes and wood-boring insects require favorable moisture conditions for growth. In addition to damaging structures, microbe growth has significant health effects that are assessed in subsection 1.3.2.

Stain fungi grow on and in timber without causing weakening or decay in the structure. Instead, they cause discoloration of wood, typically as blue or gray stains. Thus, the damage is mostly aesthetic. The significance of stain fungi is mostly as an indicator of high moisture levels that could support the growth of more hazardous fungi. The critical moisture condition for the growth and discoloring of stain fungi in timber is the moisture quotient of approximately 30 % (RH near 100 %). [8, pp. 89–90]

The growth of *mold* in structures is mostly superficial and thus the possibly arising problems are typically health-related or merely aesthetic. Mold can usually be seen as green and white blotches on the surface of the structure [8, p. 91]. Mold growth on a material is affected by several factors: the ambient relative humidity and the moisture content of the material, the prevailing temperature, the time of exposure, the type of material and its nutritive status, and the fungal species involved. For example, in pine and spruce sapwood the critical conditions for mold growth have been reported to be an exposure to the relative humidity of more than 80 % and the temperature between 5 and 50 ℃ for several weeks or months. At RH above 95 % and the temperature between 25 and 50 ℃ the required time is only a few days [9].

Rot fungus breaks down wood cells, which weakens the durability and strength of wooden structures [1, p. 291]. The decay process is initiated by the fungal hyphae that grow in the wood. The hyphae liberate digestive chemicals that break down the polymers forming the wood cells. Different rot fungi can be divided into brown rots and white rots by the color of the decayed wood. Another way of grouping rot fungi is a division based on the moisture conditions that they require for growth. The wet rots, such as the cellar fungus (*Coniophora puteana*) require moister conditions than the dry rot fungus (*Serpula lacrymans*) [8, pp. 84–85]. For example, the critical conditions for the initiation of decay caused by *Coniophora puteana* in pine and spruce sapwood at 20 ℃ has been reported to be approximately one year in a RH of 93–94 % (moisture quotient ca. 22–23 %) or one month in a RH near 100 % (moisture quotient ca. 30 %) [10]. Thus, the moisture conditions are significantly higher than those of mold fungi. Dry rot, on the other hand, can cause decay at a moisture quotient as low as 20 % (RH ca. 90 %) [8, pp. 84].

Wood-boring insects may damage wooden structures and thus affect their strength and cause deformations [1, p. 291]. Insect-related damage in timber consists typically of tunnels bored by larvae and exit holes made by adult insects that leave the structure. Some insects require the presence of rot decay that softens the wood and improves its nutritive status. The moisture content of the wood is significant even for species that do not require the timber to be decayed. A typical critical value of the moisture quotient of timber is 30 % (RH near 100 %) [8, p. 92].

1.3.2   Effects of moisture on indoor air

People spend most of the time indoors and thus are continuously surrounded by indoor air. The moisture conditions in a building affect the quality of the indoor air through several mechanisms. Excess moisture on one hand increases emissions from different construction materials and on the other hand creates suitable conditions for the growth of molds and other microbes. Indoor air quality, in turn, has an effect on the health of the people using the building.

Material emissions

Material emissions are chemical impurities that evaporate from construction materials. The chemical impurities include both corpuscular and gaseous, and both organic and inorganic compounds. Especially volatile organic compounds (VOC) are probably connected with health-related and olfactory damage [11, p. 60]. Material emissions can be divided into primary and secondary emissions. Primary emissions are caused by normal evaporation from new building materials and usually diminish rapidly with time. Secondary emissions are emissions caused by an external factor, such as moisture [12, p. 13]. Moist building materials may increase the emissions of formaldehyde, ammonia, and several other VOCs.

Significant material emissions may occur if concrete structures are covered when they are still wet. Different covering materials have different critical moisture conditions varying between the relative humidity of 80 % and 97 %. Especially chemical reactions in the combination of concrete, mortar, adhesive, and the covering material may produce harmful compounds into the indoor air. The adhesive used to attach the covering material may experience decay reactions that may develop emissions hazardous to health. The emissions have been noticed to increase significantly when relative humidity exceeds 90 %. [13, pp. 7–10]

Some fillers, adhesives, and water proofing materials include casein. Casein appears to decay at moist alkaline conditions, in which case ammonia and several other irritating VOCs may be secreted [13, p. 10] [11, p. 63]. Moisture induced decay reactions can often be perceived from a tangy, cellar-like smell. The critical moisture conditions for casein-based fillers vary between the relative humidity of approximately 75 % and 85 % [13, p. 11].

Formaldehyde in indoor air usually originates from urea-formaldehyde resin that is used in e.g. chip boards, some varnishes, and wall-to-wall carpets [11, p.66]. The rate of evaporation depends on relative humidity, the critical moisture condition being between 60 % and 70 % of relative humidity [13, p. 11].

Currently, no international directions of the authorities or standards for maximum values of chemical impurities in indoor air are available. In Finland, the Ministry of Social Affairs and Health has published guideline values for some indoor air impurity concentrations ($\mu g/m^3$) including ammonia and formaldehyde [11]. In addition, the Finnish Society of Indoor Air Quality and Climate (FiSIAQ) has formulated a classification for indoor air that includes maximum values for ammonia, formaldehyde and total volatile organic compounds (TVOC) concentrations [14]. Concentrations exceeding these values may be a sign of moisture damage.

Microbe growth

Moist building materials may support the growth of several microbes that are normally not present in indoor air. The growth of microbes depends mainly on the prevailing moisture and temperature conditions, the time of influence, and the nutritive status of the base material [9]. However, in buildings, moisture is typically the only limiting factor. The presence of some of the microbes, especially mold fungi, have been associated with different health effects.

Indoor and outdoor air always contain several different microbes and their spores. In a normal building, the species present in the indoor air are the same as outdoors. However, in a moisture damaged building the spectrum of microbes is different [15, p. 29]. Some species, referred to as *indicator microbes*, are typically found in moisture damaged buildings. The international workshop *Health Implications of Fungi in Indoor Environments* in 1992 reached a consensus of a list of indicator microbes, shown in table 1.2 [16, p. 535]. The microbes have been grouped by the minimum relative humidity that they need in the material for growth in the typical building environment. *Hydrophilic microbes* may grow only in very moist conditions, while *xerophile microbes* may grow in drier conditions. As a consequence, at an early stage of a moisture damage, the damaged material may be occupied by xerophile microbes. If the damage is prolonged, they are gradually superseded by microbes that require moister conditions until only hydrophilic microbes remain [15, p. 21]. This phenomenon is known as *succession* [17, p. 21].

Table 1.2: Indicator microbes according to Samson et.al. [16, p. 535]

relative humidity	microbe
high (RH > 90 %) hydrophilic microbes	*Aspergillus fumigatus* *Trichoderma* *Exophiala* *Stachybotrys* *Phialophora* *Fusarium* *Ulocladium* yeasts, such as *Rhodotorula* Actinomycetes Gram-negative bacteria
moderately high (85 % < RH < 90 %)	*Aspergillus versicolor*
lower (RH < 85 %) xerophile microbes	*Aspergillus versicolor* *Eurotium* *Wallemia* Penicillia

Microbe growth in buildings may manifest itself in several different ways. Even if the growth is not visible, it may be recognized from a moldy or cellar-like smell or from the symptoms of the people using the building. Microbe-related health effects may be caused by several factors including microbial volatile organic compounds (MVOCs), mycotoxins, allergens, and airborne microbe spores and fungal particles. MVOCs are chemical compounds that are released when some microbes grow. In fact, they are typically the same compounds as the VOCs of chemical origin [18, p. 53]. MVOCs also cause the typical smell of mold. Mycotoxins are toxic compounds produced by some microbes. Among the indicator list of table 1.2, especially *Stachybotrus*, *Fusarium*, and *Aspergillus versicolor* are toxigenic [16, p. 535]. In addition, some microbes include proteins that are allergens, i.e. compounds that have the ability to cause allergy. Microbe spores and fungal particles may both cause symptoms themselves and transport toxins in the indoor air. [17, pp. 32–34]

The critical moisture conditions for the growth of molds and other microbes vary in the related literature. This is partially because each microbe has unique preferences for the growth conditions. On the other hand, also the properties of the material, the time of exposure, and the temperature are significant factors. The growth of xerophile microbes may begin when the relative humidity of a material is 65–70 % [15, p.22]. On the other hand, the probability of microbe growth on building materials seems to increase considerably when relative humidity exceeds 80 % [19, p. 491]. The relative humidity of 75 % seems to be a sensible critical moisture condition for microbe growth in buildings materials. For example, a typical xerophile microbe *Aspergillus versicolor* has been reported to require a relative humidity of approximately 75 % for growth on a nutritious material at 20 ℃ [15, pp. 22].

Health effects

Moisture damages have been associated with several different health effects and symptoms in different studies. Commonly reported mold or moisture related health effects are for example:

1. *Irritative and general symptoms* such as rhinitis, sore throat, hoarseness, cough, phlegm, shortness of breath, eye irritation, eczema, tiredness, headache, nausea, difficulties in concentration, and fever

2. *Infections* such as common cold, otitis, maxillary sinusitis, and bronchitis

3. *Allergic diseases* such as allergy, asthma, and alveolitis

[20, p. 25]. The irritative and general symptoms in the first group do not cause permanent health hazards. The symptoms typically disappear within a few weeks after the end of the exposure. The same holds for repeated infections, but possibly not until after several months. However, a prolonged moisture damage may also lead to allergy or hyperergia. [21, p. 57–61]

The exact moisture induced agents that cause health effects are yet unknown. However, there seems to be a significant association. Bornehag et al. reviewed 61 studies that concern moisture related health effects concluding that there is strong evidence for a true association between dampness and health effects [22]. In addition, Peat et al. reviewed papers accessible via MEDLINE that investigate respiratory health outcomes in relation to housing characteristics or the presence of damp or mold in the home [23]. Approximately half of the reviewed studies showed a significant association between respiratory symptoms, especially cough and wheeze, and the presence of damp and mold.

1.4 Economic significance of moisture damages

In Finland alone, the different expenditures due to moisture damages are measured in billions of euros. The Finnish Society of Indoor Air Quality and Climate (FiSIAQ) assessed in 1998 the gross expenditure of poor indoor air in the Finnish building stock [24]. The report estimates the total costs of refurbishment of mold and moisture damaged buildings to be between 3 200 and 4 000 million euros, and the annual costs of indoor air -related health hazards to be approximately 2 900 million euros.

The composition of the estimated refurbishment costs of mold and moisture damaged buildings is shown in Table 1.3. The cost estimates associated with dwellings are based on two studies by the National Public Health Institute [25][26]. Partanen et al. reported in 1995 that approximately 82 % of the houses built in Finland during the 1950's to 1980's have included moisture damages with the average refurbishment costs of 1 200 euros per house [25]. Koivisto et al. reported in 1996 that in addition approximately 60 % of the apartments in high rise residential buildings built in the same time interval have included moisture damages [26]. The costs related to office and public buildings are calculated assuming that the average refurbishment costs for office buildings are 14 000 euros and for public buildings 42 000 euros per building [24, p. 24].

Table 1.3: Refurbishment costs of mold and moisture damages in Finland according to FiSIAQ [24, p. 32]

Houses	480–580 M€
High rise residential buildings	580–1 300 M€
Office and public buildings	2 200 M€
total	3 200–4 000 M€

The FiSIAQ estimate of the annual costs of poor indoor climate in Finland, 2 900 million euros, is based on evaluating the costs caused by allergies, radon induced cancers, decrease in the efficiency of employees, their absenteeism, hospital infections and passive smoking [24, p. 52]. However, the evaluation does not attempt to distinguish the proportion of moisture and mold related costs. Nguyen et al., in turn, estimated in 1998 that asthma associated with mois-

ture in dwellings costs a total of between 11 and 35 million euros and other moisture-related respiratory diseases cost between 12 and 23 million euros [27].

1.5 Methods of measuring moisture in building structures

As the previous sections demonstrate, controlling the moisture conditions in building structures is extremely important. Currently, the moisture conditions are assessed at different, separate stages of the life cycle of a building. At the time of construction, moisture measurements are often used to determine when a concrete structure is dry enough to be covered with layers of other materials. If they are covered at too early a stage, the covering materials may be damaged and a favorable growth environment for microbes may arise. On the other hand, too long a waiting period increases building costs. Another important field of application for moisture measurements is evaluating the condition of a building. This is typically done when a potential purchaser of an apartment or a house wishes to conduct a condition survey or when moisture damage is suspected to have occurred. However, with the current technology it has so far not been feasible to monitor moisture routinely in order to perceive possible problems before more serious damage occurs.

This section introduces the most common measurement methods and instruments for assessing moisture conditions both in building structures and air. The emphasis is on the methods currently used in Finland and the other Nordic countries, since these countries can be considered to be pioneers in the field of measuring moisture conditions. In addition, special attention is given to measuring moisture conditions in concrete due to its wide use and the fact that it is one of the most difficult materials for moisture measurements.

1.5.1 Surface moisture meters

Surface moisture meters are practically the most commonly used tools for measuring moisture conditions in building structures [28, p. 81]. The meters function by measuring the electrical properties of the material under investigation. The measurement procedure is fast and non-destructive, but the meters have limitations that need to be taken into account. Several manufacturers produce surface moisture meters. Some of the most common ones are shown in Figure 1.3.

Operating principle

Surface moisture meters function by measuring electrical properties, such as conductivity or dielectric constant from the surface of a material. The meters are usually equipped with conversion tables for different material groups, such as concrete, brick, wood, etc., in order to present the measurement results as
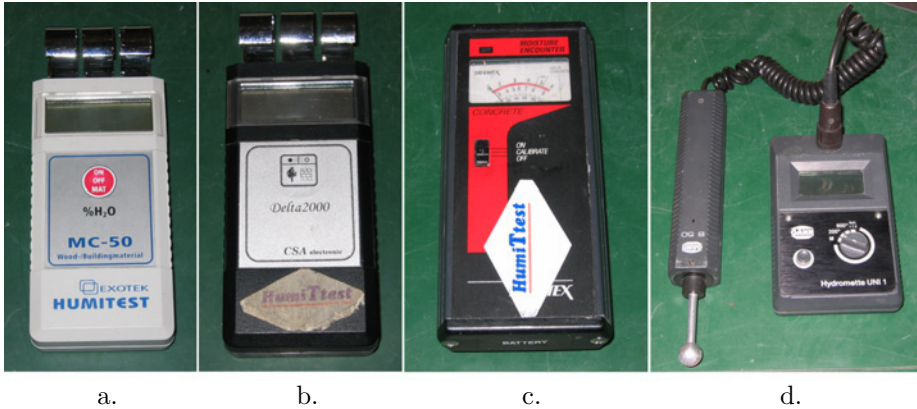
Figure 1.3: Some common surface moisture meters, a. Humitest MC-50 (Exotek Ab, Sweden), b. Delta 2000 (CSA Electronic GmbH, Germany), c. Moisture Encounter (Tramex Ltd. Ireland), d. Hydromette UNI 1 with B 50 active electrode (Gann GmbH, Germany)

calculatory moisture quotient [2, pp. 29–30].

The devices in figure 1.3 a. and b., Humitest MC-50 (Exotek Ab, Sweden) and Delta 2000 (CSA Electronic GmbH, Germany) are traditional surface moisture meters that function by measuring the dielectric constant of a material. The devices feature metal electrodes that are connected to a high-frequency voltage generator and a measuring circuit. During measuring the moisture content of an object, the electrodes are pressed against the object. The capacitance between the electrodes is then proportional to the moisture content of the material. [29]

The surface moisture meter of figure 1.3 c. is an old version of Moisture encounter (Tramex Ltd. Ireland). According to the data sheet of the current version of the device, it functions by measuring electrical resistance at a frequency of 5–25 kHz [30].

Figure 1.4 shows a perspective view (a.) and the measurement circuit (b.) of a one-electrode surface moisture meter, such as the one in Figure 1.3 d., Hydromette UNI 1 and the B 50 active electrode (Gann GmbH, Germany). The one-electrode construction aims to detect moisture at greater depths than conventional surface moisture meters. The device measures capacitance with a measurement circuit (1) that is connected to a high frequency voltage source (2). An active electrode (3) is connected with one terminal of the measuring circuit. The cooperating electrode for the active electrode is constituted by ground. As a consequence, the device actually measures the leakage current through the object under investigation and the operator. When the electrode is in contact with a material, the capacitance C_M represents the measured capacitance, C_E the capacitance between ground and the operator of the device, and C_G the capacitance between ground and the object under investigation. The capacitances C_E and C_G are assumed to be substantially larger than C_M. C_V

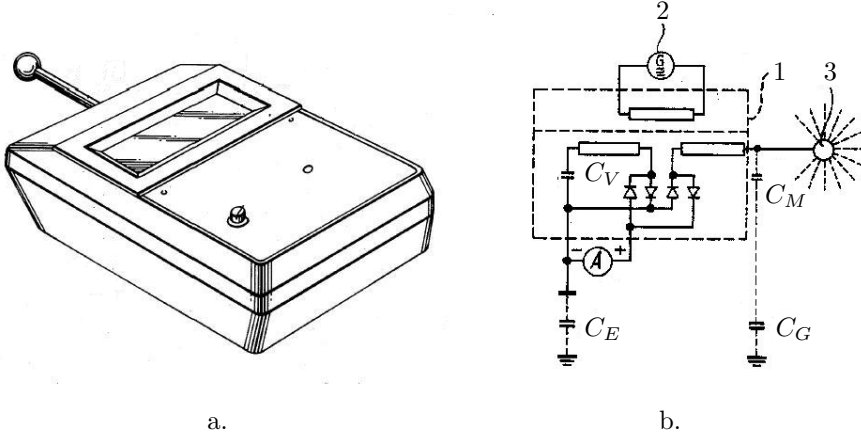is a reference capacitance that corresponds to the capacitance of air. [29]

Figure 1.4: A perspective view (a.) and measurement circuit (b.) of an instrument for measuring the moisture content of dielectric objects. The device includes a measurement circuit (1), a high frequency voltage source (2), and an active electrode (3). The capacitance C_M represents the measured capacitance, C_E the capacitance between ground and the operator of the device, C_G the capacitance between ground and the object under investigation, and C_V is a reference capacitance. [29]

Properties

The most significant advantages of surface moisture meters are their ease of use, non-destructiveness, and fastness of the measurement procedure. On the other hand, from the simple non-destructive measurement procedure follows that the measurement field typically reaches a depth of only a few centimeters. More importantly, the depth, in which moisture possibly exists, cannot be derived from the measurement results. For example, in a bathroom wall that is waterproofed and covered with tiles, a surface moisture meter can not be used to find out on which side of the waterproofing the perceived moisture is located [31, p. 7].

Surface moisture meters usually give only suggestive information about the absolute moisture content and distribution inside structures, thus the acquired readings should be compared with readings from a dry reference location in the same structure [2, p. 30]. This is because the moisture quotient readings given by different meters in the same circumstances may differ significantly. Furthermore, the electrical properties of building materials are not constant. For example, different types of concrete and different mixing ratios of water, cement and additives lead to different conductivities. In addition, metal objects, e.g. reinforcement irons and electric lines near the surface may affect the acquired reading. [31, p. 6–7]

A significant factor affecting the reliability of surface moisture meters is the

contact between the electrodes and the material under investigation [31, p. 7]. With a rough surface, the contact is weaker than with a smooth one. In addition, the person performing the measurement may unintentionally or intentionally affect the reading by applying a different force when pressing the device to the structure in different locations [2, p. 30].

Usage

Surface moisture meters are a useful tool in moisture surveys if their properties and limitations are acknowledged. Instead of looking at the absolute readings provided by the meters, they are much better suited for comparative measurements, e.g. for searching for a possible damp spot in a structure or for determining its size [2, p. 30]. Surface moisture measurements should be performed as systematically as possible to form a map of the moisture distribution in the structure. The map can then be used in evaluating the reason and comprehensiveness of the damage in terms of building physics. Conclusions reached with surface moisture meters should always be verified with a destructive measurement, such as a relative humidity measurement [5, p. 24].

1.5.2   Calcium carbide method

The calcium carbide method is a fast but destructive method for measuring the moisture quotient of materials. The method is mostly used outside the Nordic countries.

Operating principle

When calcium carbide gets in contact with water, acetylene gas is released [32]. Cameron Hugh patented in 1930 a "Process and apparatus for detecting and determining the quantity of percentage of moisture in a substance" based on this reaction [33]. The original patent was mostly intended for measuring moisture in flour, however the reaction can also be used with respect to masonry with the equipment shown in figure 1.5. The method requires a sample to be taken from the material of interest. The sample is weighed and then placed in a gas pressure vessel (1) with a calcium carbide ampoule (2) and some steel balls (3). When the vessel is shaken, the steel balls break the ampoule. As a consequence, the calcium carbide reacts with the water in the sample. A gauge (4) at the top of the vessel can be used to measure the resulting gas pressure. The quantity of the generated gas is directly proportional to the moisture content of the sample. The moisture quotient corresponding to the measured pressure can be determined from material-dependent conversion tables. [31, p. 7] [8, pp. 267–269]

Figure 1.5: Calcium carbide measurement equipment: (1) gas pressure vessel, (2) calcium carbide ampoule, (3) steel balls, (4) gauge

Properties

The calcium carbide method is a relatively fast technique for measuring moisture content. However, the problem with the method is the indirect measurement of moisture quotient through pressure. Not all concrete types and materials have conversion tables. Additionally, in the Nordic countries, most threshold values for the coatability of concrete are defined as relative humidity. A further conversion to RH may lead to misinterpretations. Another disadvantage is that the calcium carbide method requires the structure to be damaged in order to get a sample. [31, p. 7]

Usage

The calcium carbide method has been used for determining the correct time to coat concrete, especially in Central-Europe where the critical moisture conditions are usually expressed in moisture content. In Finland, where the criteria are expressed in relative humidity, the calcium carbide method is recommended to be used only in special applications, such as bridge building [31, p. 7].

1.5.3   Gravimetric method

The methods presented above can be used to measure the moisture content or moisture quotient of a material indirectly. However, moisture quotient can also be measured directly by using the gravimetric method, also known as the oven-drying method. The method is more accurate but significantly slower than the indirect methods.

Operating principle

The procedure of the gravimetric method is as follows [2, p. 29] [31, p. 8]

1. A sample of approximately 0,1–100 g, depending on the material and the accuracy of the scales used, is taken from the structure at the depth of interest. The sample is kept in a tight container or bag until the measurement, in order to prevent evaporation.

2. The sample is weighed before drying. The result is the wet mass, m_{wet}.

3. The sample is dried in an oven until all water has evaporated, i.e. the mass of the sample has ceased to decrease. The typically used drying temperature is 105 ℃. However, with hydrous materials, such as gypsum, the appropriate temperature is only 40 ℃.

4. The sample is reweighed. The result is the dry mass, m_{dry}.

5. The moisture quotient, W, of the material is calculated as

$$W = \frac{m_{\text{wet}} - m_{\text{dry}}}{m_{\text{dry}}} \times 100\%. \qquad (1.2)$$

Properties

The gravimetric method is the most accurate method for measuring the moisture content of a material [8, p. 263]. The most significant measurement errors result from the process of taking the sample, keeping it before weighing, and the weighing itself [31, p. 8]. The most significant disadvantage of the method is its slow measurement procedure compared with the indirect methods described above. The drying process typically lasts at least one day, and with e.g. mineral wool even longer [2, p. 29]. In addition, also the gravimetric method is destructive, i.e. the structure under investigation is damaged. Finally, the acquired data is the moisture quotient of the material, not the preferred relative humidity.

Usage

The gravimetric method can be used together with hygroscopic sorption isotherms to evaluate whether the material is in the capillary range. In addition, with the isotherms and the relative humidity of the surrounding air, the method can be used to determine whether the structure is drying or wetting. The drying or wetting can also be estimated by measuring the moisture content at different surfaces and depths. [2, p. 29]

Since the gravimetric method is relatively time-consuming, it is best suited for special investigations, where the requirements for accuracy are strict.

1.5.4   Relative humidity measurements

In the Nordic countries there is a strong agreement that relative humidity and temperature are the most important quantities in assessing the moisture conditions both in air and inside materials. However, measuring relative humidity, especially inside construction materials, is a demanding task. Because of these reasons, measuring relative humidity is given special attention.

Operating principle

Relative humidity can be measured with several different methods that are based on different physical phenomena. The emphasis in this section is on the electric methods since they are currently used noticeably more often than more traditional methods. However, also other methods are assessed briefly. Figure 1.6 shows some widely used relative humidity measurement devices.

Figure 1.6: Some relative humidity measurement devices, a. HMI41 indicator with HMP44 humidity and temperature probe (Vaisala Ltd., Finland), b. testo 635 thermohygrometer (testo AG, Germany), c. testo 605-H1 mini thermohygrometer (testo AG, Germany), d. testo 175-H1, humidity/temperature logger (testo AG, Germany)

The hair hygrometer and the wet and dry bulb hygrometer are devices for measuring relative humidity non-electrically. The former type is based on measuring the changes in the length of e.g. a hair or a nylon strip with changes in relative humidity. The changes in length are a result of the absorption of moisture in hygroscopic materials. Another more direct method, the wet and dry bulb method, is based on the heat loss caused by evaporation of water. In the method known as psychrometry, two thermometers are used, one of them with a dry bulb and the other with a bulb that is covered with a wet cotton wick. The temperature difference between the two thermometers is proportional to the rate of evaporation from the wet cloth which in turn is proportional to the relative humidity of the air. [34, p. 197]

As stated in section 1.1.1, the concept of dew point can also be used to assess relative humidity. That is, relative humidity can be determined from the temperature, at which moisture begins to condense on a surface. The structure of a typical dew point sensor is shown in figure 1.7. The sensor (1) includes a mirror (2) with cooling means (3) and a temperature sensing device (4). A light source (5) is arranged to direct a beam of light onto the surface of the mirror (2) and an electrical photosensitive device (6) is arranged to receive the reflected light. In the operation of the device, the mirror is cooled gradually below the ambient temperature, T, with the cooling means until a predetermined change in the level of light detected by the photosensitive device is detected, i.e. dew point is reached. The temperature of the mirror is monitored continuously in order to record the temperature drop, ΔT, where condensation occurs. [34, pp. 200–201] [35]

Capacitive sensors are the most commonly used relative humidity sensor type in building structure measurements. The sensors consist of two electrodes and
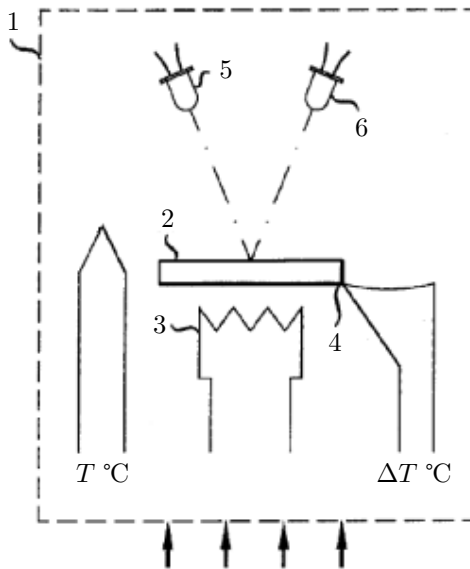
Figure 1.7: The structure of a typical dew point sensor (1) including a mirror (2) with cooling means (3) and a temperature sensing device (4), a light source (5), and a photosensitive device (6). T is the ambient temperature and ΔT is the required temperature drop. [35]

a humidity sensitive polymer placed between them. The polymer absorbs and emits water molecules from its surroundings, thus resulting in a change of capacitance. The capacitance values are converted to RH values and shown to the user with the display unit. The devices in figure 1.6 all use capacitive sensors. [31, p. 8–9]

Properties

Relative humidity measurements are considered an accurate and reliable method of measuring moisture in building structures. The accuracy of capacitive relative humidity sensors is typically ±2–3 %, which in the case of normal concrete corresponds to about ±0.2–0.3 % in moisture quotient [7, p. 115]. With regular calibration, the accuracy may be even better. However, measuring relative humidity requires expertise, since even slight variations in temperature may affect the results significantly.

Measuring relative humidity inside a material is a destructive process. As a consequence, the results apply to the exact location of measurement, but the structure is damaged. In addition, the measurement procedure may take a significant amount of time. For example, measuring the relative humidity of concrete may take several days, which is discussed below.

Usage

Relative humidity measurement devices are used in a wide range of applications in the construction environment, especially in the Nordic countries. The devices can be used e.g. to measure ambient conditions, to monitor the drying of concrete, or to verify the results of surface moisture measurements in case of a suspected moisture damage.

By definition, relative humidity sensors measure the amount of moisture in air. However, they can also be used for measuring the relative humidity of different construction materials, i.e. the relative humidity of the air inside their pores. This is typically done by creating an artificial pore either in the structure or in a test tube, and then measuring the relative humidity within. Making a hole into a structure always has an effect on its functioning in terms of building physics. For example, in a light structure, the flow of air through the hole and the conduction of heat within the probe may affect the measurement significantly [2, p. 27]. On the other hand, in measuring e.g. concrete floors, it is crucial that the artificial pores are left to steady for long enough after drilling the hole and before the measurement is made.

Measuring the relative humidity in concrete is probably the most important application of relative humidity sensors. The measurement results give information about the moisture distribution in the structure. The information can be used to evaluate the amount of excess moisture in the structure and whether the structure may be coated without a risk of moisture damage. The mea-

surements can also be used to evaluate the causes and comprehensiveness of occurred moisture damages. Measuring the relative humidity of concrete is an especially demanding task and requires expertise. [31, pp. 11–18]

Relative humidity measurements inside a structure are usually made from a drilled hole. The phases of the drill-hole measurement in concrete are illustrated in figure 1.8. The following procedure by Humittest Ltd. can be considered to be best practice in Finland [36] [37]:

1. A hole with a diameter of 16 mm is drilled into the structure with a percussion drilling machine. The hole is vacuumed clean of the drill dust and a measurement tube that reaches the bottom of the hole is assembled. The interface between the tube and concrete is sealed, the measurement tube is vacuumed clean and the end of the tube is sealed. If necessary, the measurement tube is protected with a covering. The measurement hole is then left to steady for at least 3 days.
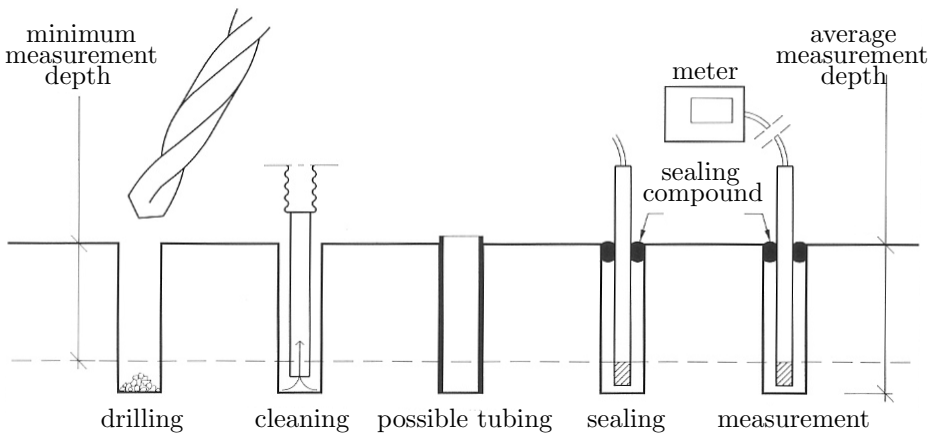
Figure 1.8: The phases of the relative humidity measurement procedure include drilling a hole, cleaning it, possibly assembling a measurement tube, sealing the hole, a waiting period of 3 to 7 days and the measurement [37].

2. A humidity and temperature probe is assembled into the measurement tube by opening the sealing at the end of the tube and resealing it around the wire of the probe. The probe is let steady in the measurement tube for at least one hour.

3. The relative humidity and temperature are read with an indicator and the results are documented together with the ID of the probe. The results are corrected with sensor-specific calibration factors.

Taking samples is a faster and more reliable method for measuring the relative

humidity of a concrete structure. Humittest Ltd.'s procedure for measuring relative humidity from a sample is the following [38]:

1. Concrete crumbs are chiseled into a test tube from a concrete surface that is 5 mm higher than the measurement depth. The sampling surface can be acquired e.g. by drilling holes in a circle and removing the concrete remaining between them. A temperature and humidity probe is sealed into the test tube so that the interface between the wire of the probe and the mouth of the test tube is tight. The test tubes and probes are transported to and from the measurement site in a case that is insulated to the constant temperature conditions of +20 ℃. The tubes are let steady in a constant temperature for at least six hours before taking the humidity readings.

2. The relative humidity and temperature are read with an indicator and the results are documented together with the probe ID. The results are corrected with the unique calibration factors.

1.6 Research objectives

The research presented in this thesis was performed at the Applied Electronics Laboratory at Helsinki University of Technology during the years 2000–2004. The aim of the research was to develop new non-destructive methods for measuring moisture conditions inside building structures. The research was performed in tight collaboration with the Finnish construction industry. As a consequence, the emphasis was on the practical applicability of the methods.

This thesis aims to present the new measurement methods and how the construction industry and the occupants could benefit from them. The specific objectives of the thesis are as follows:

1. To define the current need for new methods of measuring moisture in building structures and to select the specific problems to approach.

2. To elucidate the physical principles of the novel measurement methods and to design the practical instrumentation.

3. To verify the functionality of the methods and the instrumentation in laboratory and field measurements.

4. To generate guidelines of applying the methods in the building industry.

1.7 Problem definition

Excess moisture in building structures is evidently a problem both in respect to the health of the occupants and financially. Currently, there are several work-intensive methods for verifying suspected moisture problems and for monitoring

the drying of concrete structures. However, it has not been previously feasible to monitor moisture routinely, on a regular basis.

There seems to be a need for a new measurement system for routine monitoring of moisture in residential, commercial, and public buildings in order to perceive possible problems before more serious damage occurs. The current measurement methods and systems are not suitable for the application since they are either too unreliable and easily affected, or too work-intensive for routine use. Primary application areas of the system would be the same locations as with conventional measurement methods: the drying and long term moisture variations of concrete structures and especially structures of the bathroom area.

In order to be used in a routine moisture monitoring system, the measurement methods need to be non-destructive like surface moisture meters, since fixing the structure after repeated destructive measurements is not practical. However, the system should still be able to measure the moisture conditions at exact and predefined locations and depths, and to be able to present the results as relative humidity readings. The relative humidity readings may be adequate at applications where the temperature remains relatively constant, however generally the system should also be able to measure temperature, for the relative humidity readings to be reliable. In addition, it would be beneficial to be able to measure the ambient relative humidity and temperature in addition to the structural readings to be able to analyze the conditions more comprehensively.

The measurement methods and the instrumentation must be reliable and the results acquired should be consistent and independent of the person performing the measurements. This is not always the case with the methods currently used since they may be influenced by the operator due to ignorance or insincerity. A temptation to affect the moisture measurement results is often present. A tight construction schedule may sometimes tempt to interpret the moisture content to be lower than it is. This can be done in several different ways depending on the method used. It is important that the developed system could not be affected to get a more suitable measurement result.

To be widely adopted, the measurement system should be inexpensive. The costs of the system should be negligible in comparison with the value of the building it is applied to, and smaller than the renovation costs of a possible moisture damage. As stated in section 1.4, the average refurbishment costs of a moisture damage are of the magnitude of a thousand euros. As a consequence, the cost of the system per house or apartment should be of the magnitude of a hundred euros.

The developed measurement system should also be easy and fast to assemble and use, and it should be fit for the current construction professionals. In order for the system to be attractive, the duration of the assembly procedure should be negligent compared with the construction schedule. Thus, the assembly time should be less than one workday, preferably of the magnitude of one hour. Instead, the measurement procedure should be significantly faster than a typical

condition survey in order to be attractive. Thus, the required time should be less than half an hour, preferably of the magnitude of five minutes. The people that should be able to use the system would be, for example, the personnel of a building contractor for assembling the sensors and for controlling moisture during the time of construction, and the personnel of a maintenance company for long-term monitoring. In addition, companies that specialize in moisture measurements and condition surveys should be able to use the system.

As a secondary need, it would be advantageous if the measurement system could also function as a systematic documenting tool for moisture conditions. Practically this would mean that the measurement results could be stored within the system and, if necessary, uploaded to a computer.

1.8 Research contribution

This thesis presents several new methods for measuring moisture in building structures and the instrumentation developed for implementing them. The primary objective of the entire system is to be able to monitor moisture in buildings routinely throughout their life span. This has not been previously feasible with the prevailing equipment.

The new methods presented in this thesis are based on measuring the effects that environmental conditions have on the electrical properties of LC resonant circuit sensors. The low-cost passive sensors can be assembled inside or on the surface of structures at the time of construction or renovation. A separate reading device can then be used to measure the moisture and temperature conditions at the exact locations of the sensors, non-destructively, from outside the structure. As a consequence, the new system combines the advantages of the methods used currently, being simultaneously non-destructive, fast, easy to use, and affordable, yet reliable at an exactly defined depth.

The presented research has been carried out at the Applied Electronics Laboratory at Helsinki University of Technology. The author of this thesis has been involved with the moisture measurement research since the beginning of the research process. The theme for his research has been the moisture measurement concept and system as a whole. He has participated in surveying the existing moisture measurement field and in determining the need for new measurement methods. He has elucidated the physical principles the new measurement methods are based on and led the development of the instrumentation that implements the method practically. In addition, the author has designed and conducted experiments to verify the functionality of the system both in the laboratory environment and in the building industry. Based on the acquired results, the author has participated in generating guidelines on how the developed methods could be utilized by the building industry.

Several people have contributed to the research. The following scientific contribution is acknowledged:

Outi Valta, M.Sc., studied the application of the developed measurement concept in the measurement of relative humidity inside the pores of building structures. Her master's thesis discusses the development of a humidity sensor that is able to distinguish whether a certain relative humidity level has been exceeded [39]. As a practical realization of the research, a threshold relative humidity sensor was designed and constructed.

Tuomo Reiniaho, M.Sc., studied the technology of wireless sensors to be assembled within building structures. His master's thesis discusses especially wireless measurement of temperature and inductive transfer of energy to the sensor [40]. As a practical realization, the research produced a sensor capable of measuring both moisture conditions and temperature and of storing measurement results in the sensor.

Juho Partanen, M.Sc., studied the technology of reading sensors wirelessly. His master's thesis discusses the electronics of a reading device that couples inductively with the sensors [41]. As a practical realization, the research produced a prototype of an enhanced reading device capable of interfacing all the developed sensor types.

Being interdisciplinary, the research has contributed to several different fields of science. First of all, the methods and instrumentation are applications of different fields of electrical engineering, especially applied electronics, radio science, metrology, and embedded systems. As a consequence, some of the research results have been presented in a research report published in the Applied Electronics Laboratory publication series [42] and at the XXVIII URSI Convention on Radio Science [43]. In addition, the research relates to different fields of civil engineering, especially building physics and HVAC (Heating, Ventilation, and Air-Conditioning). Thus, research results have also been presented at the National Indoor Air Seminar [44] [45] and internationally at the 7th International Healthy Buildings Conference [46] and the 2nd International Symposium on Integrated Lifetime Engineering of Buildings and Civil Infrastructures [47].

2 Measurement method

The approach for solving the problem stated in the previous chapter is the measurement system of figure 2.1 that consists of a low-cost sensor, a separate device for indicating the measurement results, referred to as a reading device, and a wireless interface between them. There are several advantages that are gained from this kind of an approach. The sensors can be placed to the exact location of interest and then read whenever needed. As a result, the measurement procedure is fast and non-destructive as with surface moisture meters today. In addition to this, the measurements can be made accurately, and at the depth of interest, as it typically is with relative humidity measurement methods. Since the sensor itself is inside the structure, the person performing the measurement can not affect the measurement results.
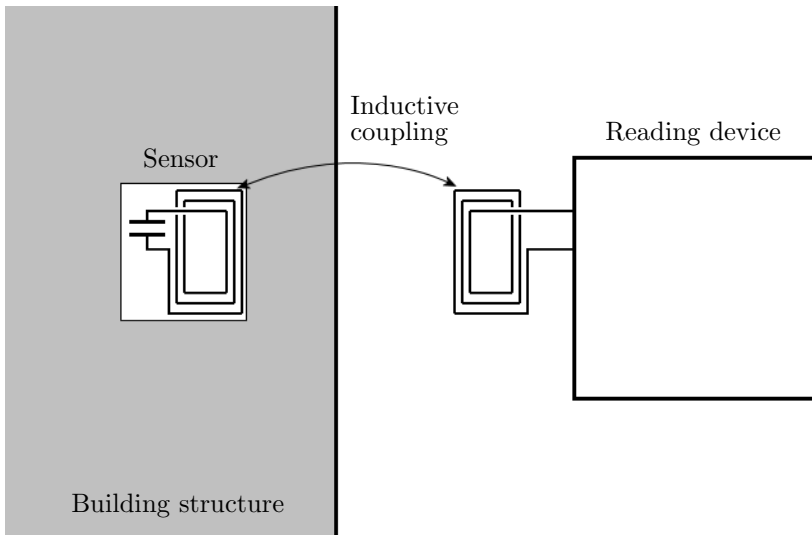

Figure 2.1: A block diagram of the measurement system including a sensor inside a building structure, a reading device and a wireless interface between them. The wireless interface has been implemented with inductive coupling between the antenna coils of the sensor circuit and the reading device.

The chosen approach can be realized either with an active or a passive sensor structure. An active sensor could be designed to perform the measurements at predetermined intervals independently of the reading interval. However, the sensor would require a battery of some sort to be included in the sensor. The life span of most batteries seems to be near 10 years at their best, while the desired operating time of the sensors is between 30 and 50 years, independent of the measurement density. With a passive structure, the measurements would

be made at the time of reading the sensors, but the life span of a sensor could be significantly longer since all necessary energy could be supplied by the reading device. As a consequence, the life span of the sensor would be dependent only on the sensor's mechanical and chemical endurance. Based on this evaluation, and cost issues, the sensor was chosen to be passive.

The passive structure chosen for the sensors is a resonant circuit that consists of a planar inductor on a printed circuit board and a surface mount capacitor in parallel with it. The sensors are laminated with a dielectric layer that, in the case of measuring moisture conditions, enables the coil to couple capacitively with a material the conductivity of which changes as a function of relative humidity or moisture content. The changes in the moisture and temperature conditions can then be sensed remotely from the electrical properties of the sensor circuit. In the research project, the sensor was chosen to be manufactured with printed circuit board technology due to the ease of manufacture, the low start-up costs and the mechanical and thermal endurance of typical circuit board materials. Other approaches that were considered include film-based coils often used in RFID transponders, and printing the sensor structure on paper with a conductive ink.

Since the sensors are passive, the energy needed for the measurement must be supplied by the reading device. The wireless interface between the reading device and the sensors has been implemented with inductive coupling since the technology involved is well known from electronic article surveillance and other RFID applications. Other possible approaches include capacitive coupling and radiating electromagnetic fields. In addition to supplying energy, the reading device also takes care of all the necessary processing of the measurement signals and indicating the measurement results to the user. The device can also be programmed to function as a more comprehensive documenting tool.

This chapter concentrates on describing the mathematical basis and the electrical phenomena involved in the developed measurement method, and on deriving generic models of the system. A more detailed description of the implemented instrumentation is presented in the following chapters.

2.1   Sensor principle

The sensors used in the measurement system are resonant circuits, the electrical properties of which are affected by the moisture content, the relative humidity, or the temperature of the environment near the sensor. In measuring all these quantities, the sensor can be described as an LC resonant circuit that is capacitively coupled with a lossy material. The environmental quantities can be read inductively from outside the structure of interest from changes in the resonant frequency and the quality factor of the sensor circuit.

This section describes the electrical phenomena that the sensor mechanism is based on and derives the basic equivalent circuit of a sensor inside a construction

structure.

2.1.1   Sensor resonant circuit

The sensor circuit is basically a parallel resonant circuit that consists of a planar inductor and a discrete capacitor connected in parallel with it. A generic equivalent circuit of the sensor structure is composed below.

Parallel resonant circuit

A circuit, with at least one capacitor and one inductor, is in resonance, when the imaginary component of its impedance is equal to zero, i.e. its impedance is purely resistive [48, p. 276]. A parallel resonant circuit, shown in figure 2.2, consists of a resistive component, R, an inductive component, L, and a capacitive component, C. The input impedance of such a circuit is

$$Z_{\text{in}} = \left(\frac{1}{R} + \frac{1}{j\omega L} + j\omega C \right)^{-1},$$ (2.1)

where j is the imaginary unit and ω is the angular frequency defined as $\omega = 2\pi f$, where f is the frequency [49, p. 303]. The impedance of a parallel resonant circuit with $R = 1$ kΩ, $C = 1$ nF, and $L = 1$ µH is sketched as a function of frequency in figure 2.3.
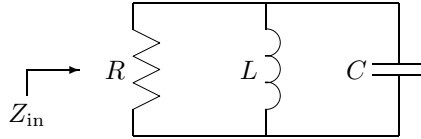
Figure 2.2: The equivalent circuit of a parallel resonant circuit includes a resistive component, R, an inductive component, L, and a capacitive component, C. Z_{in} represents the input impedance of the circuit.

The imaginary component of the impedance in equation 2.1 is equal to zero and the absolute value of the impedance reaches its maximum value, R, when $\omega^2 LC = 1$. Thus the *resonant frequency* of the circuit is given by

$$f_{\text{res}} = \frac{1}{2\pi\sqrt{LC}}.$$ (2.2)

In figure 2.3, the imaginary component of the impedance is equal to zero and the absolute value of the impedance is equal to $R = 1$ kΩ at the resonant frequency of 5.03 MHz.
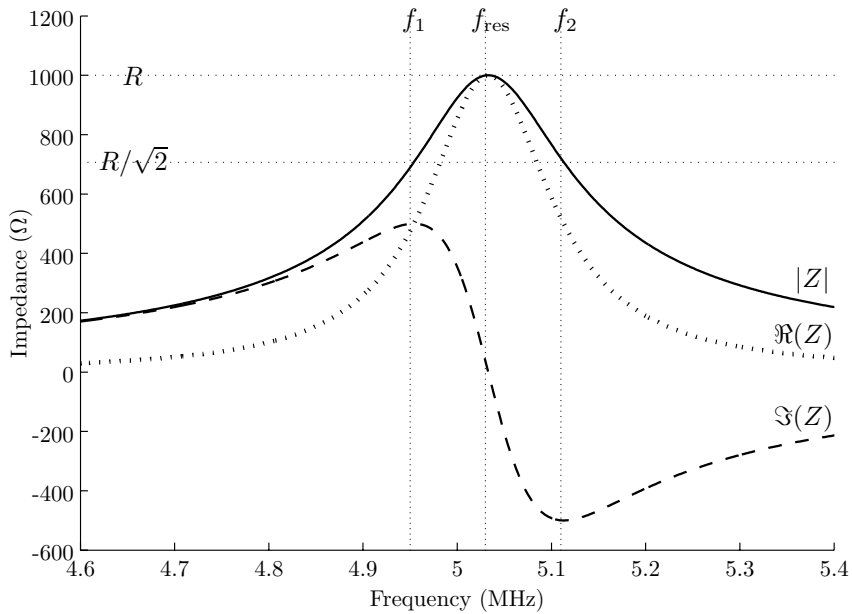
Figure 2.3: The impedance of a parallel resonant circuit ($R = 1$ kΩ, $C = 1$ nF, $L = 1$ μH) as a function of frequency. The dotted trace represents the real component $\Re(Z)$, the slashed trace represents the imaginary component $\Im(Z)$ and the solid trace represents the absolute value of the impedance $|Z|$. The horizontal lines highlight the absolute value of the impedance at resonance R and the impedance corresponding to the half power bandwidth $R/\sqrt{2}$. The vertical lines highlight the resonant frequency f_{res} and the corner frequencies of the bandwidth f_1 and f_2.

The *quality factor*, Q, of a resonant circuit is defined as

$$Q = \omega \frac{\text{(average energy stored)}}{\text{(energy loss/second)}}$$
$$= \omega \frac{W_m + W_e}{P_l}, \tag{2.3}$$

where W_m is the average magnetic energy stored in the inductor L, W_e the average electric energy stored in the capacitor C, and P_l is the power dissipated by the resistor R. Thus Q is a measure of the loss of a resonant circuit. In the case of a parallel resonant circuit

$$W_e = \frac{1}{4}|U|^2 C, \tag{2.4}$$

$$W_m = \frac{1}{4}|U|^2 \frac{1}{\omega^2 L} \tag{2.5}$$

and

$$P_l = \frac{1}{2}\frac{|U|^2}{R}, \tag{2.6}$$

where U is the voltage across the resonant circuit. By substituting equations 2.4–2.6 into equation 2.3, the quality factor at resonance yields

$$Q = \omega_{\text{res}} RC = R\sqrt{\frac{C}{L}}. \tag{2.7}$$

In figure 2.3, the quality factor of the circuit is approximately 31.6. [49, pp. 303–305]

The *bandwidth*, B, of a parallel resonant circuit is defined as the range of frequencies in which the average power delivered to the resistor R is equal to or greater than one half its maximum value. In other words, the absolute value of the circuit's impedance is equal to or greater than the impedance maximum occurring at the resonant frequency divided by $\sqrt{2}$. This condition is reached between the corner frequencies where

$$\sqrt{\frac{1}{R^2} + \left(\omega C - \frac{1}{\omega L}\right)^2} = \frac{\sqrt{2}}{R}. \tag{2.8}$$

The two solutions that yield positive values for the corner frequencies are

$$\omega_{1,2} = \pm\frac{1}{2RC} + \sqrt{\left(\frac{1}{2RC}\right)^2 + \frac{1}{LC}}. \tag{2.9}$$

Thus, the bandwidth is

$$B = f_2 - f_1 = \frac{1}{2\pi RC}. \tag{2.10}$$

As can be seen from figure 2.3, at the corner frequencies, the real component of the impedance is one half its maximum value and equal to the absolute value of the imaginary component. The bandwidth in the figure is 159 kHz. [50, p. 556]

The quality factor of a resonant circuit can also be described quantitatively as the ratio of the resonant frequency and the bandwidth

$$Q = \frac{f_{\text{res}}}{B}. \tag{2.11}$$

Thus, in the frequency domain, Q represents the relative sharpness of the resonant peak. [50, p. 557]

Planar inductor

The planar inductor used in the sensor circuit is not an ideal inductance but it also includes capacitive and resistive components. Timo Varpula, D.Sc., of VTT Information Technology has developed a numerical simulation program for the design of planar inductors on lossy substrates [51]. The equivalent circuit of the inductor used by the program is shown in figure 2.4. The equivalent circuit includes a series inductance L, and a series resistance R_s that are obtained by computing the current density distribution in the conductor. In addition, the equivalent circuit includes a parallel capacitance C_p, and a parallel resistance R_p that are obtained by deriving integral equations for equivalent surface charges that represent the conductor in the electric problem. The equivalent circuit can be used to estimate the overall impedance of the inductor at a given frequency. The circuit of figure 2.4 is used as the equivalent circuit for the planar inductors of the sensors presented in this thesis.
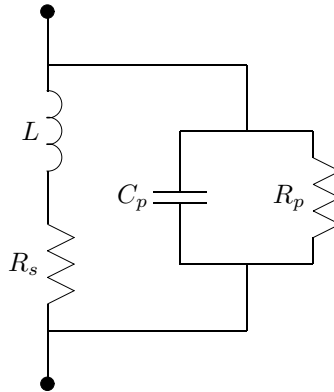
Figure 2.4: The equivalent circuit of a planar inductor on a lossy substrate [51]. L represents the inductance, R_s represents the series resistance, C_p represents the parallel capacitance, and R_p represents the parallel resistance of the coil.

Surface mount capacitor

A planar inductor of figure 2.4 is as such a resonant circuit. However, in the sensor circuit, a discrete surface mount capacitor is used in parallel with the inductor to set the resonance frequency of the circuit to a suitable range. Figure

2.5 shows a simple equivalent circuit of a ceramic multilayer capacitor below its series resonant frequency [52]. In addition to the capacitance C, the capacitor also includes an equivalent series resistance ESR and a series inductance L_s. ESR is a frequency-dependent resistance that aims to model all losses in the capacitor. The ESR of the capacitor increases the losses in the sensor resonant circuit notably and thus reduces its quality factor. In the current application, the capacitors are used at frequencies well below their series resonant frequency. As a consequence, the effect of the series inductance L_s is relatively small.

Figure 2.5: The equivalent circuit of a ceramic multilayer capacitor. C represents the capacitance, ESR represents the equivalent series resistance, and L_s represents the equivalent series self-inductance of the capacitor. [52]

Equivalent circuit of a sensor

A general equivalent circuit used for the sensors is shown in figure 2.6. The circuit is a combination of the equivalent circuits of the planar inductor and the surface mount capacitor presented above. The inductor is represented by the inductance L, the series resistance R_{Ls}, and the moisture dependent components caused by the surrounding materials, the parallel capacitance C_L and the parallel resistance R_{Lp}. The capacitor is represented by the capacitance C, the series resistance R_C, and the series inductance L_C. The circuit is essentially a parallel resonant circuit, since the series resistances R_{Ls} and R_C, and the inductance L_C appear as relatively small impedances in the operating frequency range.

The serial components of the inductor, L and R_{Ls}, and the components of the capacitor, C, R_C, and L_C, are considered to remain relatively constant in the moisture measurement application. Instead, the parallel components of the inductor, C_L and R_{Lp} change as a function of the electrical properties of the materials near the inductor. As a consequence, the resonant frequency and the quality factor of the sensor circuit depend on the surrounding materials. In the temperature measurement application, an external especially temperature dependent capacitor is used in parallel with the resonant circuit. The changes in its capacitance with temperature are expected to be significantly larger than the changes on the other components of the equivalent circuit. As a consequence, the resonant frequency of the sensor circuit is expected to depend on temperature.
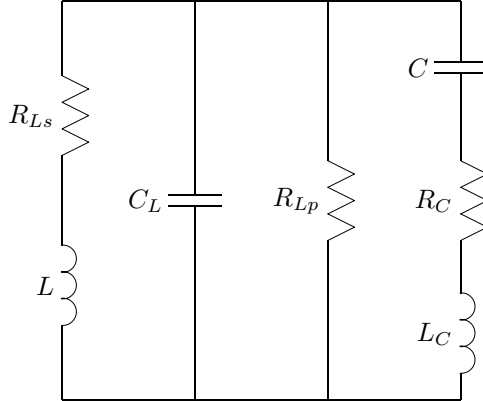
Figure 2.6: General equivalent circuit of a sensor at a given frequency. L is the inductance, R_{Ls} is the series resistance, C_L is the parallel capacitance, and R_{Lp} is the parallel resistance of the inductor. The parallel components of the inductor depend on the electrical properties of the surrounding material. C is the capacitance, R_C is the series resistance, and L_C is the series inductance of the capacitor.

2.1.2 Effect of the environment

As stated above, the parallel components of the equivalent circuit of the inductor, C_L and R_{Lp}, in figure 2.6 depend on the electrical properties of the materials surrounding the inductor. This phenomenon has been used in measuring moisture conditions. By using a material, the conductivity and dielectric constant of which change as a function of relative humidity and moisture content, near the inductor, the resonant frequency and quality factor of the sensor circuit will depend on the moisture conditions.

The developed sensor structure is such that the lossy, moisture-dependent material is not in direct contact with the conductor of the planar inductor, but there is a dielectric layer in between. Thus the turns of the inductor couple capacitively with the lossy material. As a consequence, the equivalent circuit applied for the inductor (figure 2.4) is incorrect. A more suitable equivalent circuit of the inductor would be for example the one shown in figure 2.7, where the inductor represented by L, R_s, and $C_{p'}$ couples capacitively with the lossy material represented by Z_{mat} through the dielectric material represented by C_{di1} and C_{di2}. The capacitance $C_{p'}$ represents the parallel capacitance of the inductor when it is unloaded, i.e. without the presence of a lossy material. The capacitances C_{di1} and C_{di2} depend on the physical thickness of the dielectric layer, its dielectric constant and the geometry of the capacitive coupling that may depend also on the electrical properties of the lossy material. The effective impedance of the lossy material, Z_{mat}, depends on the dielectric constant and conductivity of the material but also the geometry of the capacitive coupling. The most significant changes in Z_{mat} are expected to occur in its resistive component.
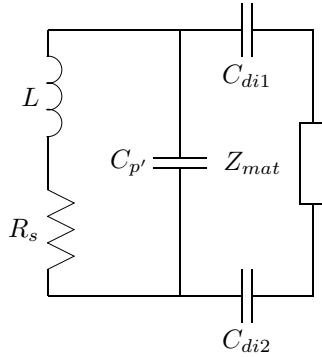
Figure 2.7: Capacitive coupling between a planar inductor and a lossy material. L is the inductance and R_s is the series resistance of the inductor, $C_{p'}$ is the unloaded parallel capacitance of the inductor, C_{di1} and C_{di2} are capacitances caused by a dielectric material. Z_{mat} is an effective impedance caused by a lossy material.

Despite the fact that that the equivalent circuit of figure 2.7 is a somewhat better approximation than that of figure 2.4 for the planar inductor that is capacitively coupled with a lossy material, the simpler equivalent circuit of figure 2.4 is used in the simulations presented in this thesis. That is, the capacitive coupling is approximated with a parallel capacitance and a parallel resistance. It should be noted that this approach yields a good approximation only at a narrow frequency band around the spot frequency where the component values are calculated.

2.2 Sensor reading principle

The resonance frequency and the quality factor of a sensor can be determined with a separate reading device, the antenna coil of which couples inductively with the sensor. The frequency response of the sensor can be measured from the impedance of the antenna coil by using either a swept measurement signal or a broadband stimulus. This section describes the phenomena that the reading device is based on.

2.2.1 Coupling between sensor and reading device

The connection between the planar inductor of the sensor and the antenna coil of the reading device is referred to as *inductive coupling* or *mutual inductance*. Below, the mutual inductance between two loops is first determined in terms of electromagnetics and then applied to form the equivalent circuit of the coupled reading device and sensor.

Electromagnetic approach

Figure 2.8 illustrates two conductive loops with the surfaces S_1 and S_2, and the contours c_1 and c_2 respectively. The loops are relatively close to one another and a current i_1 is flowing in loop 1. The mutual inductance of the loops can be determined by using the Maxwell equations. The numbering and naming conventions of the four Maxwell equations vary in the literature, so the numbering in this thesis is chosen to be the order utilized by Cheng [53].
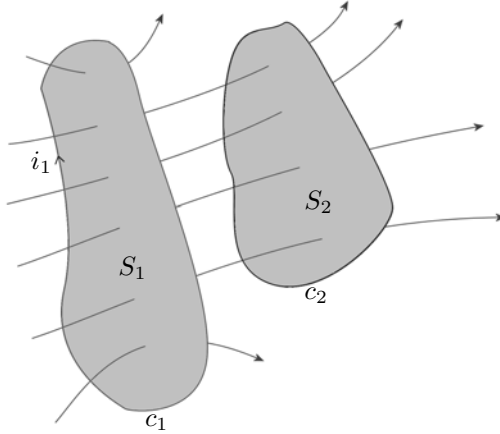

Figure 2.8: Two inductively coupled loops with the surfaces S_1 and S_2, and the contours c_1 and c_2. The current in loop 1 is denoted by i_1.

Maxwell's second equation, sometimes known as Ampère's law, states for the curl of a magnetic field that

$$\nabla \times \mathbf{H}(\mathbf{r}, t) = \frac{\partial}{\partial t} \mathbf{D}(\mathbf{r}, t) + \mathbf{J}(\mathbf{r}, t), \tag{2.12}$$

where $\mathbf{H}(\mathbf{r}, t)$ is the magnetic field strength, $\mathbf{D}(\mathbf{r}, t)$ is the electric flux and $\mathbf{J}(\mathbf{r}, t)$ the density of free currents. All of them are functions of location $\mathbf{r}$ and time t. The electric flux is linked to the electric field strength $\mathbf{E}(\mathbf{r}, t)$ with the relation $\mathbf{D}(\mathbf{r}, t) = \epsilon_r \epsilon_0 \mathbf{E}(\mathbf{r}, t)$, where ϵ_r is the relative permittivity and ϵ_0 is the permittivity of vacuum. Thus equation 2.12 indicates that both a time-varying electric field and a current flow give rise to a magnetic field. [53, pp. 322–323] [54, p. 142]

In addition, Maxwell's fourth equation states that the divergence of a magnetic field is equal to zero, that is

$$\nabla \cdot \mathbf{B}(\mathbf{r}, t) = 0, \tag{2.13}$$

where the magnetic flux density $\mathbf{B}(\mathbf{r}, t)$ can be stated in terms of the magnetic field strength $\mathbf{H}(\mathbf{r}, t)$ as $\mathbf{B}(\mathbf{r}, t) = \mu_r \mu_0 \mathbf{H}(\mathbf{r}, t)$, where μ_r is the relative permeability and μ_0 is the permeability of vacuum. Equation 2.13 indicates that

there are no magnetic flow sources, and the magnetic flux lines always close upon themselves. [53, pp. 226–227]

On the other hand, Maxwell's first equation, sometimes known as Faraday's law, states for the curl of an electric field that

$$\nabla \times \mathbf{E}(\mathbf{r}, t) = -\frac{\partial}{\partial t} \mathbf{B}(\mathbf{r}, t), \tag{2.14}$$

where $\mathbf{E}(\mathbf{r}, t)$ is the electric field strength and $\mathbf{B}(\mathbf{r}, t)$ is the magnetic flux density. Again both of them are functions of location $\mathbf{r}$ and time t. Equation 2.14 indicates that a time-varying magnetic field gives rise to an electric field. [53, p. 309]

Stokes' theorem states that the surface integral of the curl of a vector field over an open surface is equal to the closed line integral of the vector along the contour bounding the surface, i.e.

$$\int_S \nabla \times \mathbf{f}(\mathbf{r}) \cdot d\mathbf{S} = \oint_c \mathbf{f}(\mathbf{r}) \cdot d\mathbf{c}, \tag{2.15}$$

where $\mathbf{f}(\mathbf{r})$ is the vector field, c is the contour, and S is the open surface. [53, p. 59]

By integrating equation 2.14 over a surface S and by applying Stokes' theorem we get

$$\oint_c \mathbf{E}(\mathbf{r}, t) \cdot d\mathbf{c} = \int_S \nabla \times \mathbf{E}(\mathbf{r}, t) \cdot d\mathbf{S} = -\int_S \frac{\partial}{\partial t} \mathbf{B}(\mathbf{r}, t) \cdot d\mathbf{S}, \tag{2.16}$$

where c is the contour bounding the surface S. The left side of equation 2.16 is known as the *electromotive force*, emf, that is induced on the contour c [53, p. 59]. Thus, the electromotive force induced on loop 2 in figure 2.8 because of the magnetic field of loop 1 is

$$\text{emf}(t) = -\frac{\partial}{\partial t} \int_{S_2} \mathbf{B_1}(\mathbf{r}, t) \cdot d\mathbf{S}, \tag{2.17}$$

where S_2 is the surface of loop 2.

The magnetic flux density $\mathbf{B_1}(\mathbf{r}, t)$ can be calculated from equation 2.12. In this consideration, the electric flux term $\frac{\partial}{\partial t} \mathbf{D}(\mathbf{r}, t)$ can be omitted since the interest is on the magnetic field caused by the current flowing in loop 1. In order to simplify the calculation of a magnetic flux density $\mathbf{B}(\mathbf{r}, t)$, it can be stated as the curl of a *vector potential*, $\mathbf{A}(\mathbf{r}, t)$, that is

$$\mathbf{B}(\mathbf{r}, t) = \nabla \times \mathbf{A}(\mathbf{r}, t). \tag{2.18}$$

A magnetic flux density vector defined by equation 2.18 also satisfies Maxwell's fourth equation 2.13. By using an additional condition of choosing the divergence of the vector potential to be equal to zero, $\nabla \cdot \mathbf{A}(\mathbf{r}, t) = 0$, the vector

potential in free space ($\mu_r = 0$) at the location $\mathbf{r}$ caused by a current density distribution can be solved as

$$\mathbf{A}(\mathbf{r}, t) = \frac{\mu_0}{4\pi} \int_V \frac{\mathbf{J}(\mathbf{r}', t)}{|\mathbf{r} - \mathbf{r}'|} dV', \tag{2.19}$$

where $\mathbf{J}(\mathbf{r}', t)$ is the current density at location $\mathbf{r}'$, and V is the volume of the current density distribution. In the case of current loop 1, a time-dependent current flows through the loop, and equation 2.19 takes the form

$$\mathbf{A_1}(\mathbf{r}, t) = \frac{\mu_0 i_1(t)}{4\pi} \oint_{c_1} \frac{d\mathbf{c}'}{|\mathbf{r} - \mathbf{r}'|}, \tag{2.20}$$

where $i_1(t)$ is the current flowing in loop 1 and c_1 is the contour of loop 1. [53, pp. 232–234]

By substituting equation 2.18 into equation 2.17 and by using Stokes' theorem, the electromotive force is

$$\mathrm{emf}(t) = -\frac{\partial}{\partial t} \int_{S_2} (\nabla \times \mathbf{A_1}(\mathbf{r}, t)) \cdot d\mathbf{S} = -\frac{\partial}{\partial t} \oint_{c_2} \mathbf{A_1}(\mathbf{r}, t) \cdot d\mathbf{c}, \tag{2.21}$$

where c_2 is the contour of loop 2. Further, by substituting equation 2.20, the electromotive force equals

$$\mathrm{emf}(t) = -\left[\frac{\mu_0}{4\pi} \oint_{c2} \oint_{c1} \frac{d\mathbf{c} \cdot d\mathbf{c}'}{|\mathbf{r} - \mathbf{r}'|} \right] \frac{\partial i_1(t)}{\partial t} \tag{2.22}$$

The factor inside the braces is known as the mutual inductance, M, of the two loops. That is, the voltage induced on loop 2, with the polarity chosen to get a positive voltage, is

$$v_{\mathrm{ind},2} = -\mathrm{emf} = M \frac{di_1}{dt}, \tag{2.23}$$

where

$$M = \frac{\mu_0}{4\pi} \oint_{c2} \oint_{c1} \frac{d\mathbf{c} \cdot d\mathbf{c}'}{|\mathbf{r} - \mathbf{r}'|}. \tag{2.24}$$

Equation 2.24 is known as the Neumann equation. It should be noted that the mutual inductance depends only on the geometry of the loops and is symmetrical. [55, pp. 246–247]

Several formulas and tables have been published for the calculation of mutual inductances of coils of different geometries. One widely known collection is the one by Grover [56]. However, the coil geometries utilized in this research were considered to be somewhat too complicated for them. Instead, a Matlab program that directly implements the Neumann formula was developed.

Equivalent circuit

A pair of magnetically coupled loops, or coils, is generally called a transformer. The coils of the transformer are referred to as a primary coil and a secondary coil. The coupling between the coils is generally assessed in terms of the *coefficient of coupling k* defined as

$$k = \frac{M}{\sqrt{L_1 L_2}}, \qquad (2.25)$$

where M is the mutual inductance of the coils, and L_1 and L_2 are the inductances of the primary and secondary coil. The upper bound for the mutual inductance can be stated as $M \leq \sqrt{L_1 L_2}$, which gives the boundaries for the coefficient of coupling, $0 \leq k \leq 1$. The coupling coefficient is determined by a number of geometrical factors, including the number of turns of each coil, their relative positions and their physical dimensions. If k is close to zero, the coils are said to be loosely coupled and if k is close to one, they are said to be tightly coupled. Air-core transformers, such as the one formed by the reading device coil and sensor coil, are typically loosely coupled. [48, pp. 926, 931]

The two inductively coupled loops, or the transformer, discussed above, can be illustrated with the simplified equivalent circuit of figure 2.9. The two coils are represented by inductances L_1 and L_2. The inductive coupling between the coils is represented by the mutual inductance M. In addition, the currents flowing through the coils are represented by i_1 and i_2 and the voltages across the coils by u_1 and u_2.
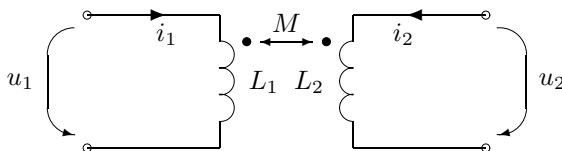
Figure 2.9: Inductive coupling between two coils, where L_1 and L_2 are the inductances of the primary and secondary coil respectively, M is the mutual inductance between the coils, and u_1 and u_2 are the voltages across and i_1 and i_2 the currents through the respective coils.

According to equation 2.23, a time-varying current through the primary coil induces a voltage across the secondary coil. When both coils are connected to electric circuits, both currents i_1 and i_2 may be nonzero. As a result, by the principle of superposition, the voltage induced across the secondary coil is a sum of the voltages caused by i_2 in the self-inductance L_2 and i_1 in the mutual inductance M. Thus, the voltage across the secondary coil is

$$u_2 = L_2 \frac{di_2}{dt} + M \frac{di_1}{dt}. \qquad (2.26)$$

The voltage induced on the primary coil can be expressed similarly. The differ-

ential expressions can also be represented with phasor expressions as

$$\begin{cases} U_1 &= j\omega L_1 I_1 + j\omega M I_2 \\ U_2 &= j\omega L_2 I_2 + j\omega M I_1 \end{cases},$$ (2.27)

where U_1 and U_2 are the phasor expressions of the voltages u_1 and u_2, I_1 and I_2 the phasor expressions of the currents i_1 and i_2, j is the imaginary unit, and ω is the angular frequency defined as $\omega = 2\pi f$, where f is frequency [48, p. 927]. The equation 2.27 can be illustrated with the equivalent circuit of figure 2.10 where the inductively coupled coils are replaced with inductances L_1 and L_2 in series with current controlled voltage sources $Z_T I_2$ and $Z_T I_1$ respectively, where the transfer impedance Z_T is equal to the impedance of the mutual inductance, i.e. $Z_T = j\omega M$.
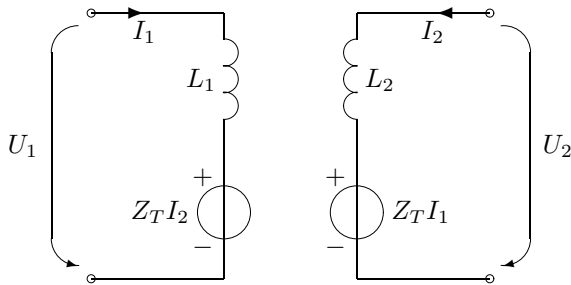

Figure 2.10: Equivalent circuit of mutually coupled coils consisting of inductances L_1 and L_2 and current controlled voltage sources $Z_T I_2$ and $Z_T I_1$, where Z_T is the transfer impedance. U_1, U_2, I_1, and I_2 are the voltages and currents of the respective coils.

Let us introduce a simplified equivalent circuit that illustrates the connection between the sensor and the reading device. Since changes in the moisture conditions and the temperature of the environment affect the quality factor and the resonant frequency of the sensor circuit, the reading device aims to acquire the frequency response of the sensor in order to determine these parameters. In figure 2.11, a current source J with a parallel resistance R_p is connected to a primary coil represented by the inductance L_1. Assuming that the resistance R_p is significantly larger than the impedance of the coil, the current I_1 through the reading device coil is equal to the current supplied by the current source J. On the secondary side, the sensor is represented by a parallel resonant circuit consisting of the inductance L_2, the capacitance C, and the resistance R. The mutual coupling between the coil of the reading device and the coil of the sensor is represented by the mutual inductance M.

Figure 2.12 shows a modified equivalent circuit of the sensor and the reading device. The mutually coupled coils have been replaced by the equivalent circuit of figure 2.10. That is, the primary coil is represented by the inductance L_1 and the current controlled voltage source $Z_T I_2$, where the transfer impedance $Z_T = j\omega M$. However, on the secondary coil, the inductance in series with a current controlled voltage source has been transformed to an inductance L_2 in parallel
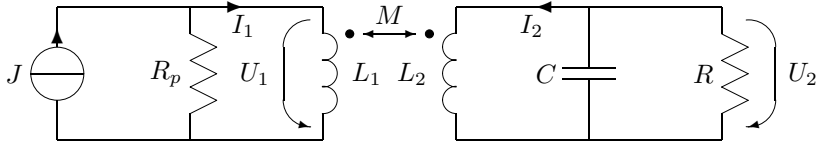
Figure 2.11: Equivalent circuit of a sensor and a reading device. The reading device features a current source J, a parallel resistance R_p, and an inductance L_1. The sensor is represented by a parallel resonant circuit of the inductance L_2, the capacitance C and the resistance R. The mutual inductance of the coils is represented by M. U_1, U_2, I_1, and I_2 represent the voltages across and the currents through the coils.

with a current controlled current source βI_1, where the current amplification factor is

$$\beta = \frac{Z_T}{Z_{L_2}} = \frac{j\omega M}{j\omega L_2} = \frac{M}{L_2}. \tag{2.28}$$

As a consequence, it is obvious that the voltage across the resonant circuit is $U_2 = \beta I_1 Z_{\text{in}}$, where Z_{in} is the input impedance of the resonant circuit as defined in equation 2.1. Further, the current I_2 can be calculated by the principle of superposition from the current of the current controlled current source βI_1 and the current through the inductance L_1 as

$$I_2 = \frac{U_2}{Z_{L_2}} - \beta I_1 = \frac{\beta I_1 Z_{\text{in}}}{j\omega L_2} - \beta I_1. \tag{2.29}$$

As a consequence, the voltage across the primary coil equals

$$\begin{aligned} U_1 &= j\omega L_1 I_1 + j\omega M \left(\frac{\beta I_1 Z_{\text{in}}}{j\omega L_2} - \beta I_1 \right) \\ &= I_1 \left[\beta^2 Z_{\text{in}} + j\omega (L_1 - \beta M) \right]. \end{aligned} \tag{2.30}$$

By substituting equations 2.28 and 2.25 into equation 2.30, the voltage across the primary coil yields

$$U_1 = I_1 \left[k^2 \frac{L_1}{L_2} Z_{\text{in}} + j\omega L_1 (1 - k^2) \right]. \tag{2.31}$$

That is, the impedance of the primary coil U_1/I_1 includes the impedance due to the self inductance of the coil scaled with the factor $(1 - k^2)$ and the impedance of the sensor resonant circuit scaled with the factor $k^2 L_1/L_2$. The real and imaginary component of the voltage U_1 with the Z_{in} of figure 2.3, $L_2 = 1$ µH, $L_1 = 1$ µH, $I_1 = 1$ A, and $k = 0.02$ are illustrated in figure 2.13.

The measured signal is the voltage that the resonant circuit sensor causes on the reading device coil. At resonance, the impedance of the resonant circuit affects the overall impedance of the reading device coil as a resistance $R_{\text{eq}} = k^2 \frac{L_1}{L_2} R$. By substituting the equations of the resonant frequency 2.2 and quality factor 2.7, the voltage caused by the sensor yields

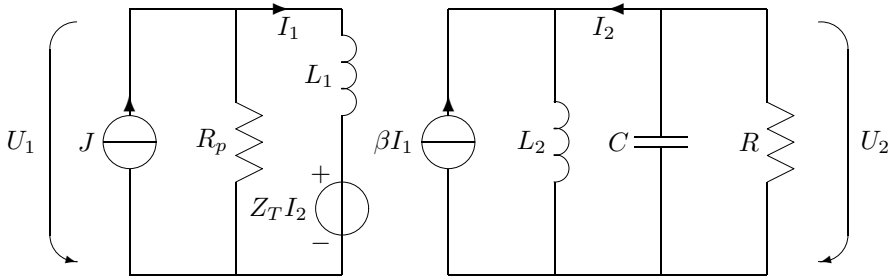$$U_S = I_1 k^2 L_1 \omega_{\text{res}} Q. \tag{2.32}$$

Figure 2.12: A modified equivalent circuit of a sensor and a reading device. The current source J and the parallel resistance R_p on the primary side, and the capacitance C and the resistance R on the secondary side remain the same as in figure 2.11. The mutually coupled coils have been replaced by the inductance L_1 and the voltage controlled current source $Z_T I_2$ on the primary side and the inductance L_2 and the current controlled current source βI_1 on the secondary side, where Z_T is the transfer impedance and β is the current amplification factor. U_1, U_2, I_1, and I_2 represent the voltages across and the currents through the coils.

That is, the magnitude of the measured signal depends on the current applied to the reading device coil, the coupling coefficient between the coils, the inductance of the reading device coil, and the resonance frequency and quality factor of the sensor. In figure 2.13, the voltage is $U_S = 0.4$ V.

Above it was assumed that the parallel resistance of the current source R_p is significantly larger than the impedance of the reading device coil U_1/I_1 i.e. the entire current J flows through the reading device coil ($I_1 = J$). In this case, a constant current flows through the reading device coil at all frequencies independent of the properties of the reading device coil and the sensor, and the mutual inductance between them. However, when this is not the case, the current through the reading device coil I_1 is no longer in phase with the current supplied by the current source J and more importantly the current I_1 depends on the impedance of the reading device coil U_1/I_1. According to equation 2.31 this means a dependence on among other things the impedance of the sensor Z_{in} and the coupling coefficient k. As a consequence, the shape of the measured signal is distorted. In addition, the distortion is the severer the higher the quality factor of the sensor is and the stronger the coupling is. This problem may be overcome by designing the current source to have a large feed impedance or by measuring the actual current through the coil and correcting the signal accordingly.

Another approach for acquiring the response of a sensor is using separate transmitter and receiver coils in the reading device. In this approach, a current is fed to the transmitter coil which is inductively coupled with the sensor coil. The voltage across and the current through the sensor coil are equal to those in the one coil approach. However, in the two coil approach the signal voltage is measured from the receiver coil that is also coupled with the sensor coil.
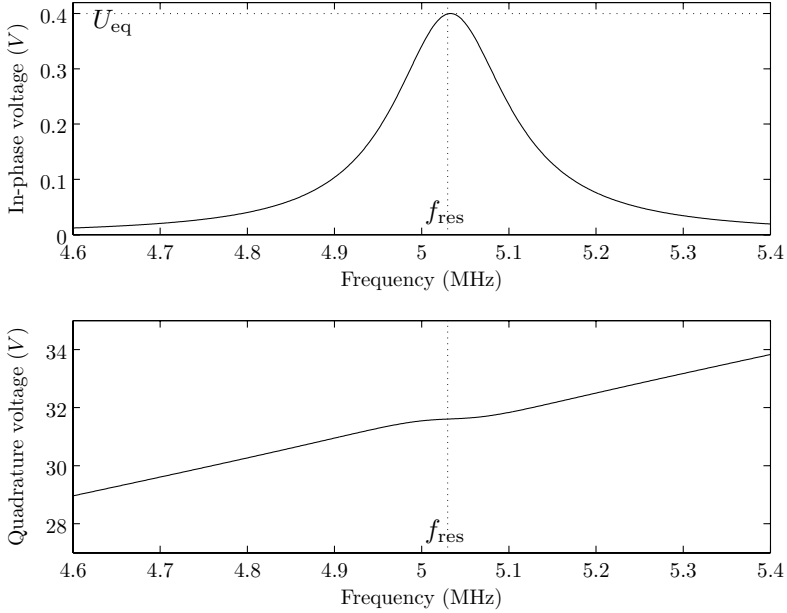
Figure 2.13: The voltage across the reading device coil as a function of frequency. The sensor is represented by the parallel resonant circuit of figure 2.3 ($R = 1$ kΩ, $C = 1$ nF, $L_2 = 1$ µH), the inductance of the reading device coil is $L_1 = 1$ µH, the current through the coil is $I_1 = 1$ A, and the coupling coefficient is $k = 0.02$. The upper figure shows the real component of the voltage, that is the component that is in phase with the current stimulus, and the lower figure shows the imaginary or quadrature component. The real component is entirely caused by the impedance of the sensor circuit, and the voltage at the resonance frequency f_{res} is equal to the maximum signal U_S. The imaginary component includes the voltage caused by the self inductance of the reading device coil and the imaginary component of the sensor response.

This approach requires that the transmitter and receiver coil are placed in a geometry where their mutual inductance is eliminated. The advantage gained from the two coil approach is that the voltage across the receiver coil results entirely from the current through the sensor coil, and the component caused by the self-inductance of the reading device coil is not included. The two coil approach is discussed in less detail, because the one coil approach was chosen for the instrumentation described in this thesis. The primary reason for the choice was the smaller amount of space required for implementing the one coil approach.

3 Sensor design

A sensor is the part of the developed measurement system that is in contact with the measured environment and transforms the measured entity into an electrical signal. Several sensor types of differing properties and cost have been developed during the research project. The principle of their operation, however, is the same. They all include resonant circuits, the properties of which change as a function of moisture content, relative humidity or temperature.

3.1 Basic sensors

The first developed sensor type was the *basic sensor*. The basic sensor was planned to be the mass product of the sensor family, so it has been constructed to be as simple and low-cost as possible. The sensor is intended to be used primarily for monitoring the moisture conditions in bathroom walls and floors in order to find signs of possible leaks. However, the basic sensor is also suitable for observing changes in the moisture conditions of several other structures. Especially the *pre-cast basic sensor* is suitable for monitoring the drying of concrete. All other developed sensor types presented in this thesis are also based on the basic sensor.

3.1.1 Objective

The objective of the development of the basic sensor is to be able to measure the moisture conditions of different building materials using the measurement method described in chapter 2 with as straightforward and cost-effective a sensor as possible. The primary application area is expected to be bathroom walls and floors, but also several other structures are considered potential.

Figure 3.1 shows the structure of the primary application area for the basic sensor, a typical bathroom wall in the Nordic countries. The innermost layer of the wall is the primary wall material, usually a concrete element, masonry or a gypsum board, possibly finished with screed. On its outer surface is the waterproofing layer which may be a plastic carpet or, in a bathroom with tiled walls as in figure 3.1, nowadays typically a waterproofing paint. Outside the waterproofing, the ceramic tiles are attached to the wall with mortar. The purpose of the waterproofing is to prevent the water used in the bathroom from penetrating into the wall structure. Thus, in a normally functioning bathroom, moisture conditions behind the waterproofing should not be affected by normal use of the bathroom. However, if the waterproofing is somehow damaged or inadequate, water may penetrate into the wall and cause a serious moisture damage. The objective of using basic sensors in bathrooms is to be able to observe such leaks

before more serious damage occurs. This requires the sensors to be assembled behind the waterproofing at the time of construction or renovation.
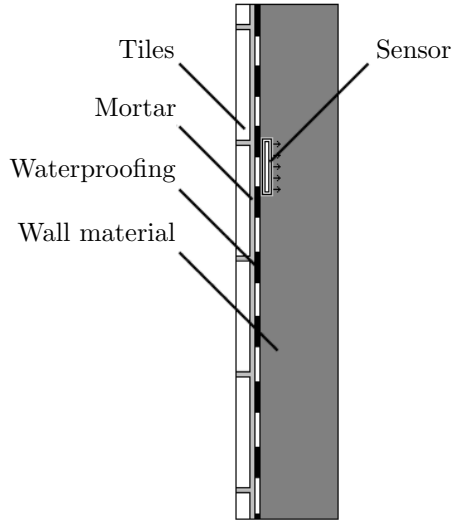

Figure 3.1: The location of the basic sensor in a bathroom wall with ceramic tiles. The tiles are attached to the wall with mortar. The waterproofing and the primary wall material are located behind the tiles. The sensor is placed behind the waterproofing in contact with the primary wall material.

In order for the measurement system to be desirable, the basic sensor must be somehow better than the measurement devices currently used, predominantly relative humidity measurement devices and surface moisture meters. This gives a desired value of ± 2 % for the measurement accuracy of the sensor. In addition, the sensors should be readable from outside the structure, i.e. the reading range should be at least 50 mm, preferably 100 mm. However, at the same time, the sensor should be sufficiently small so that it has minimal effect on the functionality of the structure. Since the sensor is left into the structure, it should function for 30 to 50 years depending on the renovation interval of the structure. Thus, the physical and chemical properties of the sensor are extremely important. Finally, the manufacturing costs of a single sensor should preferably be of the order of a few euros in order for the customer prices per apartment to be of the magnitude of a hundred euros, as estimated in section 1.7.

3.1.2 Sensor structure

A cross section illustrating the structure of the basic sensor is shown in figure 3.2. Electrically the basic sensor consists of an LC resonant circuit, the inductor of which functions both as a sensing element and an inductive antenna for

communicating with the reading device. The circuit is realized with a planar inductor (3) on a printed circuit board (2) and a surface-mount capacitor soldered in parallel with it. In order for the coupling between the sensor and its environment to be capacitive, the circuit board is covered with a polymer laminate (1). The laminate also intends to protect the sensor circuit from moisture and mechanical damage. Finally, the sensor also includes mortar (4) that is used as a layer, the electrical properties of which change as a function of the moisture conditions. In addition, the mortar fastens the sensor to the structure of interest (5).
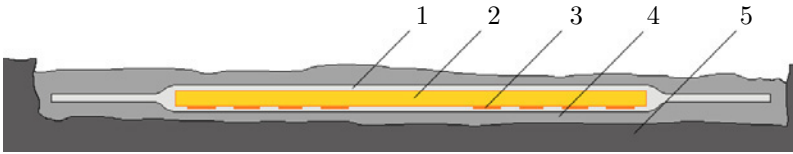

Figure 3.2: A cross section of the basic sensor inside a building structure. The sensor includes a planar inductor (3) on a printed circuit board (2). The circuit board has been covered all over with a polymer laminate (1). The sensor is fastened to the structure of interest (5) with the assembly mortar (4).

Design criteria

The sensor construction is a compromise of several different aspects. The primary application area, the bathroom application, dictates some of the criteria. Since the sensor is based on a circuit board, it is naturally assembled in contact to the structure of interest so that one of its flat sides is pressed against the structure. This side of the circuit board should thus include the planar coil that couples with the environment. In addition, the coil should also be covered with the polymer laminate and a layer of the assembly mortar. However, moisture behind the sensor should not affect the properties of the sensor since the moisture conditions outside the waterproofing depend on the normal use of the bathroom. As a consequence, the coupling between the inductor and the materials behind the sensor must be prevented.

The frequency band utilized by the measurement concept should be chosen considering a couple of aspects. First of all, according to equation 2.32 the magnitude of the signal acquired to the reading device coil from the sensor resonant peak is directly proportional to the resonance frequency of the sensor. As a consequence, it is advantageous for the frequency range to be as high as possible, but still in the range where the sensor is in the inductive near field of the coil. In addition, several standards and recommendations limit the applicable frequency range and magnetic field strength. The European Conference of Postal and Telecommunications Administrations (CEPT) has recommended certain frequency allocations to be applied for inductive applications [57, p. 40]. The widest continuous, recommended frequency allocation is the range 7400–

8800 kHz, often used in anti-theft-detection devices. At this frequency range, the European Telecommunications Standards Institute (ETSI) has set the maximum magnetic field strength 10 m away from the inductive loop system to 9 dB µA/m [58, p. 23].

The measurement accuracy of the system is a somewhat complicated compromise. First of all, the desired accuracy of ± 2 % of relative humidity requires that the basic sensor is not significantly affected by temperature or other environmental parameters within the specified operation conditions. In addition, the differences between the relative humidity readings acquired from individual sensors have to be smaller than the desired accuracy. Since the basic sensor converts the moisture conditions inside the building structure to a quality factor reading, another limiting factor for the accuracy follows from the accuracy with which the quality factor of the sensor can be determined with. According to equation 2.11, the quality factor of a resonant circuit can be determined as the ratio of the resonant frequency and the bandwidth. The effect of the accuracy of the measurement of each parameter on the calculated quality factor can be estimated by taking the differential of equation 2.11, that is

$$
\begin{aligned}
\Delta Q &= \left| \frac{\partial Q}{\partial f_{\text{res}}} \right| \Delta f_{\text{res}} + \left| \frac{\partial Q}{\partial B} \right| \Delta B \\
&= \frac{1}{B} \Delta f_{\text{res}} + \frac{Q}{B} \Delta B.
\end{aligned}
\tag{3.1}
$$

As can be seen, the quality factor is more sensitive to the measurement accuracy of the bandwidth B than that of the absolute resonance frequency f_{res}. In addition, the result is the more sensitive the higher the quality factor is.

Based on the critical moisture conditions presented in chapter 1, the most important relative humidity measurement range could be approximated to be between 65 % and 100 %. The variations in the quality factor should thus be divided evenly over this range. From this point of view, in order to acquire good accuracy, the changes in the quality factor should be as large as possible. However, according to equation 2.32, the signal acquired to the reading device coil from the sensor resonant peak is directly proportional to the quality factor of the sensor. That is, large variations in quality factor cause large variations in the strength of the measurement signal, which may lead to difficulties in the dynamics of the receiver of the reading device.

Since an individual sensor measures moisture conditions very locally, several sensors are needed in each bathroom at the most critical locations. As a consequence, the sensor should be as simple as possible in order to keep its costs low. In addition, the sensor should be sustainable, both mechanically and chemically. The mechanical endurance is important especially during the assembly process, so that the sensor is not damaged at this stage. The chemical endurance, on the other hand, is important since the sensor must remain functional inside the building structure for 30 to 50 years. Concrete, for example is an extremely alkalic environment [59, p. 852].

Printed circuit board

As stated in chapter 2, the primary inductive component of the sensor resonant circuit was chosen to be a planar inductor on a printed circuit board. The choice of the circuit board material was primarily based on electrical properties, mechanical properties and cost. The chosen circuit board material is woven glass reinforced epoxy resin, conversationally known as FR-4 according to its flame retardation class. Its electrical properties are suitable and well known. Some of the most essential parameters of the glass-epoxy material, provided by the chosen circuit board manufacturer, are shown in table 3.1. In addition, due to the good mechanical properties of the chosen circuit board material, no supporting structure is needed in the sensor. The material is also a well established industry standard among circuit board materials. As a consequence, it is easily available and cost-effective.

Table 3.1: Essential parameters of the woven glass reinforced epoxy resin circuit board material as reported by the chosen circuit board manufacturer (Elprintta Ltd., Finland). The dielectric constant and dissipation factor are reported with the conditioning C-40/23/50 (40 hours at 23 ℃ and 50 %RH) and the resistivity with the conditioning C-96/35/90 (96 hours at 35 ℃ and 90 %RH.)

parameter	value
typical volume resistivity after damp heat	10^8 MΩcm
typical dielectric constant @ 1 MHz	4.7
typical dissipation factor @ 1 MHz	0.014
thickness range	1.47–1.63 mm

The conductor material of the coil was chosen to be copper. It is more expensive than aluminium but has by far better chemical and electric properties. Copper-plated glass-epoxy is also widely used in the electronics industry. Thus, it is inexpensive and the processes involved are well known.

After choosing the circuit board and conductor materials, several parameters still remain to be optimized, including the geometry of the coil, its diameter, the number of turns, the width of and the space between the turns, and the height of the conductor. Several simulations were carried out to find suitable values for these parameters. The overall impedance of the sensor circuit was simulated with the equivalent circuit of 2.6 as a function of frequency and moisture conditions using *Aplac 7.90* (Aplac Solutions Corporation, Finland). The four components in figure 2.6 that relate to the planar inductor and its coupling with the environment, L, R_{Ls}, C_L, and R_{Lp} were obtained from simulations with a numerical simulation program *Circular coil simulator* developed in 2001 by Timo Varpula, D.Sc., of VTT Automation [51]. The mutual inductance between the simulated sensor and a loop modelling the reading device coil was simulated with a *Matlab 6.1.0.450* (The Mathworks Inc., USA) program that implements the Neumann equation 2.24.

The geometry of the inductor was chosen to be the one shown on the left in figure 3.3, a square with rounded corners. This is because, first of all, if the circuit board is square-shaped it is easy and cost-effective to cut into shape and easy to laminate. As a consequence, the inductor should be of the same shape as the board to maximize its effective area. The corners of the inductor are rounded according to good circuit design practice in order to decrease the discontinuities in the impedance of the conductor and to ease the manufacturing of the board. It was considered desirable to keep the space between the turns constant throughout the inductor so that the capacitance between the turns is more evenly distributed, thus more easily assessed. As a consequence, the radii of the corners of the outer turns are larger than those of the inner turns. It should be noted that the program used to simulate the coil assesses square-shaped inductors by estimating them with a circular coil of a calculated equivalent diameter and by transforming the acquired results to apply for a square-shaped inductor.
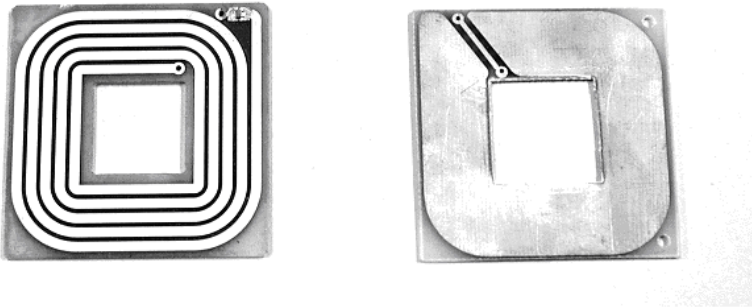
Figure 3.3: The geometry of the printed circuit board on both sides. The front side presented on the left features the 5-turn inductor. The back side on the right includes a static shield and the lead-out bridge of the inductor.

Since it was desired that the sensor would not be sensitive to the properties of the materials behind the sensor, a static shield was constructed on the backside of the circuit board. This can be seen on the right in figure 3.3. The shield does not form a closed loop or a whole plane under the coil, since that would lead to eddy currents inducing to the shield. Instead, its purpose is to short-circuit the parasitic capacitances behind the coil.

The parallel components of the inductor that change as a function of moisture conditions depend significantly also on the properties of the laminate and the assembly mortar surrounding the circuit board. As a consequence, their parameters had to be optimized in the same simulation process. The overall process required several iterations and a significant amount of trial and error. Thus, the exact simulation process can not be presented here. However, a simulation of the sensor with the finally chosen parameters is shown in the following subsection. The parameters finally chosen for the inductor are listed in table 3.2 and the resulting circuit board is shown in figure 3.3.

Table 3.2: The parameters chosen for the planar inductor.

parameter	value
Coil geometry	square
Length of side	52 mm
Number of turns	5
Width of turn	2 mm
Space between turns	1 mm
Height of conductor	40 µm

Surface mount capacitor

As stated above, a suitable range for the resonance peak of the sensor would be 7400–8800 kHz. The planar inductor as such is a parallel resonant circuit, however its resonance frequency is significantly higher than the desired range. Thus, based on the simulated properties of the planar coil, a 330 pF surface-mount ceramic multilayer capacitor (2238 861 15331, Phycomp Components, Taiwan) is connected in parallel with the inductor. Some of the most essential parameters of the capacitor are listed in table 3.3. The parameter values are obtained from the datasheet of the component [52] and from a Spice calculation program provided by the manufacturer [60]. The most important criteria for choosing this capacitor were the relatively large package that eases soldering, a small tolerance to keep the resonance frequencies of all individual sensors in the desired measurement range, a small equivalent series resistance so that the capacitor does not significantly lower the quality factor of the circuit, and cost to keep the sensors cost-effective. The properties of the capacitor have been included in the simulation model presented in the following subsection.

Table 3.3: Essential parameters of the surface-mount capacitor used in the basic sensor [52] [60].

parameter	value
Nominal capacitance	330 pF
Capacitance tolerance	± 5 %
Package size	0805
Rated voltage	50 V
Equivalent series resistance @ 8 MHz	70 mΩ
Series inductance	0.9 nH

Laminate

The circuit board of the basic sensor is laminated with a polymer layer in order to protect the circuit from moisture and contamination, and to control the effect

of the environment to the response of the sensor. The choice of the laminate material was affected by the need for high durability in an alkaline environment and in mechanical stress. The choice was also affected by the ease of attaching the laminate to the circuit board, the electrical properties of the polymer and cost. A summary of the most important polymers considered is shown in table 3.4. In the table, the materials are judged based on their compatibility with concrete and their relative costs. The most important criterion for choosing the material was its compatibility with concrete, thus polyester had to be abandoned as an alternative. In addition, PTFE appears to be considerably more expensive that the other alternatives.

Table 3.4: The compatibility of several polymers with concrete [59, p. 853] and their relative costs as surveyed by Outi Valta, M.Sc. [39, p. 35].

Polymer	Compatibility	Cost
Polyester (PET)	Poor	Inexpensive
Polyethylene (PE)	Very good	Inexpensive
Polypropylene (PP)	Very good–good	Inexpensive
Polystyrene (PS)	Very good	Inexpensive
Polytetrafluoroethylene (PTFE)	Very good	Expensive
Polyvinyl chloride -hard (PVC)	Very good	Inexpensive

The choice was finally made based on the laminates and adhesives that were easily available and widely used. A suitable combination of a polyethylene laminate and an acrylate adhesive were found and chosen to be used for the sensor. The exact electrical properties for the chosen polymer and adhesive were not available, so they were both approximated to have a relative permittivity of 2.25, a value commonly used for polyethylene. The relative permittivity of polyethylene remains nearly constant at a wide range of frequencies and temperatures [61, p. 327].

The thickness of the layer consisting of the adhesive and the laminate has also an effect on how much the quality factor and resonance frequency of the sensor change as the moisture conditions outside the sensor change. Thus, the thickness of the layer had to be included as a parameter to be optimized in the simulation model of the overall sensor. The finally chosen thickness of the polyethylene layer was 85 µm with an approximately 20 µm thick layer of acrylate adhesive.

Assembly mortar

The final component of the basic sensor is the mortar used to fasten the sensor to the building structure of interest. The function of the mortar is to reach hygroscopic equilibrium with the surrounding material and to feature predictable changes in its electrical properties as a function of relative humidity. In addition, its grain size should be such that when pressed between the sensor and the building structure, the mortar would form an adequately thick layer. In

addition, the mortar should remain available in the future without experiencing significant changes. Several materials were tested in the laboratory environment until a suitable one was found, *Vetonit 6000* (Optiroc Ltd., Finland).

To be able to include the assembly mortar in the simulation model, some information is needed about its the electrical properties at different moisture conditions. A set of measurements was performed to acquire information about the orders of magnitude in which the conductivity and the relative permittivity of the mortar vary at the chosen frequency range. In this measurement, there was no intention to compare the results to relative humidity or moisture content readings, since it is extremely difficult to balance the moisture conditions inside a block of porous material. The measurement technique is somewhat similar to the one presented by Wilson et.al. [62], however the dimensions of the setup and the used frequencies are smaller to keep the dimensions significantly smaller than the wavelength.

The electrical properties of the assembly mortar were measured with a test cell shown in figure 3.4 and an impedance analyzer, Agilent 4395A Network / Spectrum / Impedance Analyzer with Agilent 43961 RF Impedance Test Adapter (Agilent Technologies, USA). The test cell is a $50 \times 50 \times 50$ mm mold screwed together from acrylic plastic sheets. Two stainless steel electrodes have been glued on the inside of opposite faces of the mold. A thin plastic film (Plastic Spray PRF 202, Taerosol Ltd., Finland) has been sprayed on the inner surface of the electrodes. The aim of the film is to prevent galvanic contact between the electrodes and the mortar with as thin a layer as possible. The thickness of the film was measured to be less than 10 µm. The test cell includes a 50 Ω BNC connector that is connected to the electrodes with two approximately 25 mm long wires.

Figure 3.4: The test cell for measuring the electrical properties of the assembly mortar consists of a $50 \times 50 \times 50$ mm acrylic plastic mold with square shaped stainless steel electrodes on the inside of two faces. The electrodes are covered with a thin film of plastic spray. The connection to the electrodes is via a 50 Ω BNC connector.

Before making the measurements with mortar, the effect of the measurement setup was determined at the measurement frequency range 1–20 MHz. The BNC connector and the wires in the test cell together with the adapters required for attaching the test cell to the impedance analyzer were estimated to appear as a parallel capacitance in the measurement circuit. Measuring the capacitance of the test setup without the electrodes, at frequencies between 1 and 20 MHz, yielded a capacitance value of 11.7 pF. The adapters and wiring also cause an inductive component, the magnitude of which is difficult to evaluate accurately, due to the complex geometry. However, the inductive component is estimated to be of the magnitude of nH:s, which leads to an impedance of a few ohms at 20 MHz. Thus, the inductive component has been neglected from the calculations in order to simplify the used model.

The measured sample was formed by pouring fresh mortar in the mold and vibrating it in order to compact the mortar. This produced a 50 mm cube of mortar between the electrodes. The impedance of the test cell was then measured over the frequency range of 1–20 MHz, for a total of 801 points. This measurement was repeated at various times up to 32 days after the mortar was poured. The results of the measurement are shown in figure 3.5. For the sake of clarity, the results of only four characteristic measurements are shown. The first measurement, represented by the solid lines, was made three hours after pouring the mortar. The mortar was then let dry through the one open face of the cube in indoor air with the relative humidity of approximately 20–30 % and the temperature of 20–25 ℃. The dotted and the slash-dotted lines represent the results after 1 day and 8 days respectively. The last measurement, represented by the slashed line, was made after 32 days.

An approximate equivalent circuit of the impedance measurement setup is shown in figure 3.6. The capacitance of the test setup excluding the electrodes (11.7 pF) is represented by the parallel capacitance C_p. The block of mortar itself is represented by the impedance Z_{mat}. The capacitive coupling through the sprayed plastic films is represented by the capacitances C_{di1} and C_{di2}. The magnitude of their combined capacitance can be approximated from the generally known equation for the capacitance of a plate capacitor,

$$C = \epsilon_0 \epsilon_r \frac{A}{d}, \tag{3.2}$$

where ϵ_0 is the permittivity of free space, $8.854 \times 10^{-12} \frac{\text{F}}{\text{m}}$, ϵ_r is the relative permittivity of the dielectric, not specified by the manufacturer but approximated to be in the range of 2–4, A is the area of the plates, 0.0025 m², and d is the thickness of the dielectric, measured to be less than 10 µm. This approximation yields a combined capacitance value of more than 2 nF, which would appear as a reactive impedance of approximately 10 Ω at the primary measurement frequency of 8 MHz. However the actually occurring capacitance value is expected to be somewhat lower than this and to depend on the moisture content of the mortar and on the measurement frequency, since the other electrode of the plate capacitor now is the mortar block, not a highly conductive plate. Due to the
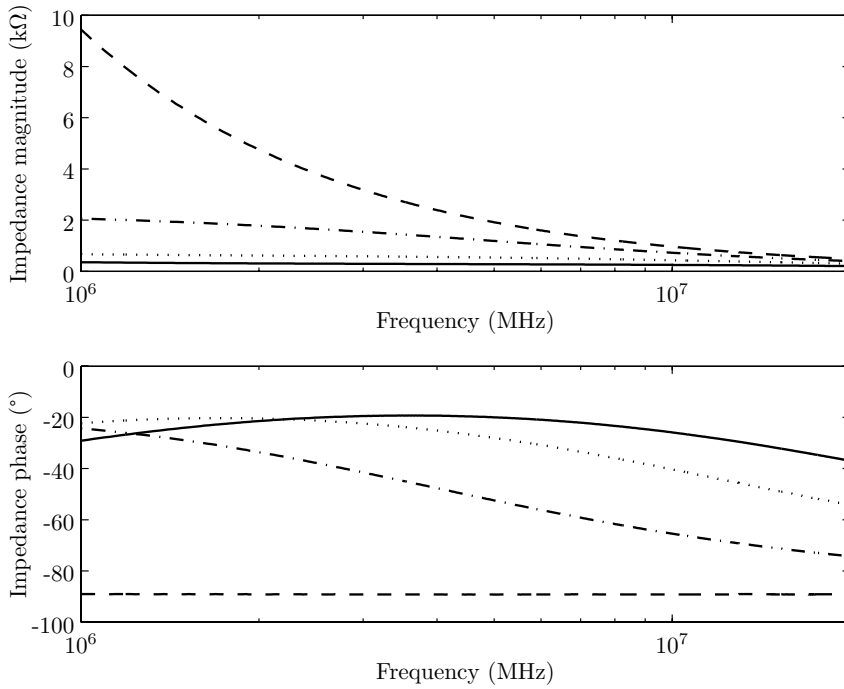
Figure 3.5: The measured magnitude and phase angle of the impedance of the test cell in the frequency range of 1–20 MHz. The solid lines represent the results at 3 hours, the dotted lines at 1 day, the slash-dotted lines at 8 days, and the slashed lines at 32 days after pouring the mortar.

lack of exact knowledge of its magnitude, the serial capacitance has been omitted in calculating the conductivity and the relative permittivity of the mortar. The most significant error is expected to occur in the relative permittivity of the mortar at high moisture content and low measurement frequencies.
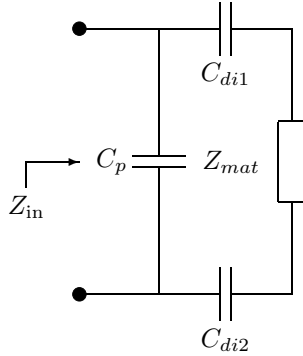

Figure 3.6: Equivalent circuit of the impedance measurement. C_p is the parallel capacitance resulting from the measurement setup, C_{di1} and C_{di2} are the capacitances caused by the sprayed plastic film. Z_{mat} is the impedance of the mortar cube.

The impedance of the mortar block, Z_{mat}, is approximated to consist of a parallel capacitance and a parallel resistance [62]. After subtracting the effect of C_p from the impedance according to figure 3.5, and omitting C_{di1} and C_{di2}, the resulting impedance can be unambiguously divided into the capacitive and resistive component. The relative permittivity of the mortar can be calculated from the capacitive component by using equation 3.2, with A as the area of the plates, 0.0025 m^2, and d as the thickness of the mortar block, 0.1 m. Correspondingly, the conductivity of the material can be calculated from the resistive component with the generally known equation

$$R = \frac{1}{\sigma}\frac{d}{A},$$

(3.3)

where σ is the conductivity of the material, d is the thickness of the mortar block, and A is the area of the plates. The calculated conductivity and relative permittivity are shown in figure 3.7. The solid lines represent the results at 3 hours, the dotted lines at 1 day, the slash-dotted lines at 8 days, and the slashed lines at 32 days after pouring the mortar.

Table 3.5 contains conductivity and relative permittivity values at the primary measurement frequency of 8 MHz at different stages of the drying of the mortar. It should be noted that the mortar cube was allowed to dry only in one direction until the measurement performed 11 days after pouring. Up to the next two measurements (12 days and 15 days) the measurement cell was opened to let the mortar dry in four directions. This explains the rapid changes in conductivity and relative permittivity at this time interval.
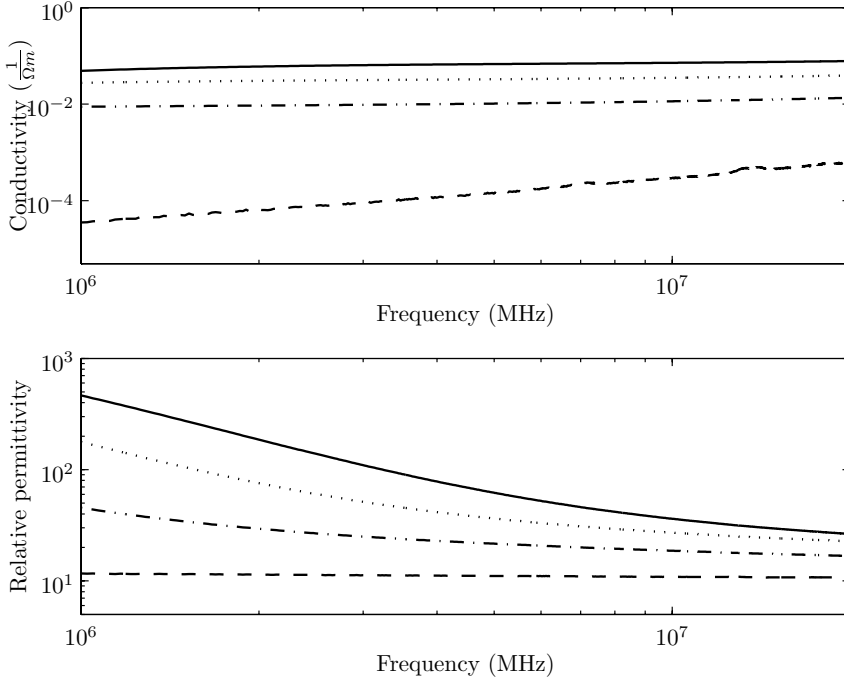
Figure 3.7: The conductivity and the relative permittivity of the mortar in the frequency range of 1–20 MHz as calculated from the measurement results. The solid lines represent the results at 3 hours, the dotted lines at 1 day, the slash-dotted lines at 8 days, and the slashed lines at 32 days after pouring the mortar.

Table 3.5: The conductivity σ and dielectric constant ϵ_r of the assembly mortar at 8 MHz at different times after pouring it.

time after pouring	σ [$1/\Omega m$]	ϵ_r
3 hours	7.04×10^{-2}	41.8
1 day	3.43×10^{-2}	29.4
8 days	1.10×10^{-2}	19.5
11 days	6.91×10^{-3}	17.5
12 days	2.37×10^{-3}	14.1
15 days	4.59×10^{-4}	11.5
32 days	2.32×10^{-4}	10.9

3.1.3 Simulation results

A simulation model was developed to investigate the functionality of the basic sensor. The applied equivalent circuit is the one presented in figure 2.6. The values in table 3.3 were used for the component values of the capacitor, C, R_C, and L_C. The series components of the inductor, L and R_{Ls}, were acquired by performing magnetic calculations with the *Circular coil simulator* as described in chapter 2. The simulations were made based on the parameters of table 3.2. The parallel components, C_L and R_{Lp}, that depend on the electrical properties of the materials around the inductor, were acquired by performing electric calculations with the same program. The simulation program supports multiple material layers only on one side of the inductor, thus the parallel components corresponding to the circuit board and the static shield were simulated separately from those of the laminate and mortar. These results were then combined to form the parallel component values. The simulated values acquired for the inductor, when surrounded by the circuit board and the static shield on one side and the laminate and air on the other are shown in table 3.6.

Table 3.6: The simulated component values of the inductor, L, R_{Ls}, C_L, and R_{Lp}, when it is surrounded by the circuit board and the static shield on one side and the laminate and air on the other.

Component	Value
L	1250 nH
R_{Ls}	393 mΩ
C_L	5.80 pF
R_{Lp}	1.3×10^9

The moisture dependent parallel components, C_L and R_{Lp}, were simulated with the electrical properties of the assembly mortar in different moisture conditions as gathered in table 3.5. The resulting component values are shown in table 3.7. The values were then placed in an Aplac simulation file that implements the equivalent circuit of figure 2.6, and the impedance of the sensor was simulated as a function of frequency. The absolute values of these frequency responses are shown in figure 3.8 where the resonance curve corresponding to the moistest mortar is the one with the left-most resonance peak and so forth. The resonance frequency and quality factor corresponding to each pair of material parameters were then calculated. These are also listed in table 3.7.

The simulation results presented above indicate the expected general trend, that as the mortar around the sensor dries, the resonance frequency and quality factor of the sensor increase. However, it seems that the quality factor of the sensor has a minimum value within the simulated conductivity and relative permittivity range. The simulated quality factor seems to vary between 28.4 and 124, which indicates a variation of the factor 4.4 in signal amplitude. In addition, the bandwidth of the sensor seems to be within the recommended

Table 3.7: The simulated moisture dependent component values, C_p and R_p, and the resonance frequency f and quality factor Q corresponding to each pair of conductivity σ and relative permittivity ϵ_r values.

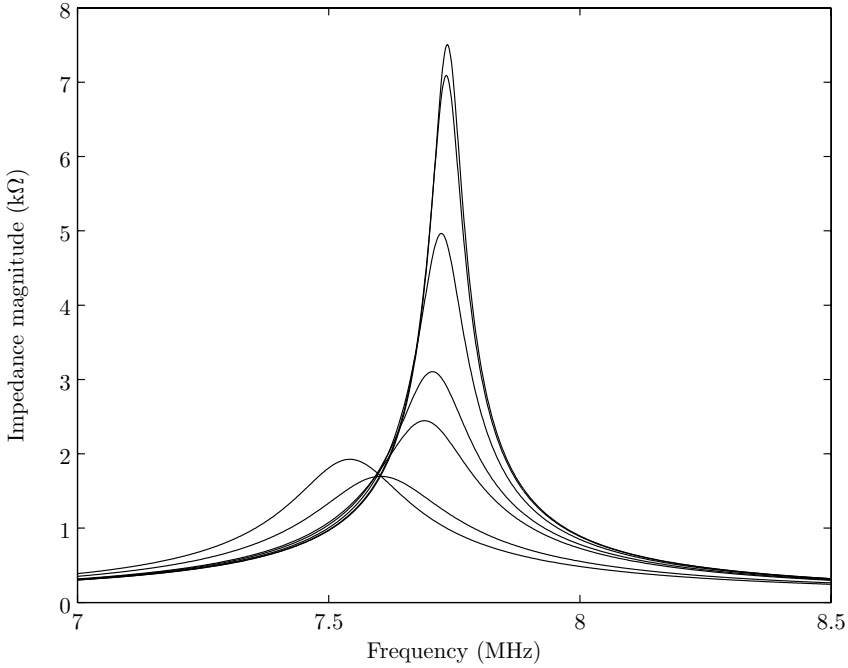| σ [1/Ωm]	ϵ_r	C_p [pF]	R_p [kΩ]	f [kHz]	Q
7.04×10^{-2}	41.8	27.2	2.57	7543	32.6
3.43×10^{-2}	29.4	21.5	2.17	7603	28.6
1.10×10^{-2}	19.5	13.5	3.53	7690	40.6
6.91×10^{-3}	17.5	12.1	5.09	7707	51.7
2.37×10^{-3}	14.1	10.5	13.1	7724	82.2
4.59×10^{-4}	11.5	9.63	62.8	7734	117
2.32×10^{-4}	10.9	9.44	122	7736	124

Figure 3.8: Simulation results for the absolute value of the sensor impedance in seven different moisture conditions. The left-most peak corresponds to the moistest mortar and so forth.

range of 7400–8800 kHz at all moisture conditions.

One of the most important criteria for the sensor design was its mutual inductance with the reading device coil. This was assessed by simulating the mutual inductance between the sensor coil and a loop with the diameter of 50 mm on the same axis. The simulations were made with a Matlab program written for the purpose, that implements Neumann equation 2.24 for two arbitrary contours divided into a finite amount of straight elements. The geometry utilized in the calculation is shown in figure 3.9. The resulting mutual inductances and the voltages induced to the reading device coil according to equation 2.32, with the quality factor and resonant frequency pairs (Q=124, f=7785 kHz) and (Q=28.4, f=7651 kHz), and the current stimulus I_1=100 mA, are shown in table 3.8.
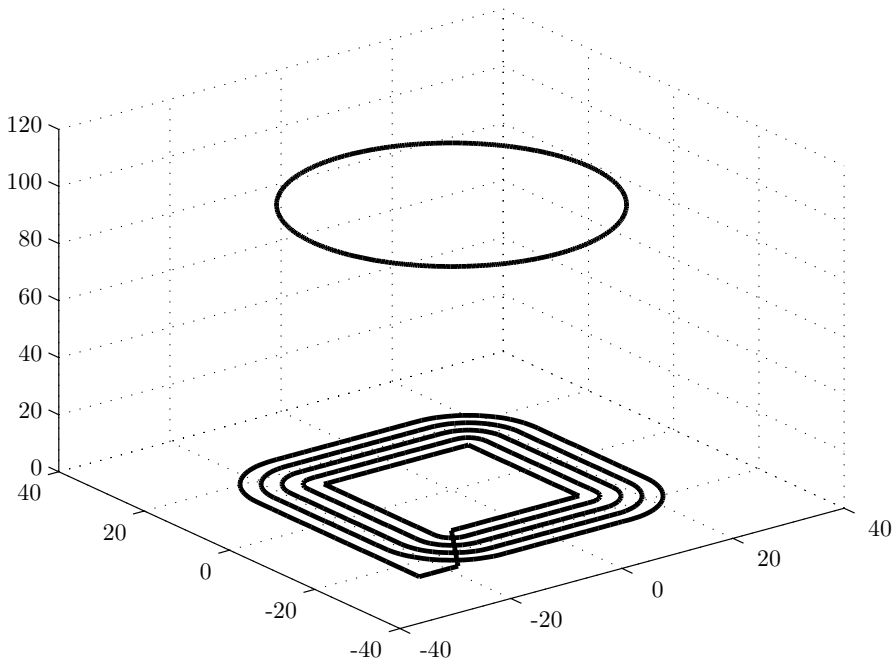
Figure 3.9: The geometry used for calculating mutual inductances with the Neumann equation. The lower contour represents the sensor coil and the upper contour the reading device coil with a 50 mm diameter. Both coils have been divided into 1000 elements for the numeric calculation of the Neumann formula. The measures in the figure are in mm.

The measurement accuracy for the quality factor and resonance frequency of the sensor results from the accuracy with which the voltages and frequencies can be measured. According to equation 3.1, a reasonable measurement accuracy of 1 kHz of the bandwidth, ΔB, would lead to an approximately 2 unit accuracy in determining the quality factor, ΔQ, when Q=124 and f=7785 kHz. In addition, the signal strength acquired from the sensor at the distance of 100 mm, 0.66–

Table 3.8: The simulated mutual inductances between the sensor coil and a loop of diameter 50 mm with different distances on the same axis, d, and the voltage induced on the loop, U_{S1} and U_{S2}, with two pairs of quality factor and resonant frequency (Q=124, f=7785 kHz) and (Q=28.4, f=7651 kHz).

d [mm]	M [nH]	U_{S1} [mV]	U_{S2} [mV]
10	129	8100	1800
20	65.6	2100	470
50	13.7	90	20
100	2.46	2.9	0.66
200	0.347	0.058	0.013

2.9 mV, seems reasonable for determining the voltage of the resonance peak and the voltage corresponding to the half power bandwidth with a reasonable, say 1 %, accuracy. With distances larger than this, it may be problematic.

Table 3.9 lists the results of a sensitivity analysis performed for the sensor structure. The analysis was performed by simulating the quality factor and resonance frequency of the sensor after changing each parameter one at a time. The table lists the ratios of relative changes of quality factor and resonance frequency to relative changes in different parameters at two moisture conditions, where Q=40.6, f=7690 kHz and Q=82.2, f=7724 kHz. Thus, the figures in the table indicate, how much and into which direction the quality factor and resonance frequency change, when a sensor parameter is changed.

Table 3.9: An analysis of the sensitivity of the quality factor and resonance frequency to several parameters of the sensor construction at two different moisture conditions.

Parameter (p)	Q=40.6, f=7690 kHz		Q=82.2, f=7724 kHz	
	$\frac{dQ}{Q}/\frac{dp}{p}$	$\frac{df}{f}/\frac{dp}{p}$	$\frac{dQ}{Q}/\frac{dp}{p}$	$\frac{df}{f}/\frac{dp}{p}$
Copper thickness	0.17	0.01	0.34	0.01
Circuit board thickness	-0.03	0.01	-0.00	0.01
Circuit board permittivity	0.00	-0.01	0.01	-0.01
Polyethylene thickness	0.42	0.00	0.15	0.00
Polyethylene permittivity	-0.41	-0.00	-0.15	-0.00
Mortar permittivity	0.30	-0.01	0.14	-0.01
Mortar conductivity	-0.58	-0.00	-0.25	-0.00
Capacitor capacitance	0.18	-0.48	-0.12	-0.49
Capacitor resistance	-0.04	0.00	-0.09	0.00

The figures in table 3.9 indicate that the resonance frequency of the sensor is significantly sensitive only to the capacitance of the surface-mount capacitor. The primary measurement parameter, the quality factor, however, is sensitive

to several parameters. The thickness of the copper layer on the printed circuit board has an effect on the series resistance of the planar coil, and thus affects the quality factor of the sensor, especially when the quality factor is high. The thickness and permittivity of the polyethylene layer, and the permittivity and conductivity of the mortar, on the other hand, have a significant effect on the quality factor when it is low, i.e. the mortar surrounding the sensor is wet. The capacitance of the surface-mount capacitor has a clear effect also on the quality factor. Interestingly, the direction of the change is different between the two different moisture conditions.

In addition to the sensitivity analysis presented above, several Monte Carlo analyses were performed using Aplac. That is, a large number of simulations were made so that the sensor parameters were varied according to their probability density functions. The variations in the properties of the mortar were left out in order to assess only the effect of the actual sensor structure. The performed Monte Carlo simulations are only indicative, since a lot of assumptions have to be made in modelling the probability density functions of each parameter.

The probability density functions of the three component values of the surface mount capacitor, C, R_C, and L_C, were modelled with a uniform distribution between the nominal value ±5 %. The manufacturer of the capacitor specifies only the variation in capacitance to be of the tolerance ±5 %. However, there is no knowledge about the actual probability density function. A single batch of the capacitors may have the same value more accurately while being significantly off the nominal value. This is typically the case, since the manufacturer may have selected parts for ±2 % tolerance purposes out of a batch of ±5 % tolerance [63, p. 66]. As a consequence, the distribution could resemble a normal distribution, with the center part missing. Thus, a uniform distribution was considered a suitable compromise, and was utilized also for the values of R_C and L_C.

The other parameters in the Monte Carlo analyses were modelled with a normal distribution. The thickness of the copper, the thickness of the circuit board, and the permittivity of the circuit board material and the laminate were estimated to vary only slightly. Thus, their probability density functions have been modelled with a normal distribution with the standard deviation of 2 % of the nominal value. The thickness of the laminate layer has been estimated to vary more due to the possibility that the adhesive between the polymer and the circuit board may not be evenly spread. Thus the probability density function of the laminate layer has been modelled with a normal distribution with the standard deviation of 5 % of the nominal value. The standard deviation for each component value of the coil, L, R_{Ls}, C_L, and R_{Lp}, was acquired by calculating the square root of the sum of squares of the standard deviation caused by each parameter. The resulting standard deviations used in the simulation are as follows: $L = 0.024$ %, $R_{Ls} = 2.15$ %, $C_L = 1.33$ %, and $R_{Lp} = 1.28$ %.

The distribution of the results of a representative Monte Carlo simulation, a 10 000 point analysis of a sensor with the nominal quality factor $Q=82.2$, and

resonance frequency f=7724 kHz, is shown in figure 3.10. The shapes of the distributions of quality factor and resonant frequency are typical of the most significant parameters. The quality factor distribution has the the distinctive shape of a normal distribution. The gaps visible in the distribution are not significant; they result from the limited frequency points of the simulation. The resonance frequency distribution, on the other hand, resembles a uniform distribution, since the capacitance of the surface-mount capacitor was modelled with one. By comparing the figure with table 3.7, it is evident that the quality factor is far more suitable to be the primary measurement parameter, since its variations are significantly smaller in comparison with the changes as a function of moisture conditions.

Since the manufacturers of typical relative humidity measurement devices specify an accuracy of ± 2 %RH, the Monte Carlo analysis presented in figure 3.10 was placed in context with similar goal values. Assuming that the quality factor of the sensor varies between 30 and 100 as relative humidity varies between 65 % and 100 %, one percentage point of relative humidity corresponds on average to two units of the quality factor. By using 82.2 ± 4 as the goal values, the performed 10 000 sample analysis resulted in a yield of 100.00 %. Thus, if the conductivity and permittivity of the mortar can be controlled reliably, the sensor construction does not limit the accuracy of the sensor from reaching the accuracy of ± 2 %RH.

3.1.4 Outcome

The development of the basic sensor led to two different applications: the plain basic sensor, to be used primarily in bathroom walls and floors, and the pre-cast basic sensor, to be used for monitoring the drying of concrete. Electrically the sensors are similar, but mechanically they are somewhat different.

Plain basic sensor

The basic sensor consists of the laminated circuit board presented above and the assembly mortar that is used to assemble the sensor into contact with the building structure of interest. A photograph of the commercial basic sensor is shown on the left in figure 3.11. The overall measures of the sensor are 80 x 80 x 2 mm. As can be seen in comparison with figure 3.3, the hole in the middle of the inductor was finally left out in order to ease the manufacturing of the sensor. In addition, a large letter S has been printed on the circuit board in order to distinguish the sensing side of the sensor circuit.

Pre-cast basic sensor

Especially in monitoring the drying of concrete, it is necessary to place the sensor deep inside the structure. This could be done with the plain basic sensor, however this would require a very deep hole to be made in order to insert the
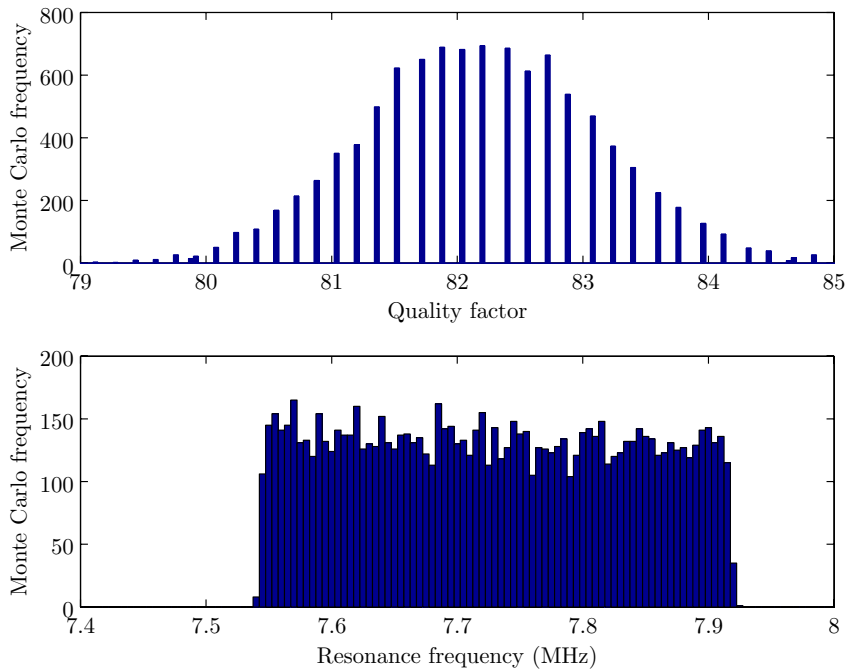
Figure 3.10: The distributions of quality factor and resonance frequency in the Monte Carlo analysis.

Figure 3.11: The commercial version of the plain basic sensor and a pre-cast basic sensor. The plain basic sensor is shown from the *sensing side* labelled with the letter *S*. The pre-cast sensor consists of a plain basic sensor inside a layer of mortar.

sensor into a concrete slab. This in turn could affect the moisture technical functionality of the structure.

The pre-cast basic sensor is a version of the sensor that can be inserted into the concrete slab already during or before pouring the concrete. The pre-cast basic sensor is a plain basic sensor that has been cast into an approximately 10 mm thick layer of assembly mortar prior to the assembly. Thus, the pre-cast basic sensor already includes the mortar layer, so that it can be either placed to its planned location before pouring concrete or alternatively pushed to the desired depth in fresh concrete. The measures of a pre-cast basic sensor are slightly larger than those of the plain sensor, being 95 x 95 x 10 mm. A photograph of a pre-cast basic sensor is shown on the right in figure 3.11.

3.2 Threshold relative humidity sensor

The *threshold relative humidity sensor* or *threshold sensor* is another sensor type that was developed based on the basic sensor. The principle of the threshold sensor is somewhat different from the basic sensor, since the threshold sensor assesses relative humidity more directly. With the threshold sensor, the relative humidity of the air surrounding the sensor, or the air within the pores of the material surrounding the sensor, changes the electrical properties of the sensor resonant circuit. The name threshold sensor follows from the property that the sensor reacts at certain relative humidity levels, thus revealing whether the relative humidity is above or below the threshold value.

The threshold sensor is aimed to be used in several different building structures and applications where it is important to know whether a relative humidity level is reached. Typical applications could be e.g. determining whether a concrete slab has dried enough to be covered with other materials, or whether the conditions inside a structure are favorable for microbe growth. The threshold sensor is also aimed to be affordable, however this criterion is not as strict as with the basic sensor.

The threshold sensor was developed and tested during the research project by Outi Valta, M.Sc.. The development process is described in more detail in her master's thesis [39].

3.2.1 Objective

The objective of the threshold sensor development was to be able to measure the relative humidity of the air inside different materials. This is because, in the Nordic countries, relative humidity is considered to be the most informative quantity for moisture conditions. In addition, the basic sensor described above is suitable for use only with dense materials, with which the assembly mortar can reach hygroscopic equilibrium with, such as concrete. The threshold sensor should be applicable to these materials but also to materials that are not so

dense, such as temperature insulation materials, and air.

Since the measurement principle of the threshold sensor is based on identifying relative humidity thresholds, several different thresholds should be available either in one sensor or in separate sensors. The thresholds should be choosable with intervals of no more than 5 % in the relative humidity range of say 70–100 %. The threshold level of the sensor should also be accurate, the accuracy being no more than ± 2 %, preferably near ± 1 %. The threshold sensor should also be readable with the same equipment as the basic sensor. That is, relative humidity around the sensor should affect the quality factor and the resonance frequency of the sensors. In addition, their values should vary in the same ranges as with a basic sensor. Otherwise, the same objectives hold for the threshold sensor as for the basic sensor. Thus, the sensor should be sufficiently small, readable from a depth of 50–100 mm, physically and chemically durable, and cost-effective. It would also be desirable for the structure of the two sensor types to be similar in order to make manufacturing more effective.

3.2.2   Sensor structure

A cross section illustrating the structure of the threshold sensor is shown in figure 3.12. Electrically the threshold sensor functions similarly to the basic sensor presented above. Mechanically, the sensor is built around the basic sensor that is realized with the printed circuit board (1) with the planar inductor (2) and the surface-mount capacitor on top of it, and the polyethylene laminate (3). On top of the sensing side of the basic sensor, is a material, the conductivity of which changes as a function of relative humidity (4) inside an air pocket (5). Finally, the sensing side of the sensor is covered with a breathing membrane (6) that passes water vapor but not liquid water. The airspace bounded by the breathing membrane functions as an artificial pore that intends to reach hygroscopic equilibrium with the surrounding material.

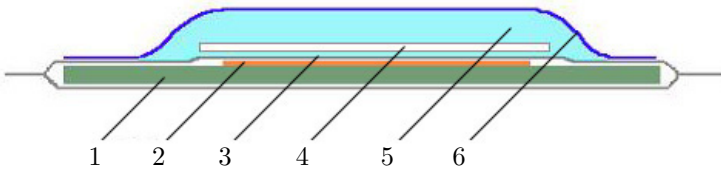*Figure 3.12:* A cross section of the threshold sensor. The sensor includes a planar inductor (2) on a printed circuit board (1). The circuit board has been covered with a polyethylene laminate (3). A material the conductivity of which changes as a function of relative humidity (4) is placed on top of the laminate inside an air pocket (5). The sensing side of the sensor is covered with a breathing membrane (6).

Breathing membrane

The function of the breathing membrane, that water can only penetrate as vapor, is to protect the reacting layer from direct contact with water and impurities. However, the membrane has to pass water vapor at an adequate rate to keep the response time of the sensor reasonable. In addition, since the membrane may be in direct contact with various different building materials, it is important that the membrane can endure the circumstances both chemically and mechanically and that the layer will not get blocked up by particles possibly present inside the building material.

Outi Valta, M.Sc., assessed several different membrane materials in terms of the properties listed above, finally concluding to the use of Goretex (W.L. Gore & Associates, USA), a PTFE-based membrane typically used in the clothing industry. According to her experiments, the chosen membrane does not pass liquid water based on a water column test in normal atmospheric pressure, the membrane passes water vapor efficiently enough for the reaction time of the sensor to be a couple of hours, and the membrane is chemically durable and thus suitable for the alkalic environment of e.g. concrete. However, the membrane material was considered expensive in comparison with the other components of the sensor. As a consequence, other possibilities should still be surveyed if the sensor is to be refined to a commercial product.

Reacting layer

The reacting layer is the sensor component the conductivity of which changes as a function of relative humidity. The change in conductivity at certain threshold relative humidity conditions has been acquired by using different salts. A saturated salt solution absorbs moisture from, and discharges moisture to the atmosphere according to how its equilibrium relative humidity compares to the relative humidity of the surrounding air. As a consequence, when the relative humidity of the air surrounding a salt exceeds the equilibrium relative humidity of the salt, the salt gets wet and the conductivity of the solution increases dramatically. The equilibrium relative humidity values are typical of each salt, thus the choice of salt determines the relative humidity threshold. The equilibrium relative humidity values for some common salts that were considered suitable for the threshold sensor are shown in table 3.10. The levels are presented at the temperature of 20 °C. Since the levels are somewhat temperature dependent, the relative humidity change per temperature change ($d\mathrm{RH}/dT$) is also presented in the list. The list has been put together by Outi Valta, M.Sc. [39, p. 29] based predominantly on the literary search by Koskelo [64, pp. 7–13].

Experiments with using salts on top of the sensor revealed that a matrix of some sort is needed to keep the salts in place. With constructions where salts were spread on top of the sensor as such, soaked into a nonwoven fabric, or bound into place with a plastic net, the salt solution slid off the top of the sensor when the salt got wet. However, a functional reacting layer was acquired by using a

Table 3.10: Equilibrium relative humidity values maintained by salts that were considered to be most suitable for the threshold sensor as assessed by Outi Valta [39, p. 29]. The relative humidity values (RH) at 20 ℃, and the temperature coefficients $d\text{RH}/dT$ are listed.

Salt	Name	RH [%] @ +20 ℃	$d\text{RH}/dT$ [% / ℃]
K_2SO_4	Potassium sulphate	97	-0.06
KNO_3	Potassium nitrate	94	-0.18
$ZnSO_4$	Zinc sulphate	90	-0.3
KCl	Potassium chloride	85	-0.16
$(NH_4)_2SO_4$	Ammonium sulphate	81	-0.07
NH_4Cl	Ammonium chloride	79	-0.13
$NaCl$	Sodium chloride	75	-0.03
KI_3	Potassium iodide	70	-0.21
$CuCl_2$	Copper chloride	68	-0.01

matrix of assembly mortar for the salt. The salt was dissolved into deionized water, which was then used to mix the mortar. A suitable amount of salt in the mortar was found to be approximately 10 % of its weight. The wet mortar was then spread as an approximately 0.5 mm thick layer on top of a plastic net located on top of the sensor. The reacting layer on top of the basic sensor is shown on the left in figure 3.13.
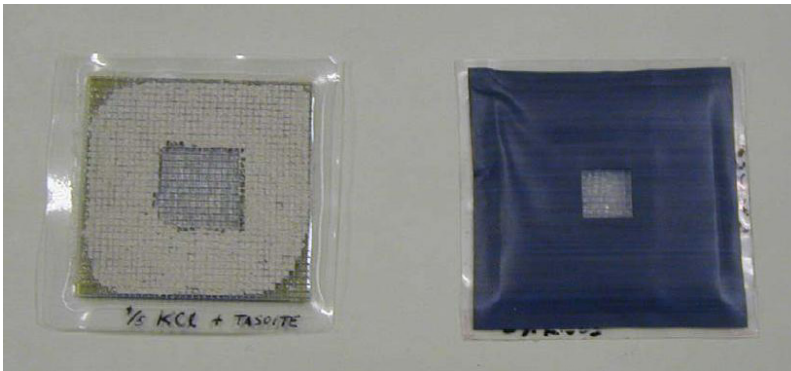

Figure 3.13: The construction of a threshold sensor. The picture on the left shows the reacting layer on top of the sensor. The layer consists of a plastic net and a mixture of the assembly mortar and the salt that determines the humidity threshold. The picture on the right shows the complete threshold sensor where the breathing membrane has been attached on top of the reacting layer.

Multiple relative humidity thresholds can be acquired in one sensor by using multiple salts. In this approach, the reacting layer is divided into separate regions each carrying a different salt. As a result, at each threshold, the salt having the corresponding equilibrium relative humidity gets wet and the quality

factor of the sensor decreases. At the highest threshold, all salts are wet and the quality factor of the sensor reaches its minimum.

3.2.3 Outcome

The development of the threshold sensor has so far led to several different prototypes. The prototypes that include only one salt in their reacting layer, and thus have only one threshold, are referred to as the 97 % threshold sensor, 94 % threshold sensor, etc. based on the salt used. In addition, several two-salt and three-salt sensors have been constructed and tested.

A threshold sensor consists of the basic sensor with a reacting layer and a breathing membrane on top of it. A photograph of a threshold sensor prototype is shown on the right in figure 3.13. The overall measures of the threshold sensor are approximately 80 x 80 x 4 mm. Such as the basic sensor, also the threshold sensor is insensitive to the moisture conditions behind the sensor. Thus the backside of the sensor can be used for assembling the sensor to the desired location, for example by attaching the sensor to a wall material with an adhesive.

3.3 Temperature and moisture sensor with escort memory

A more advanced version of the early basic sensor was developed based on the experiences acquired from the building industry. In addition to the functionality of the basic sensor, the developed *temperature and moisture sensor* includes means for measuring temperature and for identifying each sensor and storing data into it.

The need for including a temperature measurement option arose from the fact that relative humidity is extremely temperature dependent. Thus, the accuracy of measuring moisture conditions could be enhanced if also temperature could be measured at the same measurement location. In addition, most currently used moisture measurement equipment also include means for measuring temperature. As another enhancement, it was considered important to be able to give each sensor a unique identity to be able to, for example, distinguish different sensor types without actually seeing them. Storing calibration data and previous measurement results into each sensor was also considered beneficial, since it could be used to improve the accuracy of the sensor and to reveal trends in the moisture and temperature conditions of the structure under investigation.

The temperature and moisture sensor was developed and tested during the research project by Tuomo Reiniaho, M.Sc.. The development process is described in more detail in his master's thesis [40].

3.3.1 Objective

The objective of the development of the temperature and moisture sensor was to include means of measuring temperature into the basic sensor structure. In addition, the sensor was to be equipped with an escort memory for storing the identity of each sensor, possible calibration data and a small history of measurement results.

The specific objective for the temperature measurement means was to be able to wirelessly acquire temperature data from inside a building structure to append the moisture data. The temperature measurement means should also be as simple as possible, cost-effective and reliable. Once again, also this sensor should endure and function inside for example a concrete structure. In addition, the temperature sensing element and the moisture sensing element should not disturb each other's functionality.

The escort memory, on the other hand, should be able to hold a unique serial number for each sensor, possible calibration data, and the measurement results from at least 5 previous measurements. The memory should also be accessible wirelessly from outside the structure.

3.3.2 Sensor structure

The construction chosen to test the temperature and moisture sensor concept is shown in figure 3.14. In addition to the moisture sensing element (1) that is similar to the basic sensor, the sensor includes a temperature sensing element (2) that consists of a planar inductor and a capacitor, and the escort memory element (3) that has been realized with a commercial RFID transponder. Mechanically the construction of the temperature and moisture sensor is mostly similar to the basic sensor. That is, the planar inductors have been realized on a printed circuit board (A), the board has been laminated with a polyethylene layer (C) and the sensor is attached to the structure of interest with assembly mortar not shown in the picture. However, in this sensor construction, a polymer insulation disc (B) has been placed on top of the temperature sensing element and the escort memory element in order to prevent the capacitive coupling between these elements and the assembly mortar.

Temperature sensing element

Measuring temperature is one the most important and most commonly assessed practical measurement problems. Based on a literary research performed by Tuomo Reiniaho, M.Sc., in addition to a number of non-electrical measurement methods there are several different electrical methods of measuring temperature, including thermocouples, metal-resistor thermometers, thermistors, semiconductor sensors etc. [40, pp. 46–49]. However the approach chosen in the research project is a new one. A parallel resonant circuit consisting of a planar
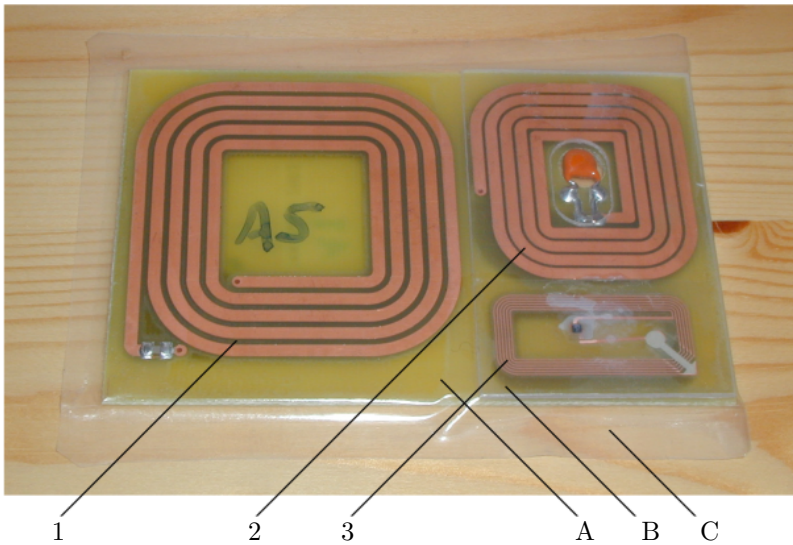
Figure 3.14: The construction of the temperature and moisture sensor. The sensor includes a separate moisture sensing element (1), a temperature sensing element (2) and the escort memory element (3). Mechanically the sensor includes the printed circuit board (A) with the copper coils and discrete capacitors, an insulation disc (B) and the protecting laminate (C).

inductor and a temperature-dependent capacitor is used as a sensing element, the resonant frequency of which is measured. The literary research revealed only cases where temperature-dependent capacitors had been used for temperature-compensating, none where they had been used for measuring temperature [40, p. 73].

In a sense, the capacitor has to be of extremely high quality: it has to be stabile and reliable, since the sensor can no longer be calibrated nor the capacitor replaced after the sensor has been assembled inside a structure. In addition, the losses of the capacitor should be as small as possible so that the quality factor of the sensor is sufficiently large. The higher the quality factor, the larger the signal acquired to the reading device coil according to equation 2.32, and the sharper the resonance curve which in turn eases determining the resonance frequency. The desired temperature dependence can be acquired by using a suitable insulator material between the electrodes of a capacitor. A sufficiently stabile and linear temperature dependence could be acquired with ceramic, class 1 capacitors. However, at the time of the research it was surprisingly difficult to find suitable commercial capacitors.

The moisture sensing element operates approximately at the frequency of 8 MHz. It was considered advantageous for the temperature sensing element to function at a frequency range near this, so that both resonance peaks could be measured simultaneously. The range chosen for the temperature sensing element was around the frequency of 9.5 MHz. The chosen range is not one recommended for inductive applications, as the range of the moisture sensing element [57, p. 40]. However, the applicable magnetic field strength is the same, 9 dBµA/m [58, p. 23].

The chosen temperature-dependent capacitor is a 330 pF Vishay Cera-Mite Low Dissipation Factor 1DF0T33 Disc Capacitor (Vishay Intertechnology Inc. USA). The stability of the capacitors was tested with a cycle test between the temperature of approximately 20 and 60 ℃. The capacitors were considered stabile, since after 40 cycles, their nominal capacitance had increased by 1 pF in average and the differences between each capacitor were quite small, ±1 pF in average. [40, pp. 74–75]

A small problem with the chosen capacitor was their relatively large losses, which would have led to a quality factor of approximately 10–15. The problem was solved by attaching a high-quality surface mount capacitor in parallel with the temperature-dependent capacitor, which results in a decrease in the losses but also a decrease in the frequency resolution of the sensing element. A 220 pF surface mount capacitor was considered appropriate.

The planar inductor of the temperature sensing element did not have as many limiting demands as the one of the moisture sensing element. The inductor was designed to have small losses, a good coupling with the reading device, a smaller area than that of the moisture sensing inductor, and an inductance that would set the resonance frequency to the desired range. The planar inductor

developed for the temperature sensor includes five turns, and the inductance of the inductor is approximately 500 nH.

The functionality of the basic sensor and the moisture sensing element of this sensor is based on the planar inductor coupling capacitively with the environment. With the temperature sensing element, however, this is an unwanted phenomenon. Thus, the electrical properties of the sensing element should not be affected by changes in the electrical properties of the materials surrounding the sensor. Similarly to the basic sensor, a static shield is used on the backside of the printed circuit board behind the inductor. However, a static shield in front of the inductor would require the use of a four-layer circuit board, which is somewhat more expensive but possibly a feasible approach. In the research project, the problem was solved by placing a sufficiently thick polymer insulator between the inductor and the laminate. Based on simulations and practical experiments, a suitable thickness for the polymer was approximately 1.1 mm.

Escort memory

The escort memory of the temperature and moisture sensor has been realized with an RFID transponder. Since both sensing elements of the sensor are read inductively, it is natural to use also an inductively coupled RFID system opposed to an electromagnetic backscatter coupling system. The frequency range around 13.56 MHz was chosen due to its wide use. In addition, the chosen range is close to the ranges of the sensing elements, which eases the design of the reading electronics.

For the prototype of the temperature and moisture sensor, the escort memory element was constructed by attaching a commercial RFID transponder on the circuit board. The transponder used in the sensor is a 14 x 31 mm tag manufactured by Rafsec Ltd., Finland. The tag includes a Philips I-CODE 1 (Philips semiconductors, the Netherlands) integrated circuit. The chip includes everything necessary to access the memory up to the reception of energy and the capacitor that tunes the resonance frequency of the tag.

3.3.3 Outcome

The final sensor prototype, shown in figure 3.14, includes the moisture sensing element that is similar to the basic sensor, the temperature sensing element, and the escort memory element. Each of the elements has a planar inductor of its own. As a consequence, the temperature and moisture sensor is somewhat larger than the basic sensor, being approximately 80 x 110 x 3 mm.

Electrically the prototype includes three resonant circuits, the resonant frequencies of which are approximately 8 MHz, 9.5 MHz and 13.56 MHz. The moisture and temperature sensing elements were planned to be read simultaneously but separately from the RFID transponder.

3.4 Conclusions

The primary objective of the sensor development was to create a sensor that can be assembled in contact with a building material and transforms the moisture conditions to an electrical signal. This objective has been reached with three different sensor structures, of which the basic sensor has been refined to be a commercial product.

As secondary objectives, it was considered desirable for the sensor to measure purely relative humidity and temperature and to be able to store data. The relative humidity measurement has been implemented partially with the threshold relative humidity sensor that can distinguish whether a certain relative humidity level has been exceeded. The temperature measurement and the escort memory, in turn, have been implemented in the temperature and moisture sensor.

Future prospects of the sensor development include developing the sensor into a wide-range relative humidity and temperature sensor applicable to all kinds of building materials and air. In addition, different sensor structures should be considered to minimize the effect of the sensor in dynamic structures and to maximize the reading range in thick building structures.

4 Reading device

A reading device is the part of the measurement system that functions as a link between the sensors and the user of the measurement system. The device is used to locate the sensors inside a building structure, to measure their electrical properties, to interpret the results as moisture and temperature conditions, and to display the results to the user. In addition, the reading device functions as a documenting tool for the system. Since the sensors are kept as simple as possible, all the intelligence in the system is inside the reading device.

The measurement functionality of the reading device is based on measuring the resonance frequency and quality factor of the sensors. To start with, these quantities were measured with several different table setups built around a signal generator, a data acquisition card and a PC with suitable measurement software. However, to be able to perform the measurements in the field, a hand-held reading device had to be developed. This chapter focuses on the design of a prototype and a commercial version of the hand-held reading device. In addition, several enhancements and suggestions for improvement are presented.

4.1 Frequency sweeping reading device

The hand-held reading device that has been given most attention during the research project is referred to as the *frequency sweeping reading device*. The name of the device follows from the method with which the device determines the frequency response of a sensor, by sweeping the measurement frequency throughout the measurement band. The research project led to the development of a frequency sweeping reading device prototype which was later refined to be a commercial product. This section describes the design and functionality of the developed reading device with the focus on the commercial version.

4.1.1 Objective

The objective of the development of the frequency sweeping reading device was to create a hand-held device for locating and measuring the resonance frequency and quality factor of the sensor circuits located inside building structures. The device should also be able to calculate and display the corresponding moisture conditions to the user. In addition, the user interface of the device should be clear and easy to use, even in poorly illuminated spaces.

To be applicable at the field, the reading device should be wireless at the time of measurement, thus it should be powered with a rechargeable or disposable battery. Despite the limitations of using a battery, the maximum reading range,

i.e. the distance between the device and a sensor, should be at least 50 mm, preferably 100 mm, and the battery should still last long enough for measuring, say, several hundreds of sensors.

Finally, the reading device should also function as a documenting tool for the measurement results. Thus, it should include a possibility to store and view the results and to later upload them to a PC.

4.1.2 Hardware design

A block diagram of the hardware of the frequency sweeping reading device is shown in figure 4.1. The hardware has been built around a microcontroller (µC) that interfaces the user via a display and a keypad, the RF electronics via a D/A converter (DAC), three FET switches, a counter and an A/D converter (ADC), and a PC via a programming interface and a serial interface. The device is powered with a battery through the power electronics.
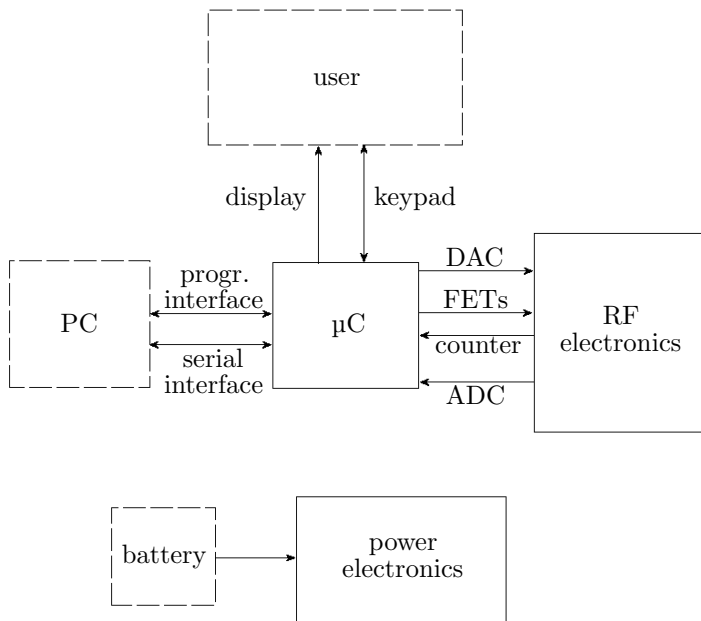

Figure 4.1: A block diagram of the hardware of the reading device. The hardware is built around a microcontroller (µC) that interfaces the user of the device, the RF electronics, and a PC. The device is powered with a battery.

The mechanical design of the hardware has been limited by the mechanics of the chosen enclosure Datec-Control XS (OKW Gehäusesysteme GmbH, Germany) shown in figure 4.2. The enclosure is quite small and hand-held, however its shape is still suitable for the design of an antenna coil. The figure also shows

the apertures processed for an LCD display and for the cable of a keypad.

Figure 4.2: The enclosure of the reading device Datec-Control XS (OKW Gehäusesysteme GmbH, Germany) with apertures processed for a display and a keypad cable.

Power electronics

The device was chosen to function with a disposable 9 V or a rechargeable 8.4 V PP3 can battery. The integrated circuits of the reading device, however, require a supply voltage of approximately 5 V. The supply voltage for them has been created with a linear regulator, LM2936 (National Semiconductor, USA).

Digital electronics

The heart of the frequency sweeping reading device is a microcontroller, AT-MEGA32, (Atmel Corporation, USA) that runs a program written in C. The key features of the used microcontroller are shown in table 4.1. In the reading device, the microcontroller is used with a supply voltage of 5 V and an external quartz crystal of 6 MHz.

The user interface of the reading device is built on a graphic liquid crystal

Table 4.1: Essential parameters of the microcontroller, ATMEGA32 (Atmel Corporation, USA) [65].

Paramater	Value
Flash program memory	32 kB
EEPROM	1 kB
SRAM	2 kB
Clock speed	0–16 MHz
Voltage	4.5–5.5 V
I/O pins	32
Peripheral features	8-channel 10-bit ADC
	2 x 8-bit & 1 x 16-bit timer/counter
	Programmable serial USART

display, LM4064 (Densitron Technologies plc, United Kingdom), and a 2x3-key matrix film keypad, BasicLine Datec Control XS (TES Frontdesign GmbH, Germany). The display includes an on-board controller, SED 1560 LSI (Seiko-Epson Corp., Japan), and a LED backlight. A graphic display was chosen for the reading device because of its versatility in the design of the user interface. The backlight was also considered necessary to be able to use the device in poorly illuminated conditions.

A serial interface has been included to the reading device in order to be able to upload measurement results to a PC. The physical interface on the reading device side is a 6-pin miniature DIN-connector which can be connected to the serial port of a PC with a suitable cable. The communication takes place between the Universal Synchronous and Asynchronous Receiver Transmitter (USART) in the microcontroller and a terminal program running on a PC. However, since the microcontroller operates with a single-ended 5 V operating voltage, and the serial port of a PC is specified to function with up to ±15 V, a transceiver (transmitter and receiver) circuit, MAX-222 (Maxim Integrated Products, Inc., USA), is used to convert signals from a voltage level to the other [66].

The resonance frequency and quality factor measurements are performed with the radio frequency (RF) electronics of the reading device, described in more detail below. The interface between the microcontroller and the RF electronics consists of an external D/A converter, the 16-bit counter and the A/D converter of the microcontroller, and three digital FETs. The 12-bit serial D/A converter, AD5320BRM (Analog Devices, USA), is used to control the measurement frequency of the RF electronics. The resulting frequency is measured with the counter and the frequency response of the sensor circuit is digitized with the A/D converter. The FETs are used as switches to turn the RF electronics on and off and to change the magnitude of the measurement signal.

RF electronics

As stated in chapter 2, the wireless interface between a reading device and a sensor has been realized with inductive coupling. Thus, the resonance frequency and quality factor of a sensor are determined from the changes that the sensor induces to the frequency response of the reading device coil. In the frequency sweeping reading device, the frequency response is acquired by sweeping the measurement frequency throughout the measurement band and measuring the impedance of the antenna coil. This is done with the radio frequency (RF) electronics of the reading device.

The RF electronics of the frequency sweeping reading device were developed in co-operation with VTT Automation, Measurement Technology, currently known as VTT Information Technology, Microsensing. The RF electronics consist of a voltage controlled oscillator (VCO), a band pass filter, a voltage controlled current source, an antenna coil, a receiver and an amplifier. A block diagram of the RF electronics together with the interface to a microcontroller and a sensor is shown in Figure 4.3.

The first stage of the RF electronics is a VCO, a voltage controlled oscillator, 74HC4046 (Philips Semiconductors, the Netherlands), that creates a square wave signal, the frequency of which is proportional to the output voltage of the D/A converter. The mapping between frequencies and voltages is defined by two external resistors and one capacitor. The external components have been chosen so that the measurement frequency band between 7.5 MHz and 8.3 MHz is covered. The band was chosen to be sufficiently wide to cover the bandwidth of the basic sensor in all moisture conditions. The output voltage of the VCO is led to the 16-bit counter inside the microcontroller through an external ripple counter 74HC4040 (Philips Semiconductors, the Netherlands) in order to be able to measure the acquired frequencies. The external counter is used to divide the frequency since the actual measurement frequencies are too large for the counter of the microcontroller.

The second stage of the RF electronics is a passive third degree band-pass filter with the pass-band starting at 7 MHz and ending at 9 MHz, thus leaving some space to adjust the measurement band within this range. The function of the filter is to remove harmonic frequencies of the square wave acquired from the VCO. The goal of the filter design was to achieve as flat a pass-band as possible by using E24 component values, with each stage of the filter consisting of an inductor and two capacitors.

The magnetic field required for the measurement is produced by feeding current to the antenna coil with a voltage controlled current source (VCCS). The current source has been realized with a bipolar junction transistor (BJT), BFQ17 (Philips Semiconductors, the Netherlands). The filtered voltage of the VCO output controls the base voltage of the transistor, which in turn controls the current through the coil that has been connected to the collector. This ap-
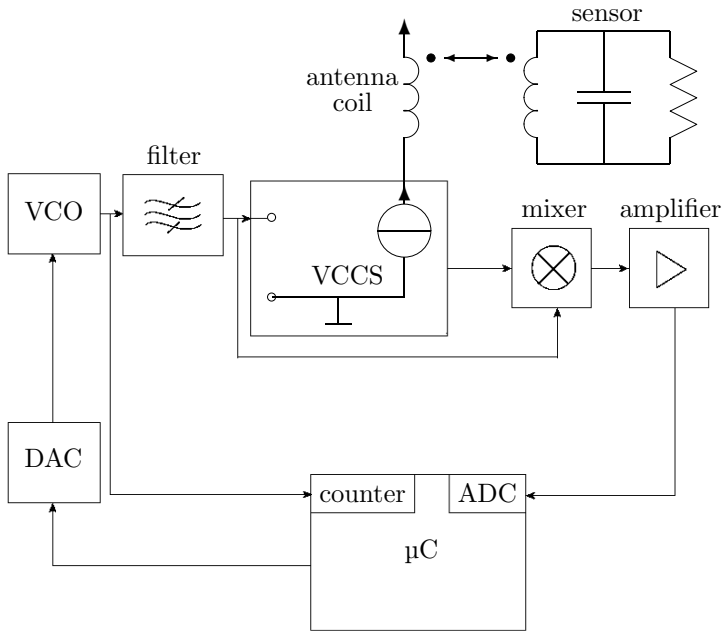
Figure 4.3: A block diagram of the RF electronics of the reading device, its interface to the microcontroller, and coupling with a sensor. The microcontroller controls the output frequency of a voltage controlled oscillator (VCO) through a D/A converter (DAC). The output frequency of the oscillator is measured with a 16-bit counter inside the microcontroller. The output signal of the VCO is also filtered and led to a voltage controlled current source (VCCS) that feeds the antenna coil. The antenna coil is inductively coupled with the inductor of a sensor resonant circuit. The signal resulting from the sensor to the antenna coil is detected, amplified, and finally digitized with the A/D converter inside the microcontroller.

proach aims to keep the feed impedance high, thus making the antenna current easily controllable. As a result, the voltage across the coil is proportional to its impedance. Since the sensor resonant circuit, that is inductively coupled with the antenna, affects its impedance, the antenna voltage also includes the properties of the sensor.

Only the real component of the coil impedance is measured, since it has, as demonstrated in chapter 2, sufficient information about the properties of the resonator: the resonance frequency and the quality factor. The real component is separated from the signal by mixing the RF signal from the collector of the transistor with the local oscillator (LO) signal of the emitter, assumed to be in phase with the coil current, using a double-balanced mixer, SA612AD (Philips Semiconductors, the Netherlands). Thus, the mixer is used as a phase detector. As a consequence, the filtered output voltage of the mixer is ideally a DC voltage proportional to the amplitude of the voltage across the antenna coil and the cosine of the phase difference between the antenna voltage and antenna current, i.e.

$$
\begin{aligned}
U_{\text{det}} &\propto |U_{\text{RF}}|cos(\Delta\phi) \\
&\propto \Re\{Z_{\text{in}}\},
\end{aligned}
\tag{4.1}
$$

where U_{det} is the voltage at the output of the detector, U_{RF} is the RF voltage across the antenna coil, $\Delta\phi$ is the phase difference between the RF and LO voltages, and $\Re\{Z_{\text{in}}\}$ is the real component of the sensor impedance according to equations 2.31 and 2.1 [67, p. 202] [49, 559–572]. Thus, if the resistance of the antenna coil is neglected, the voltage U_{det} is proportional to the real component of the impedance of the sensor. Since the VCO frequency is swept throughout the frequency band of interest, the resonance curve, characteristic of the sensor, is acquired.

The detected voltage is amplified with a differential operational amplifier configuration. The used operational amplifier is MAX4165 (Maxim Integrated Products, Inc., USA). After amplification, the signal is once again filtered and guided to the A/D converter inside the microcontroller.

Hardware outcome

Figure 4.4 shows the final outcome of the hardware development, the commercial reading device. The electronics of the reading device and the connectors for the display, keypad and serial interface have been constructed on a 4-layer printed circuit board, the outer layers of which can be seen in the figure. In addition, the display, the keypad, and a mask label have been attached to the enclosure as can bee seen from the front view (a). The behind view (b) also shows the antenna coil on the upper edge of the circuit board.
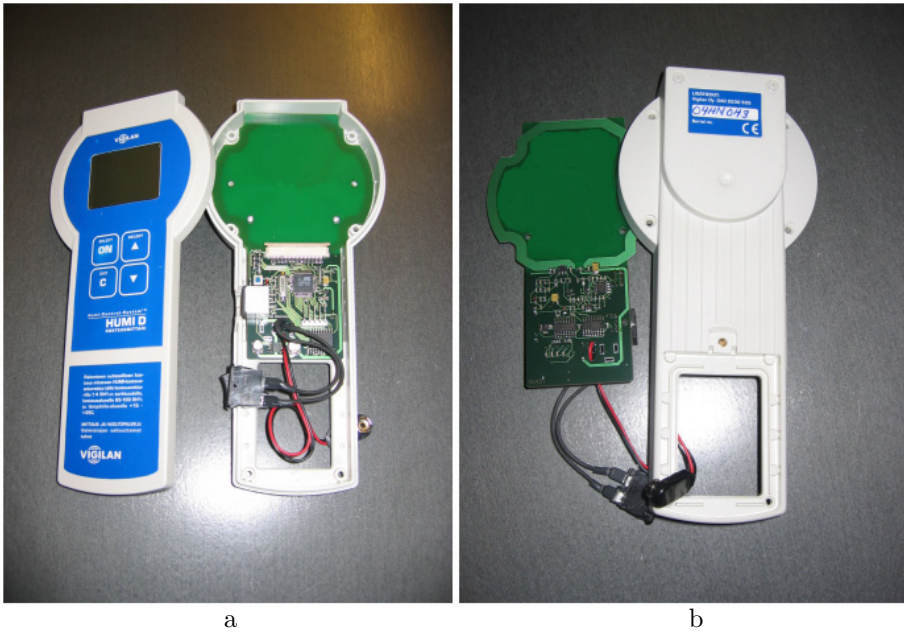
Figure 4.4: The construction of the commercial reading device from the front (a) and from behind (b) including a printed circuit board, the enclosure with the display and keypad, and several connectors and cables.

4.1.3 Software design

Figure 4.5 shows a block diagram of the software of the reading device. When the device is powered on, it performs some initializations of the peripherals and loads the stored settings into the random access memory. The program then enters the main menu, from which the settings menu, memory menu and the measurement path can be entered. The settings menu includes five changeable settings: the target of the measurement, e.g. a bathroom, the backlight of the display on / off, the contrast of the display, displaying of the quality factor and resonance frequency on / off, and language. The memory menu includes a possibility to view the status of the data memory, browse through the saved measurement results, to send them to a computer, and to clear the data memory. The measurement path, described in more detail below, includes the software for locating a sensor and for performing the actual measurement.

Development environment

The software of the reading device was developed and debugged using Atmel AVR STK500 (Atmel Corporation, USA), a starter kit and development system for the Atmel AVR microcontroller family. The programming environment used was AVR Studio 4.07 (Atmel Corporation, USA). The software was written in C and compiled with ICCAVR 6.29 (Imagecraft Creations Inc., USA).

Measurement software

The measurement path of the frequency sweeping reading device, is the part of the software that is used to find a sensor, to determine its resonance frequency and quality factor, and to calculate the corresponding relative humidity. As stated above, the resonance frequency and quality factor are calculated from the frequency response of the sensor. The frequency response is acquired by sweeping the measurement frequency throughout the measurement band of approximately 7.5 MHz to 8.3 MHz and by measuring the signal acquired to the A/D converter. The sweep is done by feeding 50 equally spaced voltages to the VCO through the D/A converter. The signals acquired to the A/D converter correspond to the real component of the impedance of the antenna coil at each frequency.

The measurement software follows the path shown in figure 4.5. Before measuring anything, the user is quoted to select and manage a file in which to store the measurement results. The measurement electronics are then turned on, and the battery voltage is measured in order to determine whether it is high enough for the measurement.

Before performing the actual measurements, some calibration measurements are made. Since the operating range of the VCO is determined with external components the values of which vary, the voltages corresponding to the end
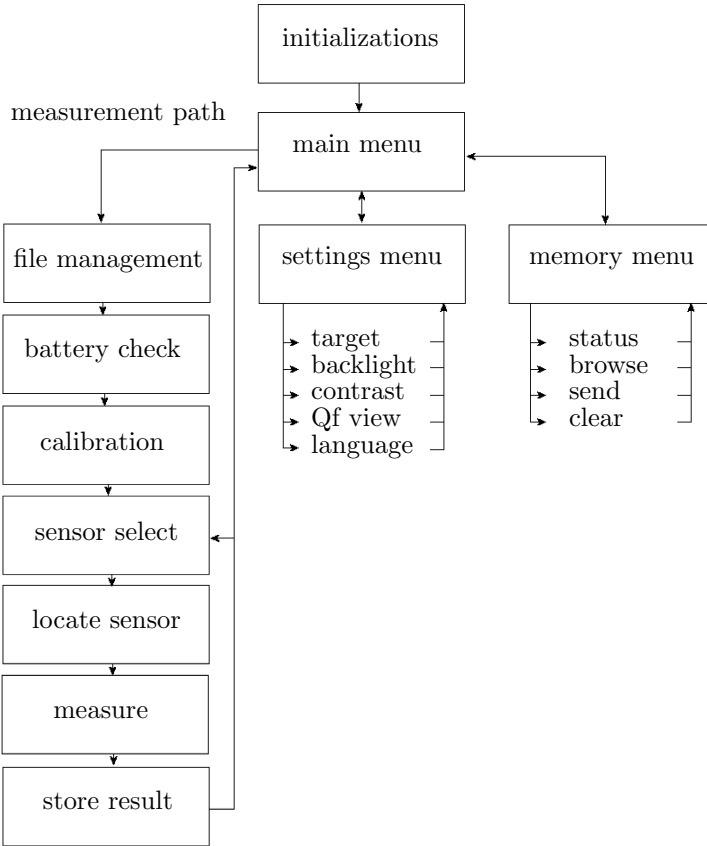
Figure 4.5: Block diagram of the software of the reading device. After initializations, the program enters the main menu. The settings menu, memory menu, and the measurement path can be accessed through the main menu. The measurement path includes managing measurement data files, checking the battery voltage, performing a calibration measurement, and for each sensor selecting it, locating it, measuring its properties, and storing the result.

points of the frequency band are measured with the counter. In addition, the base value of the measurement signal, i.e. the real impedance of the antenna coil, without a sensor involved, is measured as a function of frequency. The measurement is performed by averaging 20 sweeps of the measurement frequency span.

The next step of the measurement is selecting one of the sensors in the chosen measurement file and finding its location. The exact location is found by displaying the magnitude of the response of the sensor graphically to the user that can then move the device to the optimal location. If the reading device is taken too close to a sensor, the signal is too large for the dynamics of the receiver. On the other hand, if the reading device is too far from a sensor, the signal is too small for a reliable measurement. The locating algorithm does not allow measuring in these circumstances. The magnitude of the response is obtained by sweeping continuously throughout the measurement band, calculating the response of the sensor by subtracting the base level acquired earlier from the frequency response, and calculating the integral of the response signal. The integral is used instead of the signal amplitude because the integrals acquired from sensors of different quality factors, at the same distance from the device, are approximately equal. In addition, the maximum time for the location finding phase has been limited to 20 seconds, in order to prevent the battery from wearing down accidentally.

The actual frequency response measurement of the sensor is divided into two phases. First, 20 frequency sweeps throughout the entire measurement band are performed, and their average is calculated. The base level determined earlier is subtracted from the sweep result with adjusting according to possible changes with time and temperature. According to the resulting frequency response, the second sweep set is limited to the neighborhood of the resonance peak. The new start and stop frequencies of the sweep are determined as the points around the peak where the amplitude has reached one third of the maximum value. The second sweep set around the resonance peak is also performed by averaging 20 frequency sweeps. The peak voltage and the -3 dB points are determined and the frequencies corresponding to these points are measured with the counter. The frequency corresponding to the resonance peak is the resonance frequency, and the ratio of the resonance frequency and the -3 dB bandwidth is the quality factor.

Sensor type and material dependent calibration curves are finally used to determine the relative humidity corresponding to the quality factor and resonance frequency of the sensor. The result is displayed to the user, and the user may choose whether he wants to store the measurement results. The program then returns to selecting another sensor for measurement.

User interface software

The user interface of the frequency sweeping reading device has been built around four keys of the keypad and the graphic liquid crystal display, both of them described earlier. The graphic display allows the utilization of both text and various graphical shapes. They have been used to create menu structures, text blocks, different graphical indicators etc..

Figure 4.6a shows a screenshot from the main menu of the reading device. The menu itself includes the name of the menu and three menu items, one of which is highlighted. The two rightmost buttons of the keypad can be used to change the selection, and the two leftmost buttons to go forward and backward in the menu structure. The bar on the right indicates the voltage of the battery. Also the other menus visible in the block diagram of figure 4.5, and the user interface for managing stored measurement results function similarly, thus they are not assessed here in more detail.

Another important part of the user interface is the one for finding a sensor located inside a building structure. A screenshot of this stage is shown in figure 4.6b. In this screen, in addition to the bar on the right that indicates the battery voltage, another bar on the left shows the magnitude of the coupling with a sensor. Thus, based on this bar the user can move the device to the location optimal for the measurement. The large OK text indicates, that the prevailing location is suitable for measurement. If the device is too far from or too close to a sensor, this is also indicated to the user. Finally, the target of the measurement is shown in the upper left corner of the display.

After the measurement is performed, the results are displayed to the user. The measurement result view is shown in figure 4.6c. The view includes the measurement result as relative humidity, which is less than 65 % in the example. In addition, the quality factor and resonance frequency of the sensor circuit are shown below the RH reading if the Qf view setting is activated. A typical user of the reading device, however, would have no interest in them. The labels on the bottom of the screen indicate that the upper left button accepts and stores the measurement result and the upper right button discards the result.

4.2   Reading device enhancements

The path of the frequency sweeping reading device led to a prototype and finally to a commercial product. However, several enhancements for the reading device side were assessed, that so far have not reached the commercial product. This section describes the most promising ones: the fourier reading method, measuring ambient environmental conditions, and storing measurement results to a sensor.
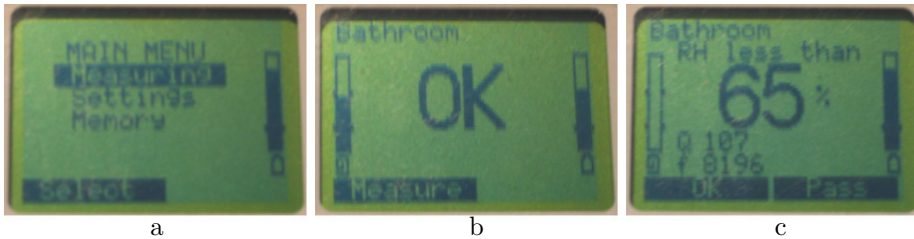
Figure 4.6: Screenshots from the user interface of the reading device: the main menu (a), locating a sensor (b), and the measurement result view (c)

.

4.2.1 Fourier reading method

A different kind of an approach for acquiring the frequency response of a sensor was also assessed during the research project. While the frequency sweeping reading device measures at one frequency at a time, the Fourier reading method uses a broadband stimulus, and acquires the frequency response with a Fourier transform. The electronics for the Fourier reading method were developed during the research project by Juho Partanen, M.Sc.. The electronics and the development process is described in more detail in his master's thesis [41].

Figure 4.7 shows a possible block diagram of the electronics of a Fourier reading device. The used broadband stimulus could be noise or a digitally synthesized signal. The stimulus signal is then amplified and filtered and used to control the current through the antenna coil. The voltage across the coil is then once again amplified and filtered and led to an A/D converter. The time-domain signal is then transformed into frequency-domain with a Fast Fourier Transform (FFT) algorithm in a digital signal processor (DSP). The resonance frequency and quality factor of the sensor can then be determined from the response and presented to the user.

Juho Partanen's master's thesis led to the development of a reading device prototype that uses a zener diode as the source for noise [41]. However, up to now, the prototype has not proven to function better as a whole than the frequency sweeping reading device.

4.2.2 Ambient temperature and relative humidity

A common practice in performing relative humidity measurements in building structures professionally, is to include the indoor and outdoor relative humidity and temperature readings to the measurement results. They provide additional information about the moisture technical status of the structures and expected changes in the near future. As a consequence, it was considered beneficial to
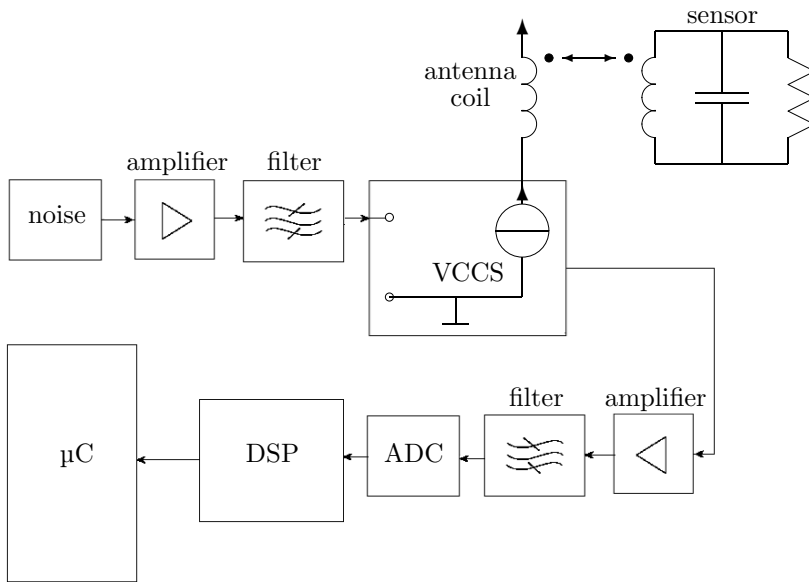
Figure 4.7: A suggested block diagram of a Fourier reading device. A noise generator is used to generate a broadband stimulus which is amplified and filtered to the exact measurement frequency band. The voltage is used to control the current through the antenna coil with a voltage controlled current source (VCCS). The sensor signal from the antenna voltage is amplified, filtered, and digitized with an A/D converter (ADC). A digital signal processor (DSP) is used to calculate a Fourier transform of the measured signal. The acquired frequency response is then transferred to a microcontroller (µC) for further analysis.

include a possibility for these measurements to the reading device.

Measuring temperature and relative humidity in indoor or outdoor air is a significantly less demanding task than measuring them inside structures. In addition, the used sensor can be easily replaced and possibly calibrated. There are several commercial sensors available for the purpose. In the research project, a digital relative humidity and moisture sensor SHT11 (Sensirion AG, Switzerland) was tested successfully in the reading device.

4.2.3 Storing measurement results to a sensor

The temperature and moisture sensor described in the previous chapter includes an escort memory for storing calibration data and measurement results. The escort memory has been realized with an RFID tag attached to the sensor. To be able to access the memory, RFID coupler electronics have to be integrated to the reading device.

RFID technology at the used 13.56 MHz frequency is reasonably well-established at the moment. As a consequence, there are several commercial RFID coupler modules available. The concept of writing measurement results to and reading from the escort memory was tested by integrating a RFID coupler, GemWave™ Medio S001 (TAGSYS, France) to the reading device.

4.3 Conclusions

The primary objective of the reading device development was to create a handheld device for locating and measuring the electrical properties of the sensor circuits inside building structures, and for calculating and displaying the corresponding moisture conditions to the user. This objective was reached with the frequency sweeping reading device that was finally refined to a commercial product.

Secondary objectives of the reading device development included a possibility to use the device as a documenting tool for measurement results and a possibility to measure temperature inside structures, and humidity and temperature in indoor and outdoor air. The documenting tool option has partially been implemented in the frequency sweeping reading device as a possibility to store measurement results and to upload them to a computer. The documenting could also benefit from storing measurement results to a sensor, which has been proven to work separately from the commercial reading device. Also, the additional measurements have been implemented and tested separately.

Future development prospects include utilizing the Fourier reading principle in the reading device and integrating the developed enhancements to the device. Finally, in addition to the hand-held reading device, a portable reading device that reaches significantly larger distances of say 30 cm could be useful in locating

and measuring sensors in thick structures.

5 Laboratory measurements

The developed measurement system and several different prototypes that implement the measurement method have been tested in numerous laboratory tests throughout the research project. The functionality of the system has been tested mainly in comparison with relative humidity measurements, since they represent the current best practice of moisture related measurements in the Nordic countries. A significant part of the measurements have been carried out at the Applied Electronics Laboratory in Helsinki University of Technology by the project staff, however some of the most important measurement results have been acquired in cooperation with Humittest Ltd. at their premises.

This chapter describes the general laboratory experiment process during the research project, and then presents the most significant experiments and their results. Finally, some conclusions are drawn based on the laboratory experiments.

5.1 General

5.1.1 Equipment

The measurement equipment used in the laboratory experiments consists of two parts, the reference measurement equipment and the tested measurement equipment.

Nearly all of the reference measurements have been performed with HMP44 and HMP42 relative humidity and temperature probes (Vaisala Inc., Finland) and the HMI41 humidity and temperature indicator (Vaisala Inc., Finland). The manufacturer of this equipment states the measurement accuracy to be ± 2 %RH ($0\ldots90$ %RH) and ± 3 %RH ($90\ldots100$ %RH) at $+20$ ℃, however even better accuracy can be reached with regular calibration [31, p. 12–13] [36]. Vaisala does not report the coverage factors of the accuracy values. A detailed analysis of the sources of uncertainty with similar probes is presented by Anders Sjöberg in his PhD. thesis [68, pp. A1 1-20]. Sjöberg reports the total standard deviation of the drilled hole measurement in concrete to be up to 3 %RH.

The quality factors and resonance frequencies of the tested sensor circuits were determined initially with a signal generator based measurement setup. The setup included an arbitrary waveform generator, Agilent 33250A (Agilent Technologies, USA), that created a sinusoidal measurement signal the frequency of which was swept throughout the measurement band. The measurement signal was led to a transmitter coil that created the magnetic field required for the

measurement. A separate receiver coil was used to acquire the signal induced from the sensor. The signal was then led to an envelope detector and further to a data acquisition card (ADC-11, Pico Technology Limited, United Kingdom) in a PC. The PC was used to calculate the resonance frequency and the quality factor of the sensor circuit and to present it to the user. A laboratory measurement setup, including the signal generator based measurement system and an HMP42 probe and an HMI41 indicator (Vaisala Inc., Finland) as reference measurement equipment, is shown in figure 5.1. Further on, as the hand-held reading device was developed, it gradually replaced the signal generator based system, since it was significantly simpler to use and considered to be more reliable.
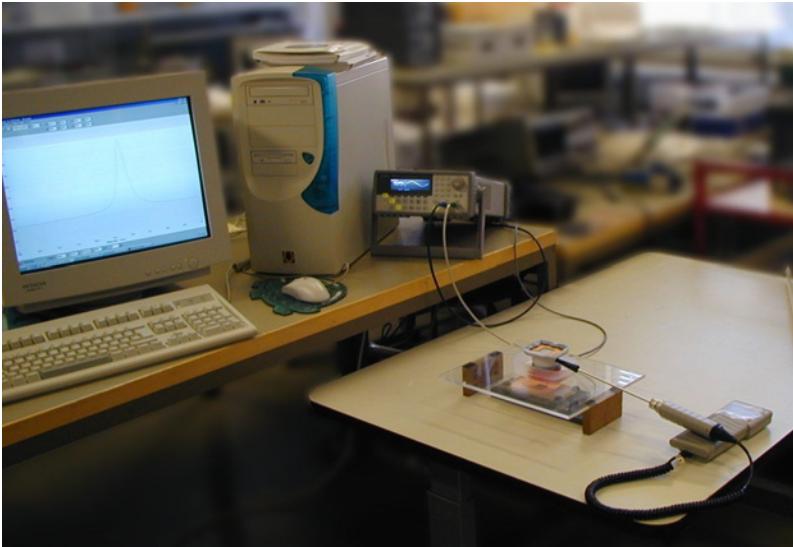

Figure 5.1: A laboratory setup for testing a sensor prototype. On the table, the prototype is in contact with an artificial pore. An HMP42 probe and an HMI41 indicator (Vaisala Inc., Finland) are used to measure the relative humidity and the temperature of the pore as a reference measurement. The quality factor and resonance frequency of the sensor prototype are measured with a setup that consists of an arbitrary waveform generator Agilent 33250A (Agilent Technologies, USA), a two-coil based coupling unit with an envelope detector, and a PC including a data logger card (ADC-11, Pico Technology Limited, United Kingdom).

5.1.2 Experiment process

At the early stage of the project, most of the laboratory measurements were performed at the Applied Electronics Laboratory in Helsinki University of Technology, even though measuring relative humidity is a demanding task that is not an area of expertise in the laboratory. However, the acquired accuracy was adequate for developing the system in the early stage. Later on in the research project, the reference relative humidity measurements were passed on to Hu-

mittest Ltd. in order to acquire the best available accuracy. Finally, Humittest Ltd. performed some of the laboratory experiments independently, thus using also the developed measurement system.

The first suggestive tests in the Applied Electronics Laboratory were used for determining a suitable structure for the sensors. As stated in chapter 3, the design of the basic sensor included the optimization of several interdependent parameters. Suitable parameters were acquired with the help of iterative simulations, however different sensor constructions were also tested in laboratory experiments with different building materials. The most significant gain of these experiments was discovering a suitable mortar used for assembling the basic sensors. Typically the experiments included assembling a sensor prototype into a thin layer of a construction material, or onto the surface of a material by using mortar. A hole was then made into the structure, to a location similar to where the sensing side of the sensor prototype is located. A relative humidity probe, typically HMP44, was then entered into the hole. The structure was then watered and let dry in cycles. The quality factor and resonance frequency readings corresponding to different relative humidity readings were measured with the signal generator based measurement setup described above. The setup of figure 5.1 could be considered a typical measurement setup.

Further on, as the sensor structure established, the focus of the laboratory experiments moved towards obtaining reliable dependency models between quality factor and relative humidity readings. Thus, the accuracy of the relative humidity measurements became a more important issue. At that stage, the relative humidity reference measurements were passed on to Humittest Ltd., since they have significant experience of measuring relative humidity in construction materials and a routine measurement and calibration process. The measurements with the developed measurement method were performed with the established sensors and the signal generator based measurement setup. However, as a prototype of the hand-held reading device evolved, the signal generator based setup and the hand-held device were used side by side.

The latest measurement results were acquired by Humittest Ltd. with an early version of the commercial measurement system. Marko Leskinen, an employee at Humittest Ltd., did his bachelor's thesis about the suitability and accuracy of the system in measuring relative humidity in building materials [69]. The thesis covers five test sets that aimed to test whether the system was ready for different field applications.

5.2   Measurement examples and results

Some representative examples of the laboratory experiments are presented. The experiments and results are divided by application into the basic sensor tests and threshold sensor tests.

5.2.1 Basic sensor

The experiments performed with the basic sensor aimed to determine the dependency between the quality factor of the sensor and the prevailing relative humidity in the material of interest, and to test the reliability of the system in different conditions. The tests were performed with respect to the two primary application areas of the basic sensor, the bathroom application and monitoring the drying of concrete.

Bathroom application

The applicability of the basic sensor in bathrooms was tested with several experiments where the basic sensor was cast into the surface parts of an assembly mortar block or attached to different materials with the assembly mortar, or a pre-cast sensor was pressed to a similar location. At the early stage of the research project, tests were performed at the Applied Electronics Laboratory at Helsinki University of Technology in order to obtain a conversion curve between the quality factor of the sensors and the prevailing relative humidity. One typical experiment is one where pre-cast basic sensors were pressed into the surface parts of blocks of two normal concrete types, floor concrete of the strength class K30 (LA30), and normal concrete of the strength class K35 (K35) (Lohja Rudus Ltd., Finland). The blocks were let dry to the relative humidity of approximately 80 %RH and then were watered again. The quality factors of the sensors were determined with the signal generator based measurement setup. The reference relative humidity, on the other hand, was determined with an HMP42 relative humidity and temperature probe and an HMI41 indicator (Vaisala Inc., Finland). The measurement results from this experiment are shown in figure 5.2. Together with the measurement results is shown the curve that the reading device uses to map quality factor readings to relative humidity. The curve has been determined empirically from this experiment and several others.

The results of figure 5.2 seem to indicate, that the basic sensor functions similarly at the surface parts of the two concrete types. Within the shown measurement data, the deviations of the measurement results from the mapping curve are less than ±2 percentage points.

Marko Leskinen presented in his bachelor's thesis an experiment where the developed basic sensors were tested in a cellular concrete board (H+H Siporex Ltd., Finland) behind two different waterproofing materials under constant moisture stress. The sensors were assembled with the assembly mortar into cavities that were made into two boards, two sensors in each, one towards the waterproofing, one the other way. Measurement pipes for HMP44 relative humidity and temperature probes (Vaisala Inc., Finland) were also installed into the board directly below the waterproofing and to a depth of 20 mm. The waterproofed boards were placed in direct contact with water. Even though waterproofing materials permeate water vapor in some extent, the relative humidity according
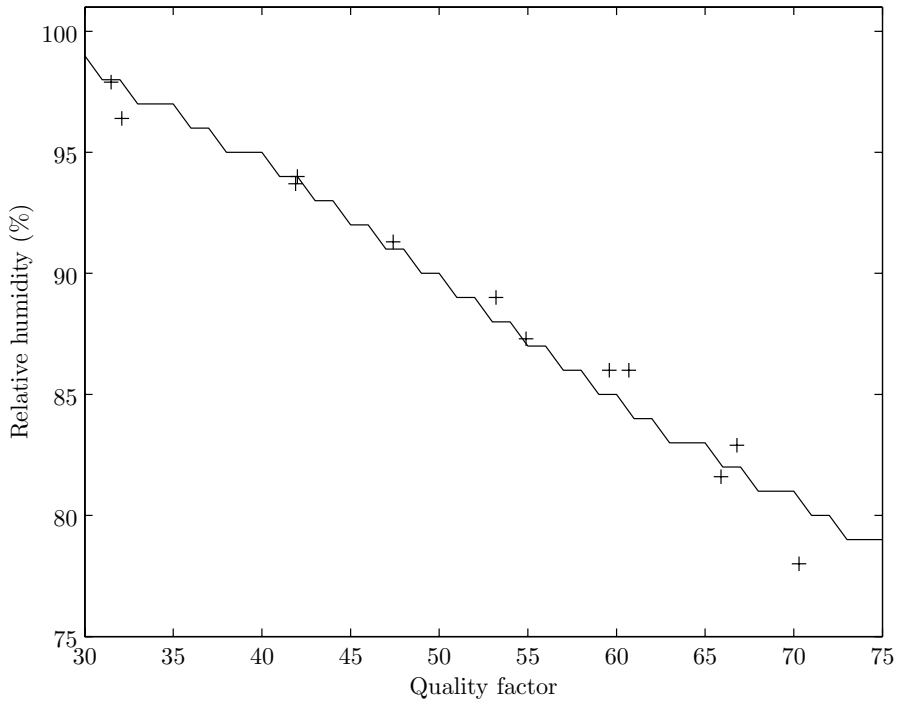
Figure 5.2: The relative humidity at the surface of LA30 and K35 concrete correspond-
ing to the quality factor of a pre-cast basic sensor. The measurement results of two
test blocks are represented by +-symbols. The solid trace represents the conversion
curve of the commercial reading device.

to the HMP44 probes nor to the basic sensors did not increase significantly. After a long moisture stress, the waterproofing layers were broken by cutting them with a knife. The relative humidity values acquired from the basic sensor facing towards the waterproofing started to increase immediately. The values acquired from the sensor facing the other way started to increase significantly after approximately 18 hours had passed from the damage. The values measured with the HMP44 probe at the depth of 20 mm started to increase significantly approximately 5 hours after the damage. Thus, it seems that in the tested material, the relative humidity does not increase significantly due to the normal use of a bathroom according to either measurement method. However, an exceptional moisture stress, such as damaged waterproofing can be perceived with either method in a matter of hours from the damage. [69]

Another test, indicative of the bathroom application, performed by Marko Leskinen, is one that aimed to test the functionality of pre-cast basic sensors under a floor covering. The test was made with three different floor covering structures, one of them a residential plastic carpet that was considered to be relatively permeable to water vapor (Upostep, Upofloor Ltd., Finland). The other two, a commercial plastic carpet Tarkett Optima (Tarkett AG, Germany) and parquet with a Tuplex sound resistant underlayment (Tuplex Corp., USA), were considered significantly less permeable. The setup was made by pressing four pre-cast basic sensors to the surface parts of three blocks of fresh normal concrete of the strength class K30 (Lohja Rudus Ltd.) each, two of them facing downwards and two of them upwards. In addition, pipes for HMP44 probes were assembled to the level of the blocks' surfaces. When the relative humidity at the depth of 30 mm inside the blocks reached 90 %, the surfaces of the blocks were grouted and a week later covered with one floor covering material each. The measurement results from the pre-cast sensors that faced down under the nonpermeable covering materials were consistent with the reference measurements. However, under the more permeable material, the downwards facing sensor did not react to the drying process significantly. Thus, it seems that the basic sensor buffers moisture similarly to the nonpermeable materials and functions better in such conditions. The measurement setup and the results are presented in more detail in Marko Leskinen's bachelor's thesis [69].

Drying of concrete

The applicability of the basic sensor in monitoring the drying of concrete has been tested with several experiments where pre-cast basic sensors have been inserted into a block of concrete. Figure 5.3 shows a typical measurement setup where two pre-cast sensors have been laid on top of fresh concrete. The sensors are then covered with a layer of concrete. As a consequence, the sensors are located at the desired depth in the block. Reference measurements are typically made with HMP44 relative humidity and temperature probes (Vaisala Inc., Finland) either from drilled and piped holes or by taking samples. Some early measurements have been performed in the Applied Electronics Laboratory at Helsinki University of Technology. However, most measurements have

been performed at the premises of Humittest Ltd. The experiments and results presented here have been presented earlier in Marko Leskinen's bachelor's thesis [69], however the interpretation is somewhat new. It should be noted, that similar results have also been acquired in other experiments.

Figure 5.3: A typical setup for evaluating the functionality of the system in monitoring the drying of concrete. Two pre-cast sensors are laid on top of fresh concrete and then covered with more concrete.

An interesting test performed by Marko Leskinen is one that aimed to resolve how a basic sensor would affect moisture migration in a concrete slab that dries only upwards. The experiment was performed with a 70 mm thick block of normal concrete of the strength class K30 (Lohja Rudus Ltd., Finland) that was allowed to dry only upwards. The basic sensors were simulated with plastic pieces, approximately the size of the sensors, that were pressed into fresh concrete at two different depths, approximately 10 and 30 mm. The relative humidity was measured with the sampling method, i.e. by taking a sample above and below the plastic piece and by determining the relative humidity of each with a HMP44 probe (Vaisala Inc., Finland). The reference measurements were done from a similar concrete block that did not include the plastic pieces. The experiment clearly indicated that the sensor does have a significant effect on moisture migration. That is, moisture is buffered below the sensor, and the relative humidity below the sensor is significantly higher than at the same depth without the presence of a sensor, and the relative humidity above the sensor is similarly lower than without a sensor. The difference is typically in the range of 5–10 %RH, but in some occasions up to 30 %RH. The experiment and the acquired results are presented in more detail in Marko Leskinen's bachelor's

thesis [69].

Marko Leskinen also performed a set of experiments that aimed to determine whether the developed measurement method is suitable for monitoring the drying of concrete. The test set was made with three different concrete types, normal concrete of the strength class K30 (NO), rapidly coverable floor concrete of the strength class K40 (NP), and self compacting concrete (IT) (Lohja Rudus Ltd., Finland). Two concrete blocks of each type, with the areas of 460 x 300 mm, and the thicknesses of 70 mm, were laid into plastic containers so that they could dry only upwards. The test blocks were equipped with four pre-cast basic sensors each, at two different depths, approximately 30 mm and 50 mm. The former corresponds to the normal measurement depth in an upwards drying slab, and the latter is a location where the relative humidity is expected to be higher. At each depth, one sensor was assembled facing upwards and another one downwards. The sensors were assembled by pushing them into the fresh concrete. In addition, holes were bored, and measurement pipes were assembled to both depths for performing reference measurements with HMP44 relative humidity and temperature probes (Vaisala Inc., Finland). The pre-cast basic sensors were read with the hand-held reading device. [69]

Based on the experiment, Marko Leskinen discovered that the relative humidity readings acquired with the developed system were systematically higher than those acquired with the reference measurements. As a consequence, the conversion curve between quality factors and relative humidity values programmed to the reading device was adjusted to better fit the measurement data. The calibration was made based on measurement results from the upwards facing sensors at the 30 mm depth in normal concrete, since it was considered to be the most typical application. Figure 5.4 shows the relative humidity measurement results acquired with HMP44 probes as a function of the quality factors of the pre-cast sensors in the application. In addition, the conversion curve programmed to the reading device is shown in the figure.

After normalizing the measurement results based on the typical application, the results from different conditions can be compared to them. Figure 5.5 shows the relative humidity measurement results acquired with HMP44 probes as a function of the quality factors of the pre-cast basic sensors in normal concrete facing down at the depth of 30 mm, and facing up at the depth of 50 mm. Figure 5.6, on the other hand, shows the relative humidity as a function of the quality factor of the sensors facing up at the depth of 30 mm in self compacting concrete and rapidly coverable concrete. In both figures, also the conversion curve, described above, is shown.

Figure 5.4 shows an approximately 3 %RH deviation between the two test blocks in the most typical application. The trends of the measurement results are, however, similar, and the conversion curve seems to fit the measurement results reasonably well. The imminent deviation results probably from the accuracy of the relative humidity measurement, that of the hand-held reading device, and the accuracy of the measurement depth in both cases.
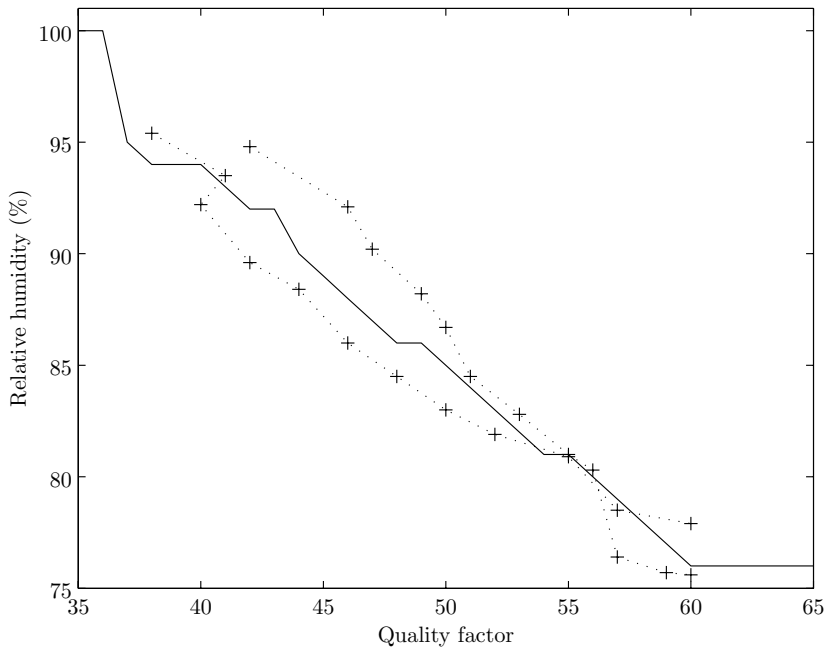
Figure 5.4: The relative humidity of normal concrete (Lohja Rudus Ltd., Finland) corresponding to the quality factors of pre-cast basic sensors placed facing up at the depth of 30 mm. The measurement results of two test blocks are represented by +-symbols. The solid trace represents the conversion curve for normal concrete, programmed to the commercial reading device.
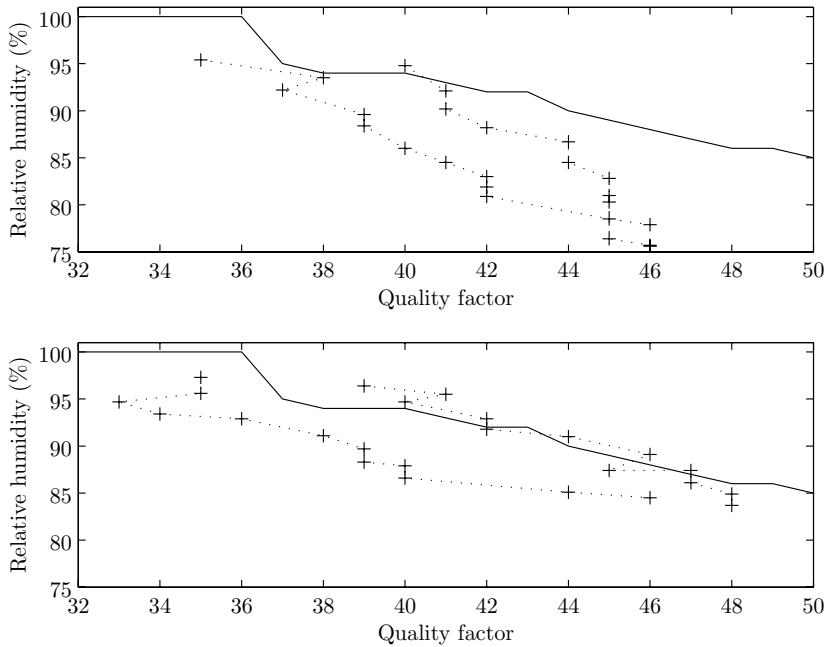
Figure 5.5: The relative humidity of normal concrete (Lohja Rudus Ltd., Finland) corresponding to the quality factors of pre-cast basic sensors. The upper graph is acquired with the sensor facing down at the depth of 30 mm, the lower graph with the sensor facing up at the depth of 50 mm. In each graph, the measurement results of two test blocks are represented by +-symbols. The solid traces represent the conversion curve for normal concrete, programmed to the commercial reading device, also shown in figure 5.4.

Figure 5.6: The relative humidity of two concrete types corresponding to the quality factors of pre-cast basic sensors placed facing up at the depth of 30 mm. The upper graph presents the results acquired with self compacting concrete (IT), and the lower one with rapidly coverable concrete (NP) (Lohja Rudus Ltd., Finland). In each graph, the measurement results of two test blocks are represented by +-symbols. The solid traces represent the conversion curve for normal concrete, programmed to the commercial reading device, also shown in figure 5.4.
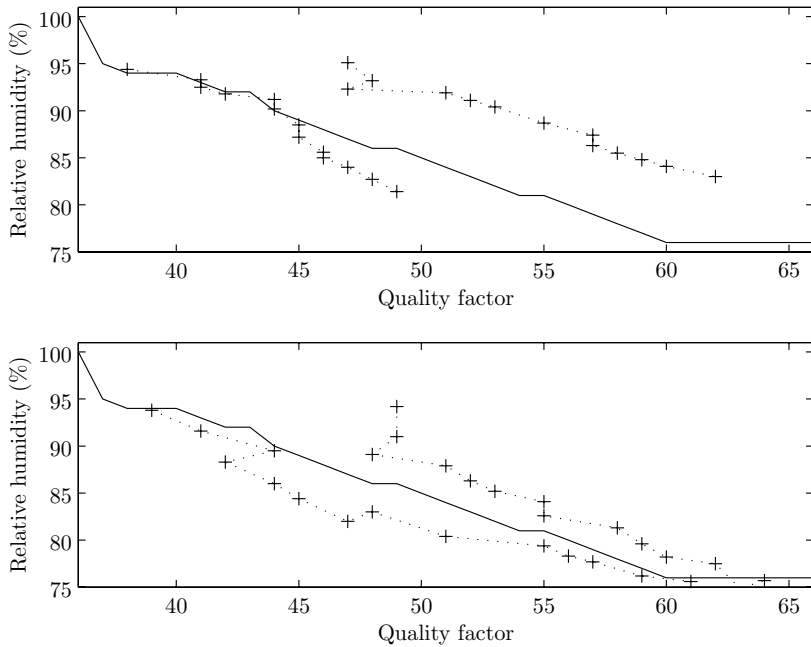
The upper graph of figure 5.5 indicates clearly, that the same conversion curve does not fit the measurement results in the case where the sensor is facing downwards. This result was expected based on the previous test of how the sensor affects moisture migration in concrete. The lower graph of figure 5.5, on the other hand, seems to indicate that the slope of the conversion curve is similar to the measurement results also at the depth of 50 mm. However, there is also a significant, on the average more than 5 %RH, deviation between the two test sets in both cases.

The upper graph of figure 5.6 shows that there is a significant deviation between the two test blocks of self compacting concrete. It seems that the sensor does not function especially reliably in this concrete type. In the lower graph, as the relative humidity decreases, the measurement results approach the conversion curve with rapidly coverable concrete. However, with wet concrete, one of the sensors does not seem to react below the quality factor of 48.

5.2.2   Threshold sensor

The threshold sensors have been tested mainly with humidity chamber measurements performed in the Applied Electronics Laboratory in Helsinki University of Technology. The tests have been performed by Outi Valta, MSc., and the results presented here are based on her master's thesis [39].

The tests have been performed in a humidity chamber, illustrated in figure 5.7, that is a tight container, the relative humidity in which can be controlled with a salt solution (1). The relative humidities that different salts tend to maintain are listed in table 3.10. An HMP42 relative humidity and temperature probe (Vaisala Inc., Finland) (2) has been placed into the chamber for reference measurements. The probe is connected to an HMI41 indicator (Vaisala Inc., Finland) located outside the container. In addition, a small fan (3) is used to even up the humidity inside the chamber. A rack that permeates air (4) has been built inside the chamber in order to bring the sensors (5) to an approximately 50 mm distance from the lid of the container. The actual measurements have been performed early on with the signal generator based measurement setup, later with the hand-held reading device (6) from on top of the lid.

Moisture chamber tests have been performed with several different threshold sensor constructions. First of all, as stated in chapter 3, different constructions were tested for the reacting layer: the salt was spread on top of the sensor as such, soaked into a nonwoven fabric, or bound into place with a plastic net. However, using mortar as a matrix for the salt was discovered to be a functional solution. Sensors including different mortar types and different amounts of salt were also tested in the moisture chamber.

Once the construction of the sensor was finalized, sensors including different salts: K_2SO_4, KNO_3, $ZnSO_4 * 7H_2O$, KCl, $(NH_4)_2SO_4$, and $NaCl$ were tested [39, p.50]. Figures 5.8 and 5.9 show the results from a moisture chamber
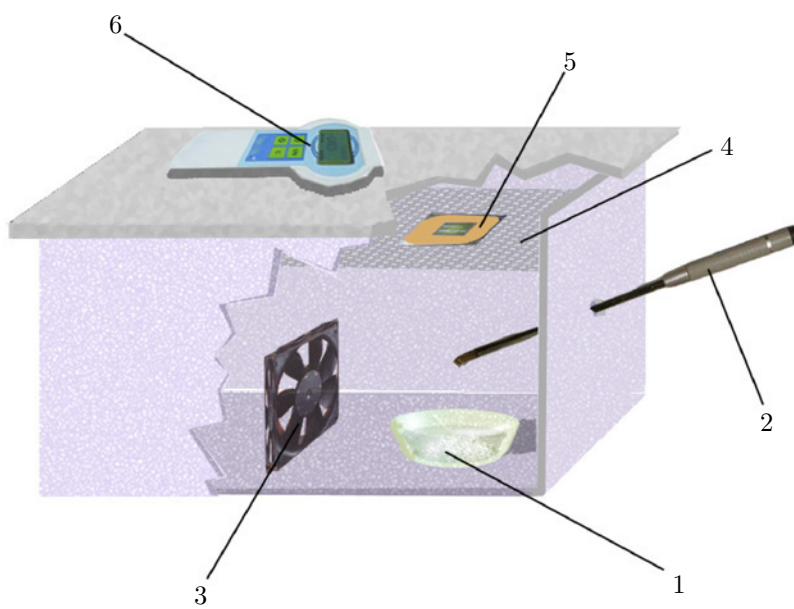
Figure 5.7: The humidity chamber includes a salt container (1), an HMP42 humidity probe (2), a fan (3), a rack (4), the tested sensors (5), and the reading device (6).

test performed with a 94 % threshold sensor (KNO_3). The experiment was performed by measuring the relative humidity in the chamber and the quality factor of a sensor during two cycles of increasing the relative humidity above the threshold and decreasing it back below it. The cycles were accomplished as follows: first the relative humidity was stabilized at approximately 81 %RH by using a $(NH_4)_2SO_4$ solution, then increased to approximately 90 %RH by switching to a $ZnSO_4$ solution, and finally at approximately 97 %RH with a K_2SO_4 solution. The relative humidity was then once again lowered to approximately 90 %RH and finally to approximately 81 %RH. The measurements were performed in sets of a few measurements with one day intervals. Figure 5.8 shows the relative humidity and quality factor as a function of time and figure 5.9 the quality factor as a function of relative humidity.
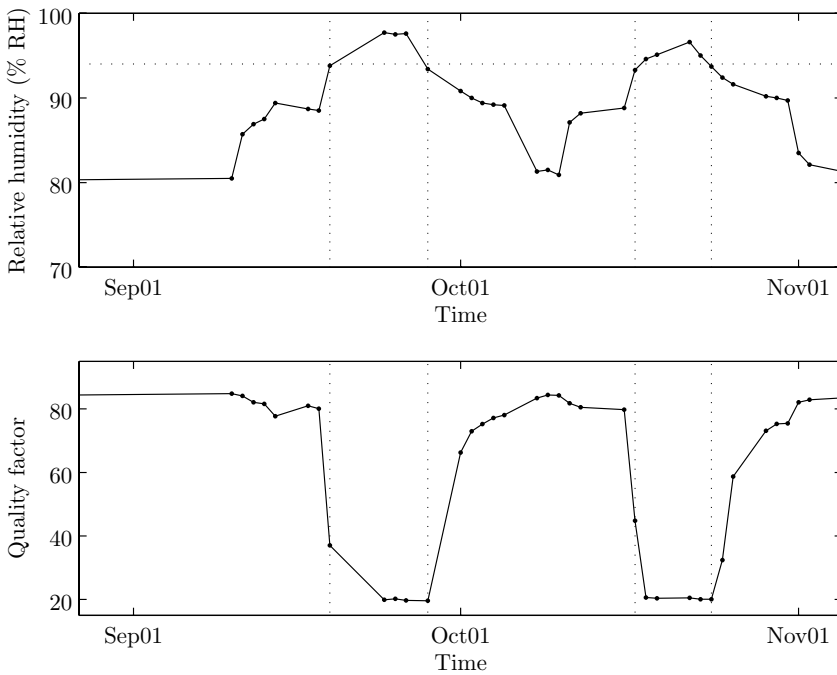

Figure 5.8: Measurement results acquired with a 94 % threshold sensor (KNO_3) in a moisture chamber. The upper graph presents the relative humidity in the chamber, measured with an HMP42 probe (Vaisala Inc., Finland) as a function of time. The horizontal line represents the 94 % threshold level of the sensor. The vertical lines represent the times corresponding to crossings of the threshold. The lower graph shows the quality factor of the sensor, measured with the signal generator based measurement setup as a function of time.

The measurement results indicate a clear change from approximately 80 to approximately 20 in the quality factor of the threshold sensor when the threshold humidity of 94 % is exceeded. As the relative humidity decreases again below

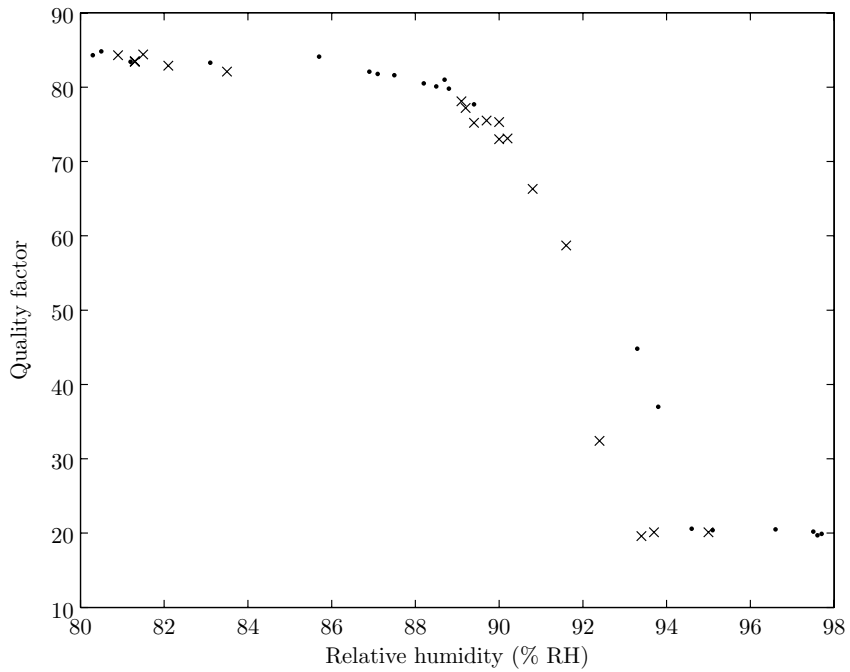*Figure 5.9:* Measurement results acquired with a 94 % threshold sensor (KNO_3) in a moisture chamber. The quality factor of the sensor, measured with the signal generator based measurement setup, is shown as a function of relative humidity in the chamber, measured with an HMP42 probe (Vaisala Inc., Finland). The results from the absorption cycles are represented with points, and from the desorption cycles as x-marks.

the threshold, the quality factor of the sensor returns to its original value, however not immediately. This causes hysteresis into the quality factor - relative humidity dependency curve of figure 5.9. It is expected to result from the hysteresis in the relative humidity - moisture content dependence of the mortar used in the sensor.

5.3   Conclusions

The performed laboratory experiments indicate, that the basic sensor seems to be ready and suitable for at least bathroom monitoring. First of all, according to the performed tests, the quality factor of a sensor can be reliably converted to a relative humidity reading. In addition, the basic sensor seems to react quickly to extreme moisture stress, such as damaged waterproofing. The sensor also seems to function more reliably under a nonpermeable material, such as typical waterproofing paints, since the sensor itself blocks some of the moisture migration in the structure.

Using the pre-cast basic sensor for monitoring the drying of concrete functions suggestively. Generally, the trends in the quality factors of the sensors follow those of the prevailing relative humidity. However, the measurement depth and the type of concrete affect the measurement significantly, and there seems to be a large deviation between measurement sets. Thus, it seems that as such the system does not function reliably enough to replace drill-hole measurements in this application area, at least in applications where absolute accuracy is important.

In the laboratory environment, the developed threshold sensors seem to be able to reliably and accurately determine whether a certain relative humidity level has been exceeded. However, there seems to be a slight hysteresis in the sensor. Typically, however, the direction of the development of relative humidity is known, and the hysteresis could be taken into account.

6 Field procedure and observations

In addition to the laboratory tests presented in the previous chapter, the developed measurement method and system have also been tested in the actual construction environment. This chapter presents some suggested guidelines of how the system could be used in different applications, and several pilot assembly cases, some of them also including preliminary measurement results.

6.1 Application guidelines

The developed measurement method and system could prove useful in several different application areas in the construction environment. Up front, the most important application areas are monitoring the bathroom area for possible leaks, and monitoring the drying of concrete at the time of construction. However, the wireless measurement procedure also provides the opportunity for measuring moisture conditions in several different structures that were previously more difficult to approach.

6.1.1 Bathroom monitoring

The primary and by far the most comprehensively studied application area for the developed system is monitoring moisture in bathrooms. The measurement problem has been presented with the objective of the basic sensor development in chapter 3. In short, the basic sensors are assembled to the bathroom walls and floors before they are waterproofed. Thus, the sensors are used to measure wirelessly the moisture conditions behind the waterproofing.

Since the basic sensors assess moisture conditions fairly locally, the used sensors should be placed to locations that are indicative of the state of the structures. Some locations that were considered important are shown in figure 6.1. Especially important locations are the ones where a lot of flowing water is present, including e.g. the vicinity of the bathroom floor drain, the wall area directly below the shower water mixer, the lower corner of the closest wall adjacent to the shower wall, the floor corner nearest to the shower, and the lower edge of the shower wall. In addition, a reference sensor should be placed to a dry location on the wall near the doorway, possibly also to a dry location on the floor. The vicinity of other water sources, such as the sink, and the washing machine, and floor penetrations below the toilet and the sink are also considered to be important locations, as is the vicinity of water pipes. A sensor could also be placed into the floor under the washing machine, and next to the sauna floor drain. The number of sensors needed for each bathroom is between six and ten, depending on its size and furnishing.

Figure 6.1: The most important assembly locations in a bathroom are places where a lot of flowing water is present, near water sources and penetrations, and at dry reference locations.

In order to apply the research results to the construction field, the first commercial product, a sensor set for bathrooms, shown in figure 6.2 was developed. The set includes ten basic sensors and everything that is needed to assemble them: two bags of the assembly mortar, two bottles of water, a container for mixing the mortar, a plastic trowel, and assembly instructions. The sensor set is meant both for construction professionals and for anyone building his own house.

Figure 6.2: The commercial sensor kit for bathrooms includes 10 sensors, two bags of assembly mortar, two bottles of water, a container for mixing the mortar, a plastic trowel and assembly instructions.

The planned assembly procedure with the sensor set is as follows. Cavities slightly larger than the basic sensor are chiselled to the walls and floor at the assembly locations. As a consequence, the sensors are beneath the surface of the structure and no further filling is needed. The dry mortar and water are mixed to form the assembly mortar. The sensors are assembled one by one into their cavities. That is, an approximately 2 mm thick layer of assembly mortar is spread on the sensing side of each sensor, and the sensor is then gently pressed into the cavity, sensing side first. The assembly mortar is let dry for approximately 10 minutes, before covering the sensors with a thin layer of the assembly mortar. The assembly is then let dry and become firm for at least one day. After that, the finishing of the bathroom can be continued normally. The assembly locations should be documented carefully into the assembly drawing or by photographing. Figure 6.3 shows a part of the sensors assembled in a relatively large bathroom before the sensors are covered with mortar.

Figure 6.3: A part of the assembled sensors in a relatively large bathroom before the sensors were covered with mortar.

6.1.2 Drying of concrete

The moisture content or the relative humidity of concrete is often measured at the time of construction, before the concrete slab is covered with layers of other materials. Manufacturers of different covering materials usually specify maximum values for the moisture conditions of the underlying concrete. If the concrete is covered at too early a stage, the covering material may be damaged or moisture may be caught under the covering. In either case, suitable conditions for microbe growth may arise. Above all, the suitable drying period is an economic issue, since waiting for the concrete to dry increases costs for the building contractor. Thus, it is important to know reliably and accurately the prevailing moisture conditions in concrete.

The prevailing best practice for the coverability measurements of concrete in the Nordic countries is a relative humidity measurement described in chapter 1. In most cases the measurement is done from a drilled hole, however the sampling method is also used. The measurements are made at depths relative to the thickness of the slab. According to best practice, the most important depth is either 40% or 20% of the thickness, measured from the surface. The depth depends on whether the concrete is allowed to dry in one or two directions respectively. The measurement depth is based on the assumption, that the surface of the slab would reach the relative humidity at the measurement depth, if the slab were covered with a fully non-permeable layer. [31, pp. 23–24]

The developed measurement system, and especially the pre-cast basic sensor, has been used in monitoring the drying of concrete. To be comparable with the prevailing practice, the measurement results are presented as relative humidity, and the same measurement depths are used. The pre-cast sensors can either be pushed into the wet concrete after laying the slab or they can be supported to the appropriate height before laying it. The second approach is preferable since the accuracy of the measurement depends on the accuracy of the measurement depth. This approach also allows the assembler of the sensors to place the sensors independently of the laying process. However, caution is necessary during laying the concrete, so that the sensors remain where supposed to.

6.1.3 Special applications

In addition to the two primary application areas presented above, the developed system has been used in some more special application areas. For example, two cases are presented below, where the system has been used to monitor relative humidity in thermal insulation and to test the functionality of the sealing of a window structure. Generally, the measurement system is applicable to any moisture and temperature measurement application, where the reading range of the system is sufficient.

6.2 Pilot assembly cases

The developed measurement method and system have been tested in numerous pilot sites and structures, concentrating mainly in bathrooms of different buildings. This section describes experiences and preliminary measurement results from pilot sites that are considered exemplary in some ways. First of all, the functionality of the system is presented in bathrooms with cases from a bathroom renovation in an apartment building, and two new one-family-houses, one of which includes a suspected leak. The functionality of the system is also tested in two applications where the drying of concrete is monitored. Finally, three special application areas are presented. Some of the cases presented here have also been presented earlier in different scientific conferences.

6.2.1 Bathroom renovation in an apartment building

A pilot assembly case in the bathrooms of an apartment building in Helsinki, Finland, is an example of applying the developed system at the time of renovation. The functionality of the system in bathrooms has been verified in other laboratory and pilot tests, so the interest in this case was mainly on the development of the assembly process. This pilot case was chosen to be presented first, since it describes a successful assembly process illustratively. The assembly process in the other presented cases is similar to the one presented here.

At the presented pilot site, the bathrooms of nine apartments were equipped

with six basic sensors each at the time of a piping renovation. The building contractor took care of assembling the sensors, which proved to be a viable solution. Separately from the pilot project, the contractor assembled the sensors similarly to hundreds of apartments in the same neighborhood. Thus, the contractor had a motivation to develop the assembly procedure. Figure 6.4 shows four photographs of the assembly process. Small cavities were chiselled for each sensor both to the floor and to the grouted wall (Figure 6.4a). The sensors were assembled by spreading a thin layer of the assembly mortar on the sensing side of each sensor (Figure 6.4b), and pressing them into the cavities (Figure 6.4c). Figure 6.4d shows some of the sensors before they were covered with mortar. All sensor locations were documented with a digital camera. The sensor locations in similar bathrooms remained the same throughout the pilot.

a

b

c

d

Figure 6.4: Assembling the sensors during the bathroom renovation: a. Small cavities were chiselled into the floor and wall, b. assembly mortar was spread on the sensing side of each basic sensor, c. the sensors were pressed into the cavities, d. the mortar was let dry for, say, ten minutes before the sensors were covered.

The construction worker that assembled the sensors had no complaints about the assembly process nor the equipment. The sensors stuck easily to the walls, and the plastic trowel included with the sensor set had proven to be suitable. According to the assembler, the assembly process in one bathroom took approx-

imately 30 minutes with the chiselling included.

6.2.2 Drying of concrete and bathroom monitoring in a one-family-house

A pilot assembly site in Heinola, Finland, is a representative example of utilizing the system in a new building. In the pilot, the sensors have been used to monitor moisture in a 250 m², 6-room, 2-storey, low-energy house shown in figure 6.5. The house has been built by Koskisen Oy Herrala Talot and it is one of the exhibition houses of the Heinola dwelling fair 2004 (Suomen Asuntomessut). This pilot assembly case has also been presented in the Integrated Lifetime Engineering of Buildings and Civil Infrastructures conference (ILCDES 2003) in Kuopio, Finland, in December 2003 [46].

Figure 6.5: The pilot assembly site, a 2-storey house in Heinola, in February 2003.

In this pilot site, the moisture conditions are monitored in two stages. At the first stage, during construction, the drying of the concrete base floor and intermediate floor slab was monitored in order to determine when they are dry enough to be covered with other materials. At the second stage, the moisture technical behavior of the most critical structures of the building, mainly in the bathroom area, is assessed throughout the life of the building.

Drying of concrete

The drying of the base floor concrete slab was measured with basic sensors and pre-cast basic sensors. The pre-cast sensors were assembled at the time of

laying the concrete by pressing the sensors into the wet concrete at the depth of interest, in this case between 40 and 50 mm. A total of four sensors were assembled to this depth. In addition to this, two pre-cast basic sensors and five plain basic sensors were assembled to a depth of approximately 10 mm, to be used in both monitoring stages.

The drying of the intermediate floor concrete slab was monitored with four pre-cast basic sensors. The concrete was laid on composite floor sheets, so the slab was allowed to dry only upwards. The sensors were placed at approximately 20 mm depths in different rooms. One of them was pressed into the wet concrete, the other three were tied to the iron reinforcement, as shown in figure 6.6, prior to laying the concrete.

| a | b |

Figure 6.6: Assembling the pre-cast basic sensors. a. The sensors were tied to the iron reinforcement and b. the concrete slab was laid.

All of the assembled sensors could be measured with a reading device in a couple of minutes. The acquired relative humidity readings at different depths were used to evaluate when the slab could be waterproofed or covered with parquet. After the slab has been covered, the sensors can still be used to monitor the development of the moisture conditions inside the structure.

Long-term monitoring

The second stage of measuring moisture conditions in the pilot assembly site is long-term monitoring. The monitoring aims to find signs of possible leaks and increasing moisture content before actual moisture damage occurs. The sensors are assembled into the walls and the floor at the most critical locations, by using the assembly mortar. At this site, a total of 15 sensors are used for long-term monitoring, 13 of them are located in the bathroom and sauna area shown in figure 6.7. The bathroom has two showers on one separating shower wall. The wall on the left of the shower wall is an exterior wall and the wall on the right is a separating wall. The monitoring is concentrated near the showers and the

two floor drains. The monitoring is partly done using the sensors already used for monitoring the drying of the base floor. The long-term monitoring sensors on the floor were assembled to the following locations:

1. Next to the bathroom floor drains, with a 50 mm distance from each drain (2 sensors)

2. In the corner of the shower wall and the exterior wall on the left, with a 50 mm distance from both walls

3. In the middle of the exterior wall on the left, with a 50 mm distance from the wall

4. Next to the sauna floor drain, with a 50 mm distance from the drain

Outside the picture, two sensors have also been placed near the other floor drains in the base floor. In addition to these floor sensors, eight sensor were assembled to the bathroom walls. They were placed to the following locations:

5. Directly below the shower mixers, with a 150 mm distance from each mixer (2 sensors)

6. On the lower edge of the shower wall, with a 50 mm distance from the floor, between the showers

7. On the lower edge of both walls adjacent to the shower, with a 100 mm distance from the floor, and 1000 mm from the corners (2 sensors)

8. To the corners of the shower wall and the adjacent walls, with a 100 mm distance from the floor and from the corner (2 sensors)

9. A reference sensor in a dry wall near the doorway.

The basic sensors both in the walls and the floor were assembled with the assembly mortar before waterproofing. Thus, they measure moisture conditions behind the waterproofing, and moisture resulting from normal use of the bathroom does not affect the sensors.

During the research project, the sensors were read twice with approximately a one month interval. After the owner of the building has moved in, he can continue the monitoring process by reading the sensors for example twice a year.

6.2.3   Bathroom with suspected leaking floor drain

A pilot assembly case that took place in a one-family-house in Hollola, Finland, is a representative case where the developed measurement system has revealed
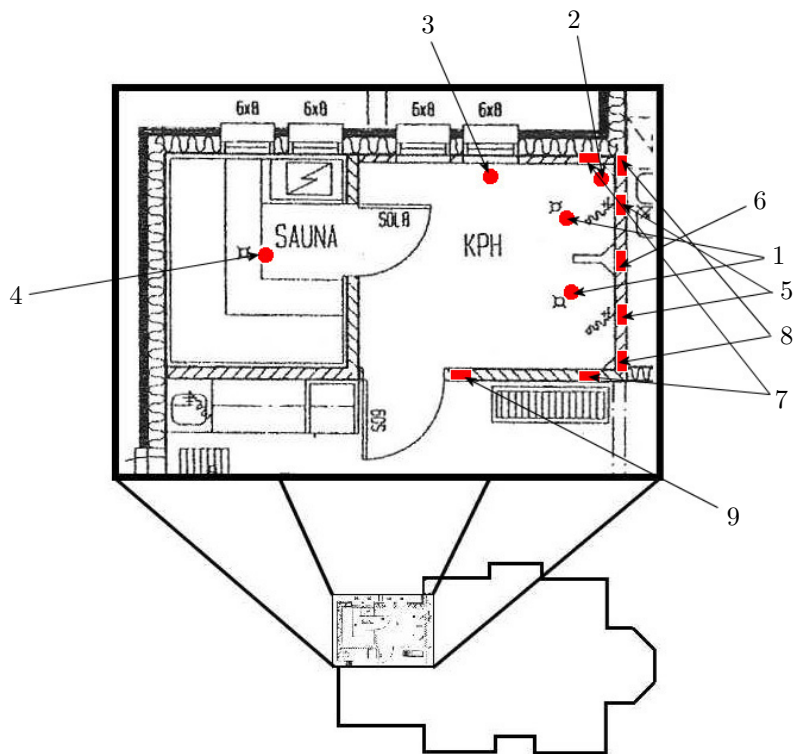
Figure 6.7: The floor plan of the bathroom area with the sensor locations in the floor (1–4) and in the walls (5–9).

a suspected leak in the bathroom. The assembly site is a one-storey, wooden house, and one of the first sites where the system was piloted in monitoring the functionality of a bathroom. The measurement results acquired from this site have also been presented at the National Indoor Air Seminar in Finland in 2004 (Sisäilmastoseminaari 2004) [45].

The floor plan of the bathroom area is shown in figure 6.8. The walls of the bathroom are block structures that have been finished with ceramic tiles. The shower wall and the wall on its left are separating walls, and the wall on its right is an outer wall. The floor of the bathroom is a ground slab that has been finished with floor tiles.
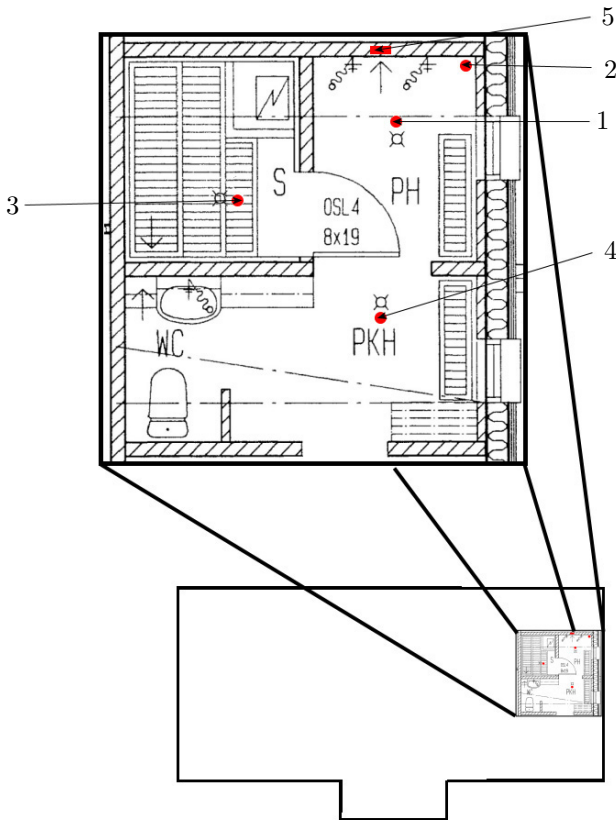

Figure 6.8: The floor plan of the bathroom area with the sensor locations in the floor (1–4) and in the shower wall (5).

Assembly process

At the presented pilot site, a total of six basic sensors were assembled into the structures. The aim was to position the sensors to the most critical locations in terms of moisture physics. In the bathroom, the sensors were assembled, as can be seen in figure 6.8, next to the the floor drain (1), to the lower end of the shower wall (5), and to the floor at the corner of the shower wall and the outer wall (2). In addition, sensors were assembled next to the floor drains in the sauna (3), the changing room (4), and the utility room.

The sensors were assembled before the floor was waterproofed, thus they measure the moisture conditions of the structure behind the waterproofing, and the normal use of the shower should not affect the measurement results. The basic sensors were assembled by spreading a thin layer of the assembly mortar on the sensing side of each sensor and by pressing the sensors against the structure under investigation. When needed, a small cavity was made into the structure so that the sensor would not complicate assembling the tiles. After assembling, the sensors were covered with mortar. Figure 6.9 shows some of the sensors during the assembly process. The process took approximately 20 minutes. After the mortar had dried, the floor was ready for waterproofing.

Measurement results and discussion

At the moment, the sensors at the pilot assembly site have been read four times, the first of which was timed before the waterproofing, and the other times after the bathroom had been taken into use. Reading all the sensors at the site takes approximately five minutes. Figure 6.10 shows graphically the measurement results from four of the six sensors. The sensors in the utility room and the sauna have been left out for the sake of clarity. In these locations, the development of the moisture conditions is similar to the results acquired from the floor corner and the floor drain of the dressing room. The error tolerances shown in the figure correspond to the ± 3 percentage point accuracy reported by the commercial manufacturer of the developed measurement system. The figure indicates that the relative humidity acquired from the only sensor assembled to the wall has remained at approximately 72 percent. The floor, instead, has dried even after taking the bathroom into use, according to the sensor in the corner, and the sensor near the floor drain of the dressing room. However, relative humidity near the shower floor drain has risen to approximately 96 percent after taking the shower into use.

The joint between the floor drain, and the structures and waterproofing is one of the most common moisture problems in bathrooms [70, p. 47]. The local increase in relative humidity, after taking the bathroom into use, suggests that the joint may leak. Full confidence of this could be acquired by performing a destructive relative humidity verification measurement. However, verification measurements or corrective actions have so far not been considered necessary. On the other hand, according to previous experience, there is no reason to
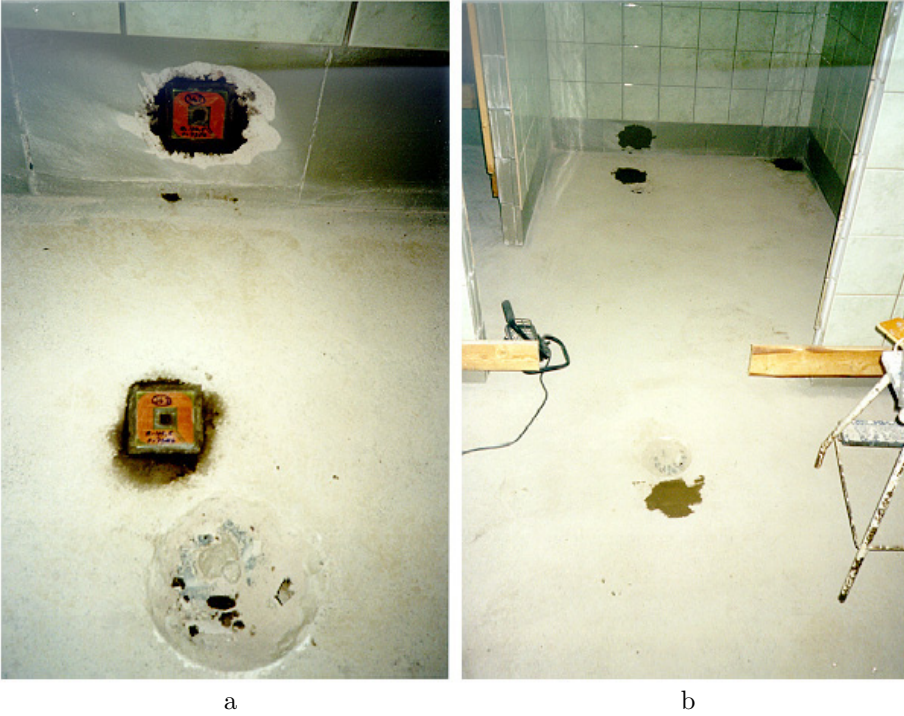
a   b

Figure 6.9: Assembling the sensors to the structures: a. the sensors next to the shower floor drain, and at the lower end of the shower wall, before they were covered with mortar, b. the same sensors together with the sensors at the floor corner of the shower wall and the outer wall, and next to the changing room floor drain, after covering with mortar.
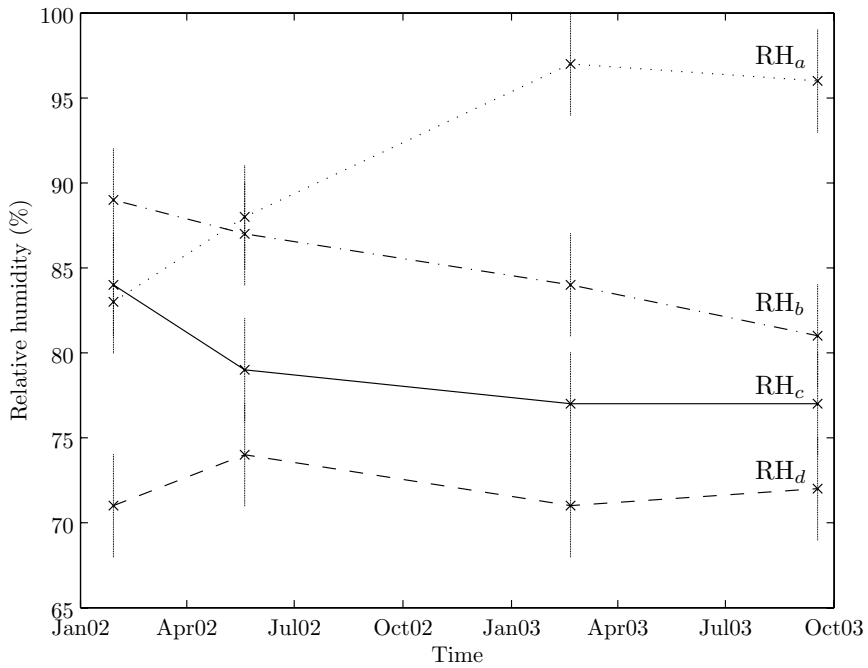
Figure 6.10: Relative humidity measurement results acquired with the developed system near the shower floor drain, RH_a, at the floor corner of the shower wall and the outer wall, RH_b, near the floor drain of the dressing room, RH_c, and at lower end of the shower wall, RH_d, at four occasions in the years 2002–2003.

suspect that the measurement results acquired with the develop measurement system would not be accurate. The monitoring is continued.

6.2.4 Measuring moisture in a multi-layered floor structure

The functionality of the developed measurement system in a multi-layered floor structure was tested in a school classroom in Helsinki, Finland. The floor of the room was renovated because of previously occurred moisture damage. The construction of the floor after the renovation is shown in figure 6.11. One 50 mm thick grooved (5) and one plain (4) expanded polystyrene (EPS) thermal insulation board were placed on top of an old ground slab (6). A filter cloth (3) was placed on top of them and a new reinforced concrete slab was laid (2). The structure was finally covered with plastic flooring (1).
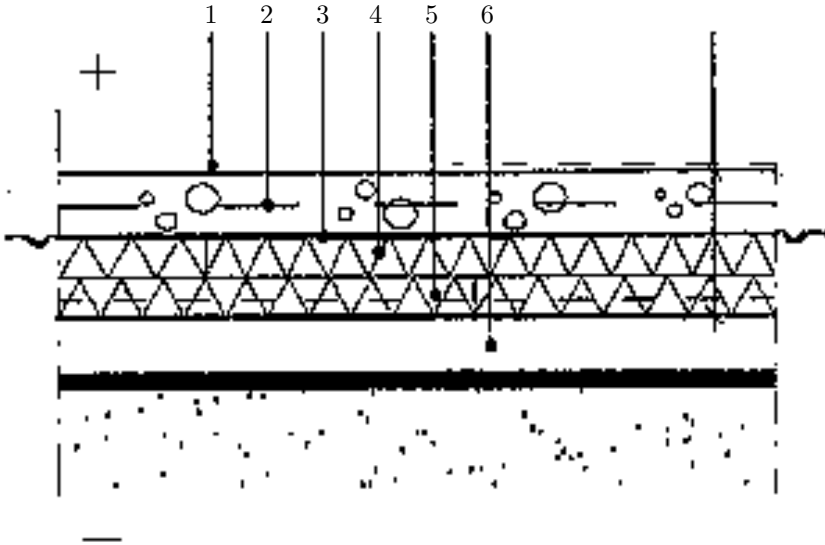

Figure 6.11: The construction of the floor: plastic flooring (1), reinforced concrete slab (2), filter cloth (3), 50 mm EPS board (4), 50 mm grooved EPS board (5), old ground slab (6)

The structure under investigation was equipped with some of the developed sensors side by side with measurement pipes for HMP44 humidity and temperature probes (Vaisala Inc., Finland). The pipes and the HMP44 probes were assembled by Humittest Ltd. that also performed the reference measurements. Two separate measurement sets were performed at the site. First of all, the drying of the new concrete slab was monitored, and after it was covered, the long-term functionality of the structure was monitored for over a year.

Drying of the concrete slab was monitored with two upwards facing pre-cast basic sensors and two HMP44 probes in the middle of the room, one of each at the two depths of 15 and 30 mm. The pre-cast sensors were pressed into the laid concrete as shown in figure 6.12c.

The long-term functionality of the structure was monitored with both the developed sensors and HMP44 probes at three locations: at the outer edge of the room, i.e. near the outer wall, in the middle of the room, and at the inner edge of the room, i.e. near the wall opposite to the outer wall. At each location, the monitoring was made at three depths: below the lower surface of the thermal insulation, i.e. at the interface of layers 5 and 6, above the upper surface of the thermal insulation, i.e. at the interface of layer 2 and 3, and at the surface of the laid concrete slab, i.e. at the interface of layers 1 and 2. Thus, pipes for the humidity probes were assembled to a total of nine points in the room.

The sensors of the developed measurement system were assembled to the same three depths. Below the thermal insulation, basic sensors were assembled in contact with the ground slab at the three measurement locations, by using the assembly mortar. In addition, two 10x10 cm sensors were assembled at the outer edge and the middle of the room. The 10x10 cm sensors are early prototypes of a somewhat larger sensor that aims to function similarly to the basic sensor. All sensors were assembled with the sensing side upwards. A photograph of the assembly process, also showing a 10x10 cm sensor, is shown in figure 6.12a. Above the thermal insulation, pre-cast basic sensors were taped to the filter cloth at the three measurement locations. The sensor at the inner edge was assembled with the sensing side downwards, the other two with the sensing side upwards. This assembly phase, and two of the measurement pipes can be seen in figure 6.12b. At the surface of the reinforced concrete slab, plywood board pieces, slightly larger than the basic sensor, were pressed into the laid concrete. After the concrete had dried, the pieces were removed, as shown in figure 6.12d, and basic sensors were assembled to the resulting holes, with the sensing side downwards, by using the assembly mortar.

Measurement results and discussion

The plan was to read the sensors at the surface with the hand-held reading device. The sensors attached to the filter cloth above the thermal insulation and the 10x10 cm sensors below the thermal insulation were to be read with a portable measurement system built around a signal generator. The basic sensors below the thermal insulation were not expected to be readable with the prevailing equipment. However, as the reading equipment is enhanced, measuring them may become possible.

The sensors, that were assembled to the depths of 15 mm and 30 mm in the new slab, were used to test the functionality of the system in monitoring the drying of concrete and to determining when the slab could be covered. The concrete slab was laid on the 3rd of March 2003. Figure 6.13 shows the measurement

a

b

c

d
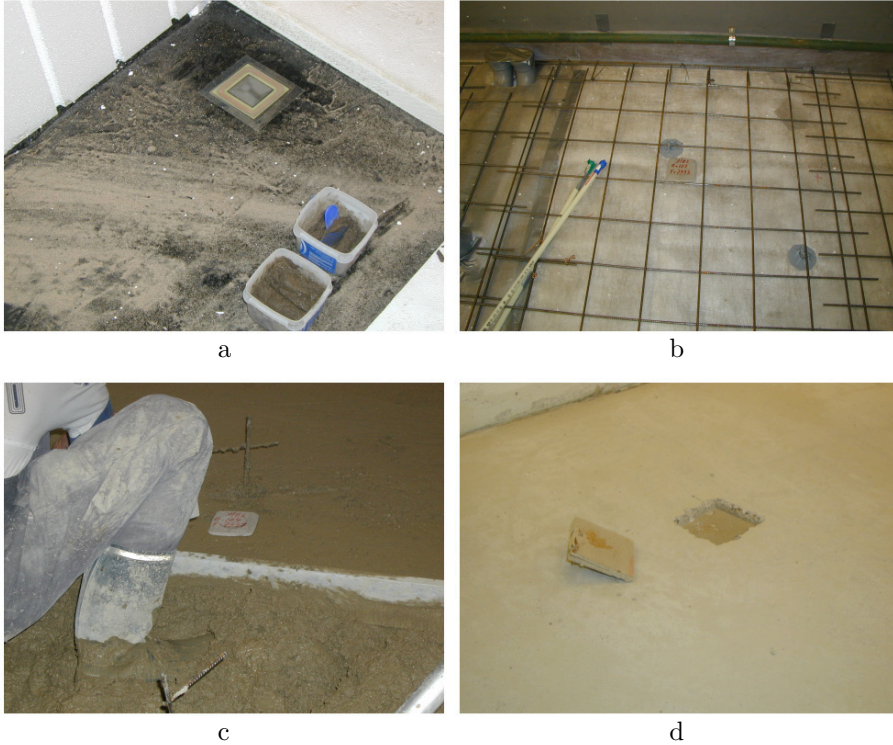
Figure 6.12: Assembling the sensors: a. basic sensors and 10x10 cm sensors were assembled below the thermal insulation by attaching them to the ground slab with the assembly mortar, b. pre-cast basic sensors were assembled above the thermal insulation by attaching them to the filter cloth prior to laying the concrete slab, c. pre-cast basic sensors, used to monitor the drying of concrete, were pushed into the wet concrete, d. basic sensors were assembled to the surface of the concrete slab into holes made with pieces of plywood board.

results at different depths on the 17th of March 2003. The slab was covered with plastic flooring two weeks later, on the 31st of March 2003.
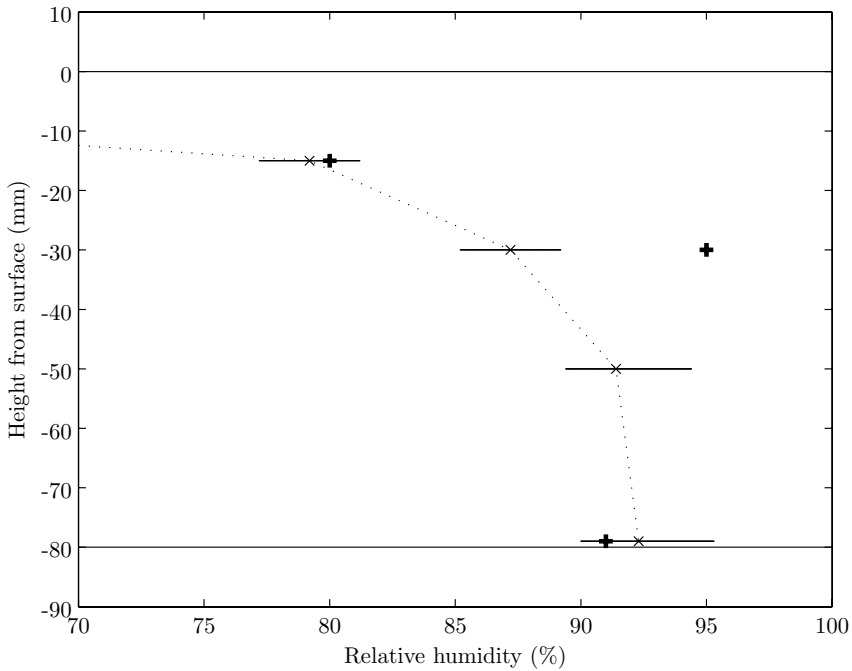

Figure 6.13: Relative humidity measurement results at different depths in the laid reinforced concrete slab. The measurement results acquired with Vaisala HMP44 are indicated with x-marks and their error margins with the horizontal lines. The results acquired with the developed system are indicated with the +-marks. All of the sensors face upwards.

The results of figure 6.13 indicate, that the results acquired with the developed sensors are within the measurement accuracy of the HMP44 probes at the depths of 15 mm and 80 mm. However, at the depth of 30 mm, the result acquired with the pre-cast basic sensor is significantly higher than that of the HMP44 probe. This may be because the mortar surrounding the basic sensor can not desorb moisture to the concrete quickly enough in comparison with the dynamics of the structure at this depth.

The long-term functionality of the multi-layered structure was monitored with single measurements that were performed approximately one week, 4 weeks, 8 weeks, 12 weeks, 5 months, 6 months, 10 months, and 15 months after the slab was laid. A part of the measurement results with both measurement methods is shown in figures 6.14 and 6.15.

From the measurement results at the surface of the new slab, it can be seen that the difference between the readings from the developed system and the

Figure 6.14: Relative humidity near the inner wall of the room measured with the HMP44 probes (+) and the developed sensors (x). The upper graph shows the results from the surface of the new slab, and the lower graph from the upper surface of the thermal insulation. All of the sensors face downwards.
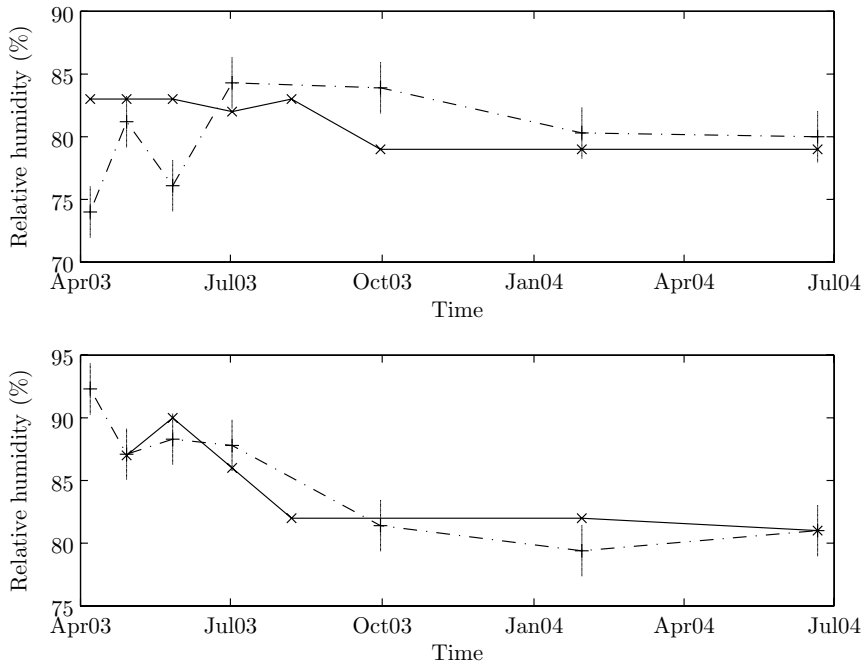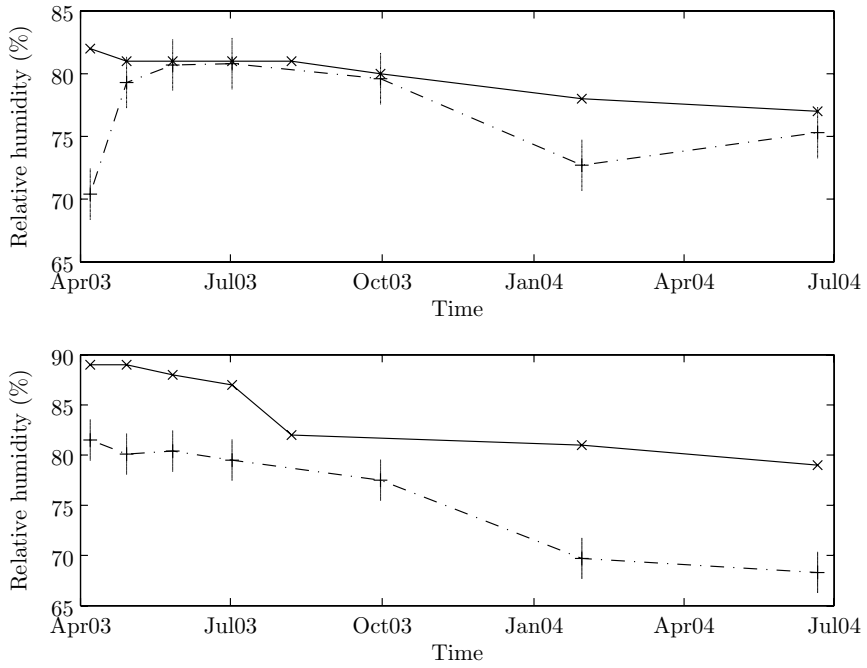
Figure 6.15: Relative humidity near the outer wall of the room measured with the HMP44 probes (+) and the developed sensors (x). The upper graph shows the results from the surface of the new slab, and the lower graph from the upper surface of the thermal insulation. The upper sensor faces downwards and the lower one upwards.

HMP44 probes is initially quite large. This is suspected to be because the sensor blocks some of the diffusion of moisture in the structure resulting in a higher moisture content accumulating below the sensor before the structure is covered with the plastic flooring. After covering the structure, the relative humidity at the surface of the structure, according to the HMP44 probes, increases as expected, however this can not be noticed with the developed system. At the end of the measurement set, the results acquired with the methods seem to agree reasonably well, except for the measurements near the outer wall in January 2004. In this measurement, the relative humidity according to the HMP44 probes has decreased, only to increase again to the next measurement. The developed system has not reacted to this change.

The measurement results at the upper surface of the thermal insulation in figure 6.14 are also promising, especially toward the end of the measurement interval. However in figure 6.15, the results acquired with the HMP44 probe are significantly lower than with the developed system. The results obtained with the developed system at the two locations, however, are similar. The orientation of the sensor does not seem to affect the measurement result.

The measurement results acquired with the 10x10 cm sensors located below the thermal insulation are also promising. At the moment, the measured quality factors and resonance frequencies could not be converted to a relative humidity reading due to the lack of suitable conversion tables. However, the trends of the measurement results are similar to those acquired with the HMP44 probe.

Summary

The measurement results acquired from this pilot site indicate that the developed system could be applicable for monitoring moisture in a multi-layered structure. However, as such the sensors do not react to the most dynamic changes in the moisture conditions of the structure. In some cases this could be considered to be a good thing. In addition, the results acquired with the developed system seem to agree more with the results acquired with the reference measurement as time passes. Thus, as it is, the system seems to be most fit for long-term monitoring. Also the 10x10 cm sensors proved to be a promising sensor construction for long reading ranges.

The sensor reading technology was not yet mature for this kind of an application. With the current hardware, only the sensors at the surface of the new slab could be read with the hand-held reading device. Measuring with the hand-held device is significantly simpler and faster than using the signal generator-based system. In addition, most measurement experiences have been acquired with the hand-held device, thus its results are considered more reliable.

The pilot site also provided experience about assembling the sensors. Attaching the sensors to the ground slab and to the filter cloth worked fine. However, assembling the sensors to the laid concrete is somewhat problematic, since the

exact assembly depth was difficult to determine. Still, the measurement accuracy during the drying phase depends, above all, on the accuracy of the measurement depth. As a possible solution, a small stand has been tested in order to set the sensor to the correct depth prior to laying the concrete. Using the plywood piece as a mould for the sensors on the surface proved to be a functional solution.

6.2.5   Measuring relative humidity inside a thermal insulation

A pilot test site in Ryttylä, Finland, is an example of how the developed relative humidity sensors could be used in monitoring moisture conditions inside thermal insulation materials. The test site is a wooden one-family house, where Termex wood-fiber thermal insulation (Termex Ltd., Finland) [71] has been used in the outer walls. At the time of assembling the sensors, there was very little experience of using the developed system in coarse materials, thus both the functionality of the sensors and the attachment mechanism were new. During the same pilot test, there was an interest to find out how the sensors affect the distribution of moisture within the insulation material. In addition, the ambient relative humidity and temperature sensor used in the reading device, SHT-11 (Sensirion AG, Switzerland), was tested in the structure. However, the results acquired from the SHT-11 sensors are not assessed in this context.

The behavior of the thermal insulation, in terms of building physics, was monitored at two locations in the outer walls of the house: in one bedroom, and in the bathroom. As a reference measurement, Humittest Ltd. assembled pipes for HMP44 humidity and temperature probes (Vaisala Inc., Finland) into the wall, and later performed the actual measurements. In both locations, the pipes and probes were assembled to measure the conditions at the outer surface of the insulation, at the inner surface, and half-way. In the bedroom, an extra pipe was assembled with a PVC piece, of the size of a threshold sensor, attached to the inner edge of the opening of the pipe. The aim of this measurement pipe was to find out, how a sensor would affect the humidity distribution inside the structure.

In this pilot test site, different threshold relative humidity sensors were tested. As presented in chapter 3, a threshold sensor consists of a basic sensor covered with a reacting layer and a breathing Goretex (W.L. Gore & Associates, USA) membrane. Each sensor is supposed to react when a certain humidity threshold is exceeded, depending on the salt used in the reacting layer. In this pilot test, threshold sensors featuring the thresholds of 44 % (K_2CO_3), 75 % ($NaCl$), 81 % ((NH_4)$_2SO_4$), 85 % (KCl), 94 % (KNO_3), and 97 % (K_2SO_4) were used. The sensors assembled to each location are listed in table 6.1.

The sensors at the outer surface of the thermal insulation were assembled by taping them to the wind-protective panel outside the insulation layer. The sensors located half-way in the thermal insulation and at its inner surface were

Table 6.1: The thresholds of the sensors at different locations in the bedroom and the bathroom.

Room	Location	Thresholds
Bedroom	Inner surface	44 %, and 75 %
	Half-way	75 %, 81 %, 85 %, and 94 %
	Outer surface	44 %, 75 %, 85 %, and 97 %
Bathroom	Inner surface	75 %, and 81 %
	Outer surface	85 %, 94 %, and 97 %

attached to an elastic anti-slip mat that was tightened between the framework of the wall, in such a way that the thermal insulation could still be sprayed into place. Four assembled sensors can be seen in figure 6.16a. Figure 6.16b shows the pipes for the HMP44 probes and the wires that connect to the SHT-11 sensors, and figure 6.16c the complete measurement setup in the bedroom wall. Figure 6.16d shows the bedroom wall from the outside before the boarding was completed. At that stage, the outermost sensors could be read with the hand-held reading device.

Measurement results and discussion

Figure 6.17 presents the relative humidity and temperature measurement results, acquired by Humittest Ltd. with the HMP44 probes, halfway in the bedroom wall during the years 2003–2004. The solid traces represent the results from the pipe with the PVC piece on its inside, and the slash-dotted traces without the piece. The presented results are from the winter time when both the relative humidity and the temperature differences between the indoor and outdoor air are the largest. The PVC piece seems to cause a slight temperature difference between the probes, the temperature behind the piece being approximately 1.0 ℃ larger on the average. Thus, it seems that either the PVC piece conducts temperature from its inner surface to the probe, or the locations of the probes are not exactly at the same depth in the insulation. The difference in relative humidity, however, is more significant, with the relative humidity behind the PVC piece being approximately 5.0 percentage points smaller. The difference is expected, since the absolute humidity inside the building is somewhat larger than that of the outdoor air, thus moisture diffuses from the inside out. It seems that the piece slightly restrains the diffusion, thus leaving a slightly smaller absolute humidity behind the piece. This results in the smaller relative humidity visible in figure 6.17.

The test setup of the threshold relative humidity sensors proved to be somewhat unsuccessful. The acquired measurement results from the bedroom wall are shown in table 6.2. As can be seen from the table, not one of the 10 sensor assembled to the bedroom wall had reacted fully at the times of measurement. It should be noted that all the quality factor measurement results half-way in

Figure 6.16: Measurement setup in the thermal insulation of the bedroom wall: a. two threshold sensors taped to the wind-protective panel and two sensors attached to an anti-slip mat tightened between the framework of the wall, b. the pipes for the HMP44 probes and the connection of the SHT-11 sensors, c. the entire measurement setup in the bedroom wall, d. measuring the outermost sensors from outside the building.
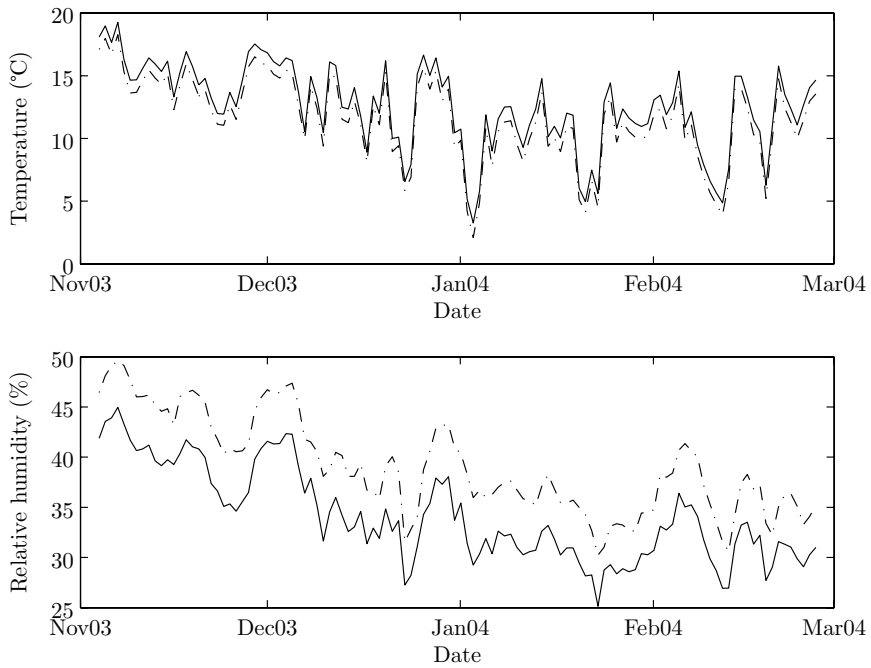
Figure 6.17: Temperature and relative humidity measurement results halfway in the bedroom wall, at noon, during the years 2003–2004, acquired with HMP44 probes and a logger. The solid traces represent the results behind the PVC piece, and the slash-dotted traces without it.

the thermal insulation and the results on the outer surface after June 12th 2003, were acquired with the portable measurement setup built around a signal generator, and their results are not as accurate as the ones acquired with the hand-held reading device. However, it is obvious that the quality factors of all the sensors are above 100. Among the measurement results, there is only one case where a threshold sensor definitely should have reacted, the 44 % sensor in the outer wall, in June 12th 2003. In this case the relative humidity around the sensor has been above the threshold value for a long time. In addition, there are some cases where the relative humidity exceeds the nominal threshold, but the temperature is significantly lower than 20 ℃, in which the nominal thresholds are determined. However, most of the threshold sensors feature thresholds that are so high, that a significant failure in the structure would be needed for them to react.

Table 6.2: Measurement results from the three locations in the bedroom wall. The relative humidity (RH) and temperature (T) readings were measured by Humittest Ltd. with HMP44 probes (Vaisala Inc., Finland). The quality factors of each threshold sensor were measured with the hand-held reading device or a portable measurement system built around a signal generator.

Location	Date	RH	T	Quality factor					
		[%]	[℃]	44	75	81	85	94	97
Inner	Feb 3rd 2003	45	11.1	105	103	-	-	-	-
	Jun 12th 2003	37	24.0	103	103	-	-	-	-
	Oct 8th 2003	32	23.1	107	111	-	-	-	-
	Jan 30th 2004	16	20.8	110	108	-	-	-	-
	Jun 21st 2004	33	23.3	106	106	-	-	-	-
Half-way	Feb 3rd 2003	70	2.2	-	110	112	102	105	-
	Jun 12th 2003	53	21.2	-	111	115	106	112	-
	Oct 8th 2003	50	16.0	-	126	130	120	119	-
	Jan 30th 2004	34	10.0	-	124	123	111	119	-
	Jun 21st 2004	43	20.3	-	116	119	112	111	-
Outer	Feb 3rd 2003	90	-5.2	106	106	-	103	-	106
	Jun 12th 2003	60	20.1	105	113	-	107	-	110
	Oct 8th 2003	67	11.1	-	-	-	-	-	-
	Jan 30th 2004	60	2.1	119	120	-	-	-	-
	Jun 21st 2004	52	18.6	111	118	-	111	-	115

Summary

The most significant experience gained from the presented pilot case is how an obstacle, the size of a basic or threshold sensor affects the moisture distribution in a coarse structure. The effects seem to be of such magnitude, that they significantly affect the measurement of relative humidity and temperature, because of the dynamic nature of the structure. However, it seems that the sensors do

not hinder the normal functionality of the structure. As a consequence, the construction of the sensor should be refined to be more permeable to water vapor, in order to be suitable for the application. This could be done by e.g. perforating the sensor. In the current form, for example the orientation of the sensor would influence the acquired measurement result significantly, since moisture is buffered to the moisture source side of the sensor, and the humidity behind the sensor is lower than normally.

The threshold relative humidity sensors have not shown signs of functioning. This may be partly because the threshold levels chosen for the sensors at each location are somewhat too large when taking into account the temperature dependence of the relative humidities at which the salts react. Another possible cause is that small filaments of the Termex thermal insulation have blocked the Goretex membrane surrounding the sensors so that it no longer permeates water vapor. A more positive observation was, that all the sensors have remained readable also in this kind of a structure.

6.2.6 Testing the success of window renovation

A slightly different application of the developed system is one that took place in a window renovation in a Finnish hospital. The location is a 16-storey-high concrete structured building that has been built in the early 1960's. The building has experienced leaks in its outer wall structure. The water has also migrated to the plate structure inside the wall causing microbe growth that has harmed the indoor air quality in the building. An experimental renovation was done to a small part of the wall structures in order to find out whether the proposed renovation model is suitable. The functionality of the structure was tested with the developed measurement system.

At the time of renovating the structure, basic sensors were assembled above and below the window. The suggested assembly locations of the sensors are shown in figure 6.18a. The sensors were attached to the wooden surface (7) of the block masonry (6) with the assembly mortar, before smoothing the surface (3). Figure 6.18b shows the actual sensor locations in one room.

Measuring the sensors has been left primarily for the organization responsible for the building. However, a brief visit to the location approximately one year after the renovation, revealed a significant rise in relative humidity at some locations. The measurement results have been backed up by an observation reported by the hospital staff, that water has penetrated the window structure into the room.

6.3 Conclusions

The experiences gained from applying the developed method and system into the actual construction environment indicate, that the system functions rea-
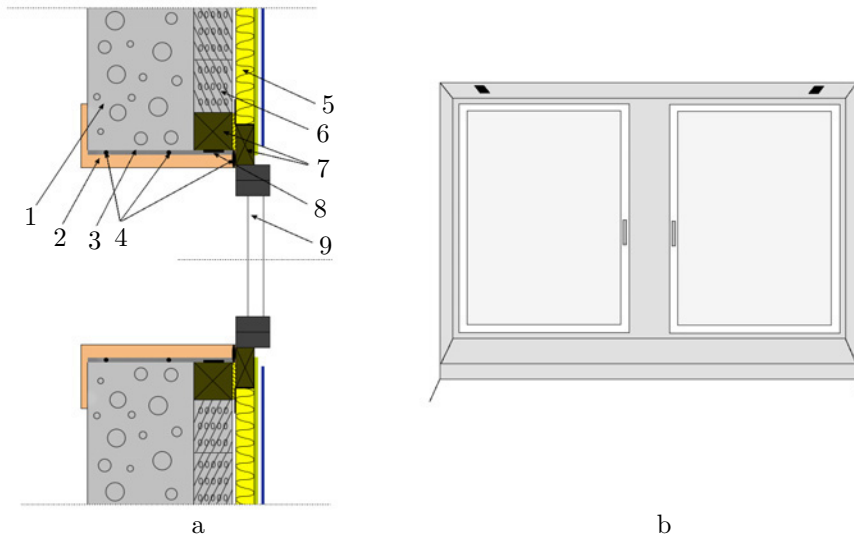
Figure 6.18: The window structure with the suggested sensor locations (a) and the sensor locations in one of the windows (b). The structural picture includes a concrete element (1), plywood finishing (2), smoothing mortar (3), sealing compound (4), thermal insulation (5), block masonry (6), a wood structure (7), the sensor (8), and the window (9).

sonably well, especially in the bathroom moisture monitoring application. The assembly process seems to function, and the commercial sensor set is suitable for the purpose. However, it is crucial that whoever assembles the sensors is motivated and documents the locations of the sensors accurately. The measurement concept only works if the sensors can be located and action is taken according to their readings. Some resistance has also been met to the adoption of the system, since surface moisture meters can be more easily used to get a suitable reading when behind schedule.

In more dynamic structures, such as in monitoring the drying of concrete, the system does not seem to react to the most rapid changes in the moisture conditions of the structure. This is probably partly because the sensor blocks the migration of moisture in the structure. As an enhancement suggestion, the sensor should be made more permeable to moisture by e.g. drilling holes into the sensor structure. On the other hand, the fact that the sensor neglects short-term variations, could be considered an advantage, if the sensor is used to monitor long-term changes.

7 Discussion and conclusions

A definite need for a new method for routine monitoring of moisture in building structures was recognized in the construction industry. Specifically, the new method had to be non-destructive, yet able to measure the moisture conditions at exact and predefined locations inside the structures. The results were to be presented as the relative humidity of the materials, preferably together with the local temperature, and the ambient relative humidity and temperature. In addition, the system had to be reliable, consistent, and independent of the operator. Further, the system had to be be inexpensive, easy and fast to assemble and use, and it had to be suitable for the current construction professionals. It was also considered advantageous, if the measurement system could also function as a systematic documenting tool for moisture conditions.

The approach chosen to fill the defined need was a new measurement method that uses sensors that are assembled inside the building structures at the time of construction or renovation, and a separate reading device for reading the sensors wirelessly from outside the structure. The chosen approach has proven successful in filling the needs and the specific requirements listed above. As a consequence, the developed measurement method is a functional solution for preventing many problems caused by moisture in building structures. Thus, it can be used to diminish the exposure of inhabitants to health risks caused by moisture. In addition, the system functions as a tool for evaluating the condition and quality of constructions. All these benefits can be acquired with a minimal economic input and loss of time.

The development of the instrumentation that implements the measurement method has also been successful. Several different sensors of differing properties and cost have been developed for different applications. In addition, a fully functional reading device has been developed. The device can be used to reliably determine the quality factors and resonance frequencies of different sensors at the range of 30–70 mm, and to display the results to a user as relative humidity. However, the functionality and the reliability of the system still varies somewhat between different application areas. At suitable conditions, the system functions as accurately as professionally performed relative humidity measurements. The reading device can also be equipped with means to document measurement results, and to measure ambient relative humidity and temperature.

The bathroom application was early on chosen as the first area of focus for the research. The laboratory tests and their results presented in chapter 5 show that the basic sensor concept is functional, especially when the sensor is assembled underneath an impermeable layer, such as the waterproofing typically used in bathrooms. The practical experiences and the pilot assembly cases presented in

chapter 6, on the other hand, have proven that the assembly and measurement processes are straightforward and functional. In addition, utilizing the developed system in bathrooms has unquestionably proven to give information about the moisture technical performance of bathrooms that would be difficult, if not impossible, to acquire with earlier equipment. As an option, a temperature sensing element and an escort memory can also be attached to the basic sensor to add extra functionality.

Another, a significantly broader and more demanding application area assessed, was monitoring the drying of concrete. Both the laboratory experiments of chapter 5 and the practical experiences of chapter 6 have indicated that using the pre-cast basic sensor in concrete gives suggestive information about its moisture conditions. The difficulties seem to be related to the migration of moisture in dynamic structures. First of all, the sensors do not seem to react to the most rapid changes in moisture conditions. This could be considered an advantage or a disadvantage. However, the pre-cast basic sensors also seem to function differently in different concrete types and at different assembly depths. The problems are suspected to result from the sensor blocking the migration of moisture, different salts migrating differently in different concrete types, and the effect of different pore structures in the moisture migration between the assembly mortar and the surrounding concrete. Nevertheless, the measurement method is practical, especially when the same sensors are used both in monitoring the drying of concrete and in the bathroom application. However, absolute conclusions about the moisture conditions in the structure should not be drawn based on the results acquired with the measurement method. Instead, in critical applications, verifying measurements should be made with traditional relative humidity measurements.

Measuring relative humidity in air directly, and thus also the relative humidity inside the pores of materials, has also been one important application area for the method. The most significant amount of research has been conducted with the threshold relative humidity sensor. In laboratory experiments, presented in chapter 5, the threshold sensor has proven to be able to reliably determine whether a certain relative humidity threshold has been exceeded. However, the functionality of threshold sensors has not yet been proven with field experiments.

The customer's costs of utilizing the measurement system are relatively low. At the moment, only the bathroom application has reached the state of a commercial product. The customer price for the sensors required in a single bathroom is around 100 euros. Thus, the costs are negligent in comparison with the construction or renovation costs. The price of the reading device, on the other hand, is around 1000 euros. However, a typical occupant does not need a device of his own. To conclude, the measurement system can be considered to be inexpensive.

Currently, the greatest challenges in the measurement system lie in creating an infrastructure around the usage of the technique. The measurement system must be in the best interest of all parties involved with the building process.

Thus, effort must be put into convincing all parties of the advantages gained. More knowledge about the adoption of the system and its long-term durability is constantly gained from the pilot assembly sites and the sites where the commercial measurement system has been applied. In addition, if the measurement system becomes more common, several objective evaluations of the system are expected to take place in the construction industry.

The developed measurement system as such includes several areas that could be enhanced. The existing sensors could be assembled deeper into the structures of interest, if the maximum reading range of the reading device was somewhat longer. The reading range could be increased with several different ways, e.g. by increasing the area of the antenna coil, adding more turns to the coil, using a larger measurement current, or using more sophisticated signal processing such as the Fourier reading method discussed briefly in chapter 4.

In addition to the reading device, several enhancements could be made in the sensor technology. The monitoring of dynamic structures, such as drying concrete, could function more reliably, if the sensor structure was made more permeable to moisture by using different materials, or by reducing its area perpendicular to the moisture gradient. The latter could be accomplished e.g. with a different sensor coil design, a different orientation of the sensor, or adding holes to the sensor circuit board. It would also be extremely beneficial, to be able to develop the sensor into a wide-range relative humidity and temperature sensor that would function in free air as well as in all kinds of construction materials. A promising method for implementing it is using conductive polymers as the reacting layer in a sensor.

The future of the measurement system lies very likely in automatic monitoring. Currently the functionality of the measurement system depends on a person that reads the sensors regularly. However, it would be beneficial if the system could monitor moisture automatically at regular intervals in several locations, and indicate the results or possible warning signals in a common indicator device. This could be accomplished by equipping the sensors with simple radio transmitters. This approach, however, would increase the costs of the sensors significantly.

To conclude, this thesis presents new methods and instrumentation for measuring moisture in building structures. The research has been successful, and the thesis has reached the specific objectives stated for it. The first objective was to define the current need for new methods of measuring moisture in building structures and to select the specific problems to approach. The most significant need was discovered in routine monitoring of moisture, specifically in bathrooms and concrete structures. The measurement problem was defined carefully and processed into exact specifications for the measurement system. The second objective was to elucidate the physical principles of the novel measurement methods and to design the practical instrumentation. The chosen approach was a measurement system that consists of low-cost sensors, a separate device for reading them, and inductive coupling between the sensors and the device. After

elucidating the physical principles involved in the approach, several different sensors and a functional reading device were developed to implement the methods. The third objective was to verify the functionality of the methods and the instrumentation in laboratory and field measurements. Results acquired from extensive tests in the laboratory environment, and preliminary results from the field indicate that the methods and instrumentation function in the most important application areas. The fourth objective was to generate guidelines of applying the methods in the building industry. The information acquired from the experiments was reported to the building industry as instructions and specifications of the system.

This thesis contributes new methods for measuring moisture in building structures, several new passive moisture and temperature sensors, a hand-held device for reading the sensors wirelessly, and preliminary measurement results and experiences from using the system in the construction industry.

Bibliography

[1] Lars Erik Nevander and Bengt Elmarsson. *Fukthandbok: praktik och teori (Moisture handbook: practice and theory, in Swedish)*. Svensk byggtjänst, Solna, Sverige, 1994.

[2] *Kosteus- ja homevaurioituneen rakennuksen kuntotutkimus (Condition investigation of a moisture and mold damaged building, in Finnish)*. Ministry of the Environment, Helsinki, Finland, 1997.

[3] Dick Björkholtz. *Lämpö ja kosteus: rakennusfysiikka (Temperature and moisture: building physics, in Finnish)*. Rakennustieto, Helsinki, Finland, 1997.

[4] Joseph Lstiburek and John Carmody. *Moisture control handbook : principles and practices for residential and small commercial buildings*. John Wiley & Sons, New York, USA, 1994.

[5] Ari-Veikko Kettunen. *Kosteuskartoitusopas vesivahinkojen tapauksessa (Moisture survey guide in case of water damage, in Finnish)*. Helsinki University of Technology, Espoo, Finland, 2000.

[6] Kirsi Torikka, Tarja Hyypöläinen, Jussi Mattila, and Ralf Lindberg. *Kosteusvauriokorjausten laadunvarmistus (Quality control of moisture damage repairments, in Finnish)*. Tampere University of Technology, Department of Civil Engineering, Tampere, Finland, 1999.

[7] Lars-Olof Nilsson. *Hygroscopic moisture in concrete - drying, measurements & related material properties*. Division of Building Materials, Lund Institute of Technology, Lund, Sweden, 1980.

[8] Alan Oliver. *Dampness in buildings. Second edition revised by James Douglas and J. Stewart Stirling*. Blackwell Science Ltd., Oxford, UK, 1997.

[9] H. Viitanen. Modelling the time factor in the development of mold fungi in wood - the effect of critical humidity and temperature conditions. *Holzforschung*, 51(1):6–14, 1997.

[10] H. Viitanen. Critical time of different humidity and temperature conditions for the development of brown rot decay in pine and spruce. *Holzforschung*, 51(2):99–106, 1997.

[11] *Asumisterveysohje: asuntojen ja muiden oleskelutilojen fysikaaliset, kemialliset ja mikrobiologiset tekijät (Guideline for dwelling health: physical, chemical and biological factors in housing and other living premises, in Finnish)*. Ministry of Social Affairs and Health, Helsinki, Finland, 2003.

[12] Martti Viljanen, Ari-Veikko Kettunen, Mari Makkonen, Riikka Kangas, and Päivi Järnefelt. *Rakenneratkaisut ja sisäilman laatu, 1990-luvun asuinkerrostalotutkimus (Structural solutions and indoor air quality, a research of a 1990's multistorey apartment block, in Finnish)*. City of Helsinki, Environment center, Helsinki, Finland, 1998.

[13] Pentti Lumme and Tarja Merikallio. *Betonin kosteuden hallinta (Controlling moisture in concrete, in Finnish)*. Suomen Betonitieto Oy, Forssa, Finland, 1997.

[14] *Sisäilmastoluokitus 2000 (Indoor air classification 2000, in Finnish)*. Finnish Society of Indoor Air Quality and Climate, Espoo, Finland, 2001.

[15] B. Flannigan and P.R. Morey. *Rakennusten kosteus- ja homevaurioiden toiminta (originally: Control of moisture problems affecting biological indoor air quality, in Finnish)*. ISIAQ-guideline: Task force I - 1996. Finnish Society of Indoor Air Quality and Climate, Helsinki, Finland, 1996.

[16] Recommendations. In R.A. Samson, B. Flannigan, M.E. Flannigan, A.P. Verhoeff, O.C.G. Adan, and E.S. Hoekstra, editors, *Health Implications of Fungi in Indoor Environments*, pages 529–538. Elsevier Science, Amsterdam, The Netherlands, 1994.

[17] Markku Seuri and Marjut Reiman. *Rakennusten kosteusvauriot, home ja terveys (Moisture damage in buildings, mold, and health, in Finnish)*. Rakennustieto Oy, Helsinki, Finland, 1996.

[18] Marjut Reiman. In Virpi Leivo, editor, *Opas kosteusongelmiin - Rakennustekninen, mikrobiologinen ja lääketieteellinen näkökulma (A guide to moisture problems - A constructional, microbiological and medical viewpoint, in Finnish)*, chapter 4. Kosteusvaurioihin liittyvä mikrobikasvu (Microbe growth related to moisture damage), pages 48–55. Tampere University of Technology, Department of Civil Engineering, Tampere, Finland, 1998.

[19] Anna-Liisa Pasanen, Pentti Kalliokoski, and Matti Jantunen. Recent studies of fungal growth on buildings materials. In R.A. Samson, B. Flannigan, M.E. Flannigan, A.P. Verhoeff, O.C.G. Adan, and E.S. Hoekstra, editors, *Health Implications of Fungi in Indoor Environments*, pages 485–493. Elsevier Science, Amsterdam, The Netherlands, 1994.

[20] Ulla Haverinen. *Modeling moisture damage observations and their association with health symptoms*. National Public Health Institute, Kuopio, Finland, 2002.

[21] Jukka Uitti. In Virpi Leivo, editor, *Opas kosteusongelmiin - Rakennustekninen, mikrobiologinen ja lääketieteellinen näkökulma (A guide to moisture problems - A constructional, microbiological and medical viewpoint, in Finnish)*, chapter 5. Kosteus- ja homevauriomikrobien terveysvaikutukset

(Health effects caused by moisture and mold damage microbes), pages 56–63. Tampere University of Technology, Department of Civil Engineering, Tampere, Finland, 1998.

[22] C.-G. Bornehag, G. Blomquist, F. Gyntelberg, B. Järvholm, P. Malmberg, L. Nordvall, A. Nielsen, G. Pershagen, and J. Sundell. Dampness in buildings and health. *Indoor air*, 11(2):72–86, 2001.

[23] J.K. Peat, J. Dickerson, and J. Li. Effects of damp and mold in the home on respiratory health: a review of the literature. *Allergy*, 53(2):120–128, 1998.

[24] Olli Seppänen and Jari Palonen. *Sisäilmaston kansantaloudelliset vaikutukset (The effects of indoor climate on national economy, in Finnish)*. Finnish Society of Indoor Air Quality and Climate, Helsinki, Finland, 1998.

[25] Pertti Partanen, Esa Jääskeläinen, Aino Nevalainen, Tuula Husman, Anne Hyvärinen, Leena Korhonen, Teija Meklin, Kai Miller, Pertti Forss, Jari Saajo, Irmeli Röning-Jokinen, Matti Nousiainen, Risto Tolvanen, and Ilpo Henttinen. *Pientalojen kosteusvauriot - Yleisyyden ja korjauskustannusten selvittäminen (Moisture damages in houses - investigating their frequency and costs of refurbishment, in Finnish)*. National Public Health Institute, Kuopio, Finland, 1995.

[26] Jari Koivisto, Esa Jääskeläinen, Aino Nevalainen, Tuula Husman, Teija Meklin, Mikko Vahteristo, Seppo Heiskala, Pertti Forss, Jukka Turpeinen, and Irmeli Röning-Jokinen. *Asuinkerrostalojen kosteusvauriot - Yleisyyden ja korjauskustannusten selvittäminen (Moisture damages in high rise residential buildings - investigating their frequency and costs of refurbishment, in Finnish)*. National Public Health Institute, Kuopio, Finland, 1996.

[27] T. T. Lien Nguyen, Tuomo Pentikäinen, Pekka Rissanen, Mikko Vahteristo, Tuula Husman, and Aino Nevalainen. *Health-Related costs of moisture and mold in dwellings*. National Public Health Institute, Kuopio, Finland, 1998.

[28] Markku Rantama, Ari-Veikko Kettunen, Esko Kukkonen, Kristina Saarela, and Olli Seppänen. *Terve talo -teknologiaohjelma 1998-2002 loppuraportti (final report of the Finnish Healthy Building technology program, in Finnish)*. National Technology Agency of Finland, Helsinki, Finland, 2003.

[29] Friedrich Hirth. Instrument for measuring the moisture content of dielectric objects. US Patent 4,588,943, May 1986.

[30] Tramex Ltd. Tramex moisture encounter data sheet. http://www.tramexltd.com/pdf/moistenc.pdf, visiten February 23rd 2005.

[31] Tarja Merikallio. *Betonirakenteiden kosteusmittaus ja kuivumisen arviointi (Measuring moisture and estimating drying of concrete, in Finnish)*. Betonikeskus ry, Jyväskylä, Finland, 2002.

[32] International Programme on Chemical Safety. International chemical safety card: Calcium carbide. http://www.inchem.org/documents/icsc/icsc/eics0406.htm, visited February 23rd 2005.

[33] Hugh Frefman Cameron. Process and apparatus for detecting and determining the quantity of percentage of moisture in a substance. GB Patent 335,308, September 1930.

[34] G.W. Bundrett. *Criteria for moisture control*. Butterworth & Co. (Publishers) Ltd., London, UK, 1990.

[35] Frank G. Cooper. Cycling chilled mirror dewpoint hygrometer including a sapphire optical mirror. US Patent 5,507,175, April 1996.

[36] Humittest Ltd. Betonin suhteellisen kosteuden (RH) mittaus porareiästä (Measuring the relative humidity of concrete from a drilled hole, in Finnish). Appendix of field log.

[37] Confederation of Finnish Construction Industries. *Betonin suhteellisen kosteuden mittaus RT 14-10675 (Measuring the relative humidity of concrete, in Finnish)*, 1998.

[38] Humittest Ltd. Betonin suhteellisen kosteuden (RH) mittaus näytepalamenetelmällä (Measuring the relative humidity of concrete by taking a sample, in Finnish). Appendix of field log.

[39] Outi Valta. Rakenteisiin sijoitettavan suhteellisen kosteuspitoisuuden mitta-anturin kehitys (Design of a humidity sensor to be assembled within structures, in Finnish). Master's thesis, Helsinki University of Technology, Espoo, Finland, 2002.

[40] Tuomo Reiniaho. Rakenteisiin sijoitettavan langattoman anturoinnin kehitystyö (Design of wireless sensor technology to be assembled within construction, in Finnish). Master's thesis, Helsinki University of Technology, Espoo, Finland, 2003.

[41] Juho Partanen. Electronics of a reading device for inductively coupled sensors. Master's thesis, Helsinki University of Technology, Espoo, Finland, 2004.

[42] J. Voutilainen, O. Valta, E. Tommila, and R. Sepponen. Novel measurement method of humidity within construction structures. Electronic Publications E 2, Helsinki University of Technology, Applied Electronics Laboratory, Espoo, Finland, 2002.

[43] J. Voutilainen, J. Partanen, T. Reiniaho, E. Tommila, and R. Sepponen. Wireless moisture measurement technique. In *Proceedings of the XXVIII Convention on Radio Science & IV Finnish Wireless Communication Workshop*, pages 155–158, Oulu, Finland, 2003.

[44] J. Voutilainen, J. Partanen, T. Reiniaho, E. Tommila, and R. Sepponen. Uusi menetelmä rakenteiden kosteuden seurantaan (A new method of monitoring moisture in building structures, in Finnish). In *Sisäilmastoseminaari 2003, FiSIAQ Report 19*, Espoo, Finland, 2003. SIY Sisäilmatieto Oy.

[45] J. Voutilainen, E. Tommila, J. Partanen, and R. Sepponen. Märkätilan kosteuden seuranta rakenteita rikkomatta (Monitoring moisture in a bathroom non-destructively, in Finnish). In *Sisäilmastoseminaari 2004, FiSIAQ Report 22*, Espoo, Finland, 2004. SIY Sisäilmatieto Oy.

[46] J. Voutilainen, E. Tommila, J. Partanen, T. Reiniaho, and R. Sepponen. Lifetime moisture monitoring system for buildings. In *Proceedings of the Second International Symposium, ILCDES 2003, Integrated Lifetime Engineering of Buildings and Civil Infrastructures*, pages 337–342, Kuopio, Finland, 2003.

[47] J. Voutilainen, J. Partanen, T. Reiniaho, E. Tommila, and R. Sepponen. A novel technique for measuring moisture in constructions and application examples. In *Proceedings of the 7th Healthy Buildings Conference (Healthy Buildings 2003), Vol. 2*, pages 770–775, Singapore, 2003.

[48] Leonard S. Bobrow. *Fundamentals of electrical engineering*. Oxford University Press, Inc, USA, second edition, 1996.

[49] David M. Pozar. *Microwave engineering*. John Wiley & Sons, Inc, USA, second edition, 1998.

[50] James W. Nilsson and Susan A. Riedel. *Electric circuits*. Addison-Wesley, USA, fourth edition, 1993.

[51] Timo Varpula. *Optimising planar inductors*. Technical Research Centre of Finland, Espoo, Finland, 2000.

[52] Phycomp Components. *Class 1, NP0 50/100/200/500 V noble metal electrode surface-mount ceramic multilayer capacitors, data sheet, Rev. 6*, 2001.

[53] David K. Cheng. *Field and Wave Electromagnetics*. Addison-Wesley, USA, 1989.

[54] Daniel R. Frankl. *Electromagnetic theory*. Prentice/Hall, USA, 1986.

[55] Henry E. Duckworth. *Electricity and magnetism*. Holt, Rinehart and Winston Inc. USA, 1960.

[56] Frederick W. Grover. *Inductance calculations: working formulas and tables*. Instrument Society of America, USA, 1973.

[57] European Conference of Postal and Telecommunications Administration (CEPT). Relating to the use of Short Range Devices (SRD), ERC Recommendation 70-03, April 2004.

[58] European Telecommunications Standards Institute (ETSI). ETSI EN 300 330-1 V1.3.1, Electromagnetic compatibility and radio spectrum matters (ERM); Short range devices (SRD); Radio equipment in the frequency range 9 kHz to 25 MHz and inductive loop systems in the frequency range 9 kHz to 30 MHz; Part 1: Technical characteristics and test methods, June 2001.

[59] Karin Pettersson. *Beständighet hos vissa material i förbindelse med betong (Durability of some materials in contact with concrete, in Swedish)*, pages 849–853. Svensk byggtjänst, Sweden, 1994.

[60] Phycomp Componentes. *Phycomp MLCC Spice Calculation Program - MLCCSpice v1.3*, 2001.

[61] Arthur R. von Hippel. Tables of dielectric materials. In *Dielectric materials and applications, Papers by twenty-two contributors*. The Technology Press of M.I.T. and John Wiley & Sons, Inc. USA, 1954.

[62] J.G. Wilson and H.W. Whittington. Variations in the electrical properties of concrete with change in frequency. *IEE Proceedings A*, 137(5):246–254, 1990.

[63] Tim Williams. *The circuit designer's companion*. Butterworth-Heinemann Ltd., Oxford, UK, 1991.

[64] Taina Koskelo. Kosteuden siirtyminen puussa - kuppikokeiden suoritusohje (Moisture migration in wood - instructions for performing a cupping test, in Finnish). Report 4, Helsinki University of Technology, Laboratory of Structural Engineering and Building Physics, Espoo, Finland, 1994.

[65] Atmel Corporation, USA. *ATmega32(L) Preliminary Complete, data sheet*, December 2003.

[66] International Telegraph and Telephone Consultative Committee. CCITT Recommendation V.28: Electrical characteristics for unbalanced double-current interchange circuits. In *CCITT Blue Book*, volume 8.1, pages 211–215. ITU, Geneva, Switzerland, 1989.

[67] Arto Lehto and Antti Räisänen. *RF- ja mikroaaltotekniikka (RF and microwave technology, in Finnish)*. Otatieto, Espoo, 2001.

[68] Anders Sjöberg. *Secondary emissions from concrete floors with bonded flooring materials : Effects of alkaline hydrolysis and stored decomposition products*. Chalmers University of Technology, Göteborg, Sweden, 2001.

[69] Marko Leskinen. Rakennekosteuden langaton seurantajärjestelmä (Wireless humidity measurement system in concrete structures, in Finnish). Bachelor's thesis, Helsinki Polytechnic Stadia, 2003.

[70] *Kosteus rakentamisessa: RakMK C2 opas (Moisture in construction: guide to the Finnish building regulations C2, in Finnish)*. Ministry of the Environment, Helsinki, Finland, 1999.

[71] Confederation of Finnish Construction Industries. *Termex-lämmöneristeet RT K-36382 (Termex temperature insulation, in Finnish)*, August 2002.